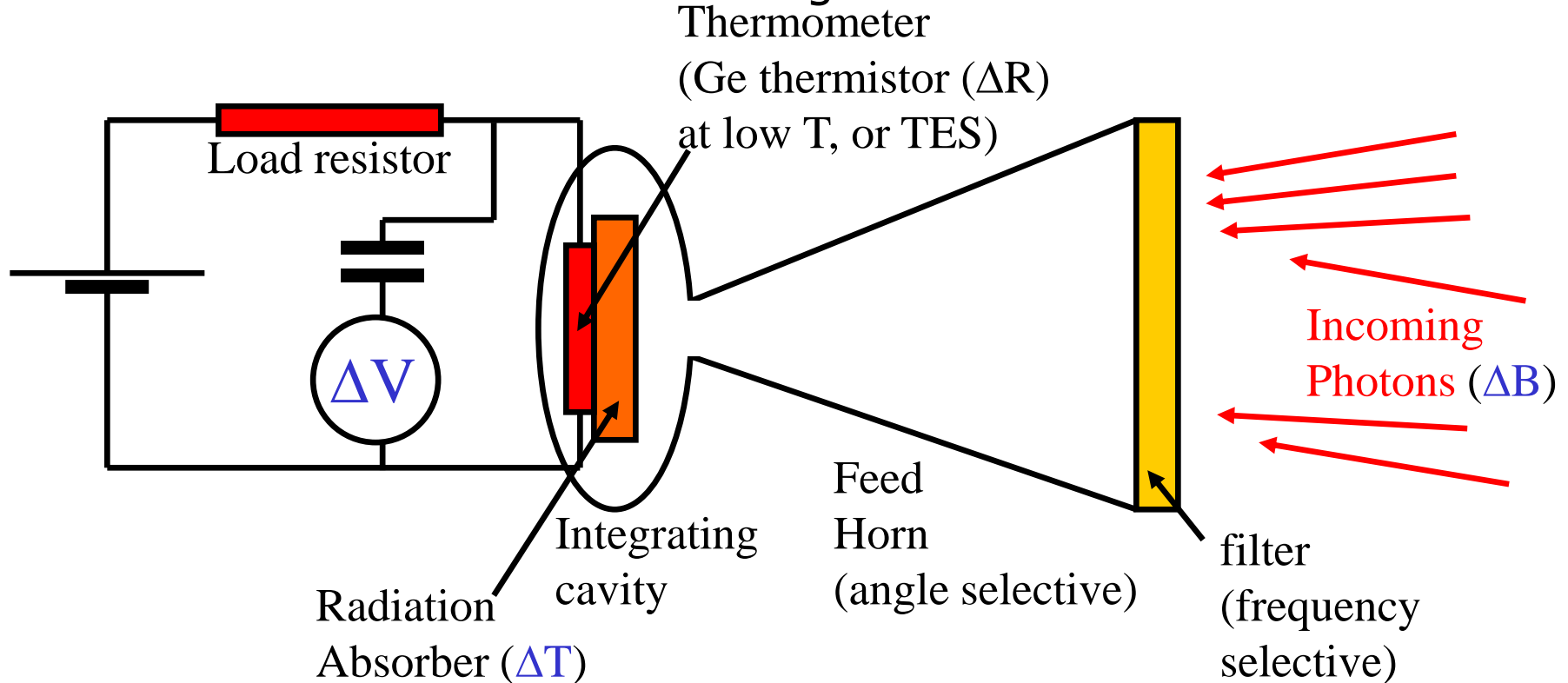


# Cryogenic Bolometers

- For FIR & mm-waves spectroscopy we need very wide band detectors. Bolometers provide the optimal choice: they are sensitive from mm-waves to the visible range.

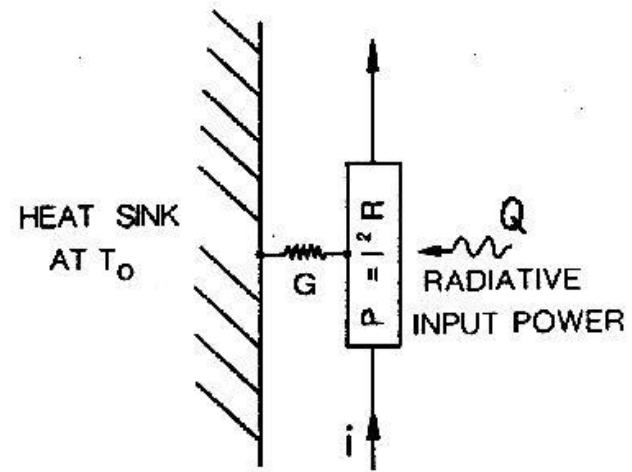


- Fundamental noise sources are Johnson noise in the thermistor ( $\langle \Delta V^2 \rangle = 4kTR\Delta f$ ), temperature fluctuations in the thermistor ( $\langle \Delta W^2 \rangle = 4kGT^2\Delta f$ ), background radiation noise ( $T_{\text{bkg}}^5$ ) → need to reduce the temperature of the detector and the radiative background.

# Cryogenic Bolometers

- In steady conditions the temperature rise of the sensor is due to the background radiative power absorbed  $Q$  and to the electrical bias power  $P$ :

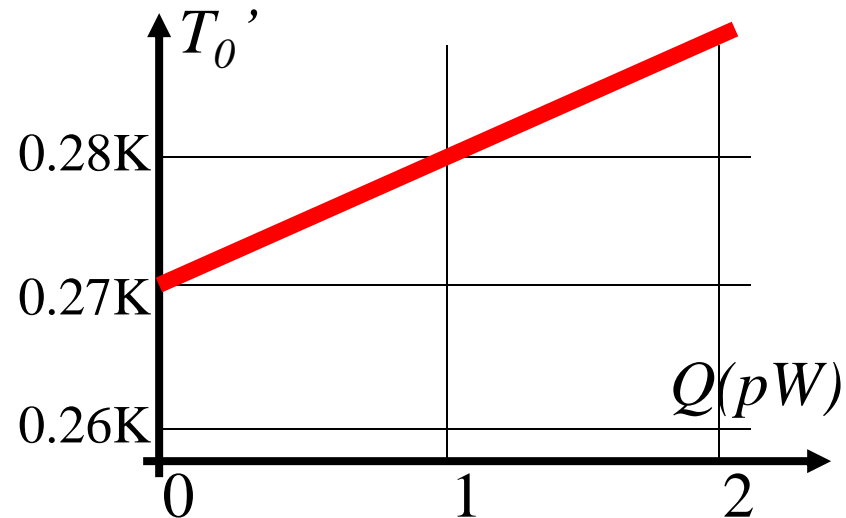
$$G(T - T_0) = Q + P$$



- The effect of the background power is thus equivalent to an increase of the reference temperature:

$$P = G \left[ T - \left( T_0 + \frac{Q}{G} \right) \right] = G(T - T_0')$$

$$T_0' = T_0 + \frac{Q}{G}$$



# Cryogenic Bolometers

- In presence of an additional signal  $\Delta Q e^{j\omega t}$  (from the sky)

$$C \frac{d\Delta T}{dt} + G_{eff} \Delta T = \Delta Q \quad \rightarrow$$

$$\left| \frac{dT}{dQ} \right| = \frac{1}{G_{eff} \sqrt{1 + \tau^2 \omega^2}}$$

$$\tau = \frac{C}{G}$$

- There is a tradeoff between high sensitivity and fast response. **The heat capacity  $C$  should be minimized** to optimize both.
- Using a current biased thermistor to readout the temperature change:

Small sensor  
at **low temperature**

$$\alpha = \frac{T}{R(T)} \frac{dR(T)}{dT} \Rightarrow dV = idR = i\alpha R dT / T$$

Responsivity  $\rightarrow$

$$\mathfrak{R} = \frac{dV}{dQ} = i\alpha \frac{R}{T} \frac{dT}{dQ} = \frac{i\alpha R / T}{G_{eff} \sqrt{1 + \tau^2 \omega^2}}$$

# Cryogenic Bolometers

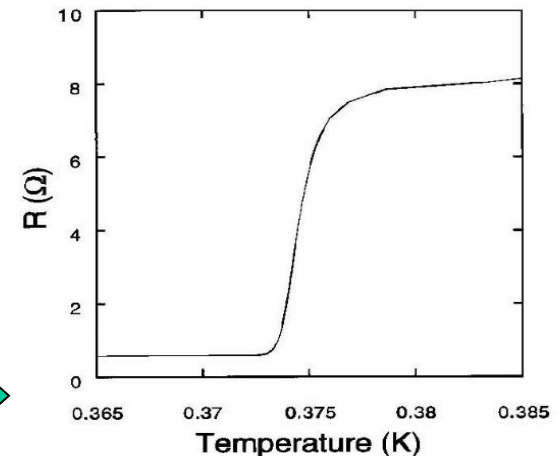
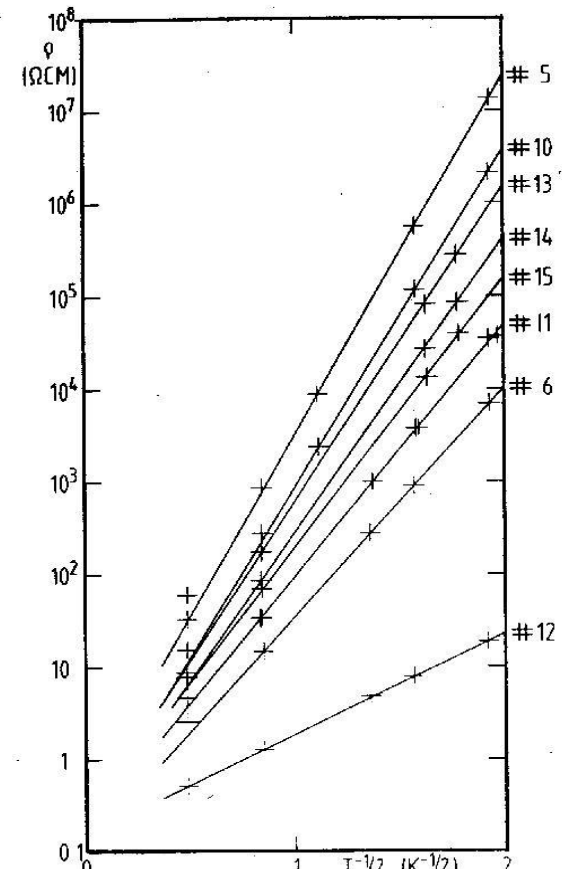
$$\alpha = \frac{1}{R(T)} \frac{dR(T)}{dT}$$

$$\mathfrak{R} = \frac{i\alpha R}{G_{eff} \sqrt{1 + \tau^2 \omega^2}}$$

- A large  $\alpha$  is important for high responsivity.
- Semiconductor (Ge) thermistors:
- Superconducting **transition edge thermistors (TES)**:

$$\frac{\alpha}{T} \approx -10K^{-1}$$

$$\frac{\alpha}{T} \approx 1000K^{-1}$$



# Intrinsic NEP of Cryogenic Bolometers

- Johnson noise in the thermistor

$$\frac{d\langle \Delta V_J^2 \rangle}{df} = 4kTR$$

- Temperature noise

$$\frac{d\langle \Delta W_T^2 \rangle}{df} = \frac{4kT^2 G_{eff}}{G_{eff}^2 + (2\pi f C)^2}$$

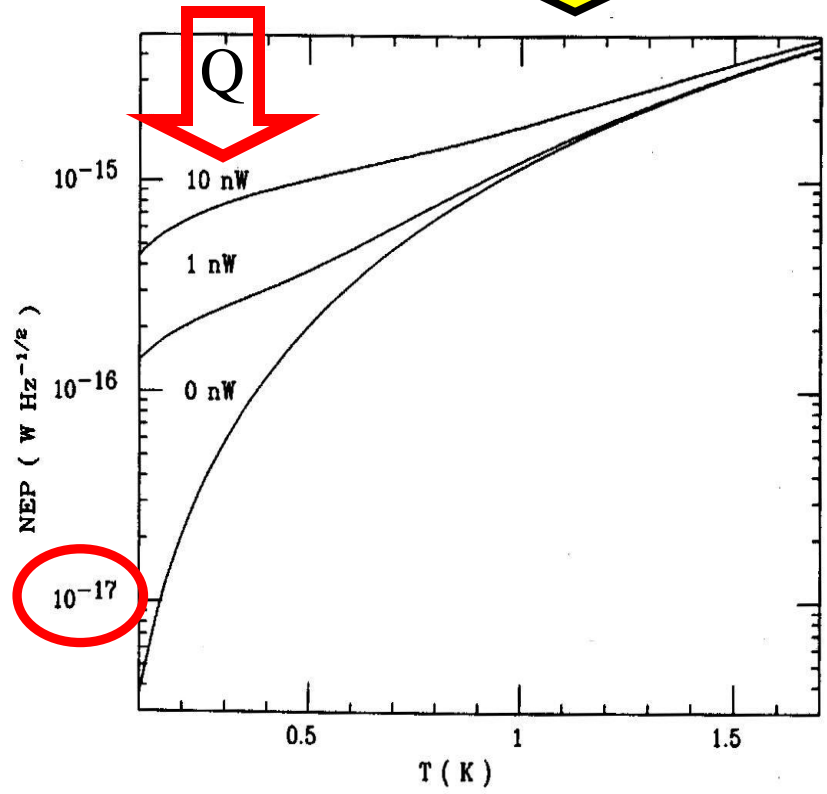
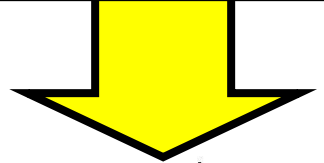
- Photon noise

$$\frac{d\langle \Delta W_{Ph}^2 \rangle}{df} = \frac{4k^5 T_{BG}^5}{c^2 h^3} \int \epsilon \frac{x^4 (e^x - 1 + \epsilon)}{(e^x - 1)^2} dx$$

- Total NEP (fundamental):  $\rightarrow$

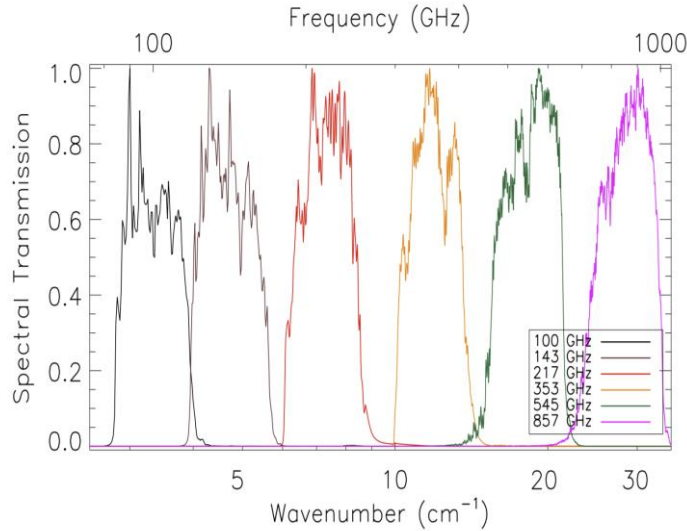
$$NEP^2 = \frac{1}{\mathcal{R}^2} \frac{d\langle \Delta V_J^2 \rangle}{df} + \frac{d\langle \Delta W_T^2 \rangle}{df} + \frac{d\langle \Delta W_{Ph}^2 \rangle}{df}$$

Need of low temperature and low background



# Performance of semiconductor (Ge) spider-web bolometers: the case of Planck-HFI

see A&A 536, A4 (2011)



- Spider webs in 6 frequency bands
- Photon-noise limited by the radiative background in deep space (CMB + 30K mirror)

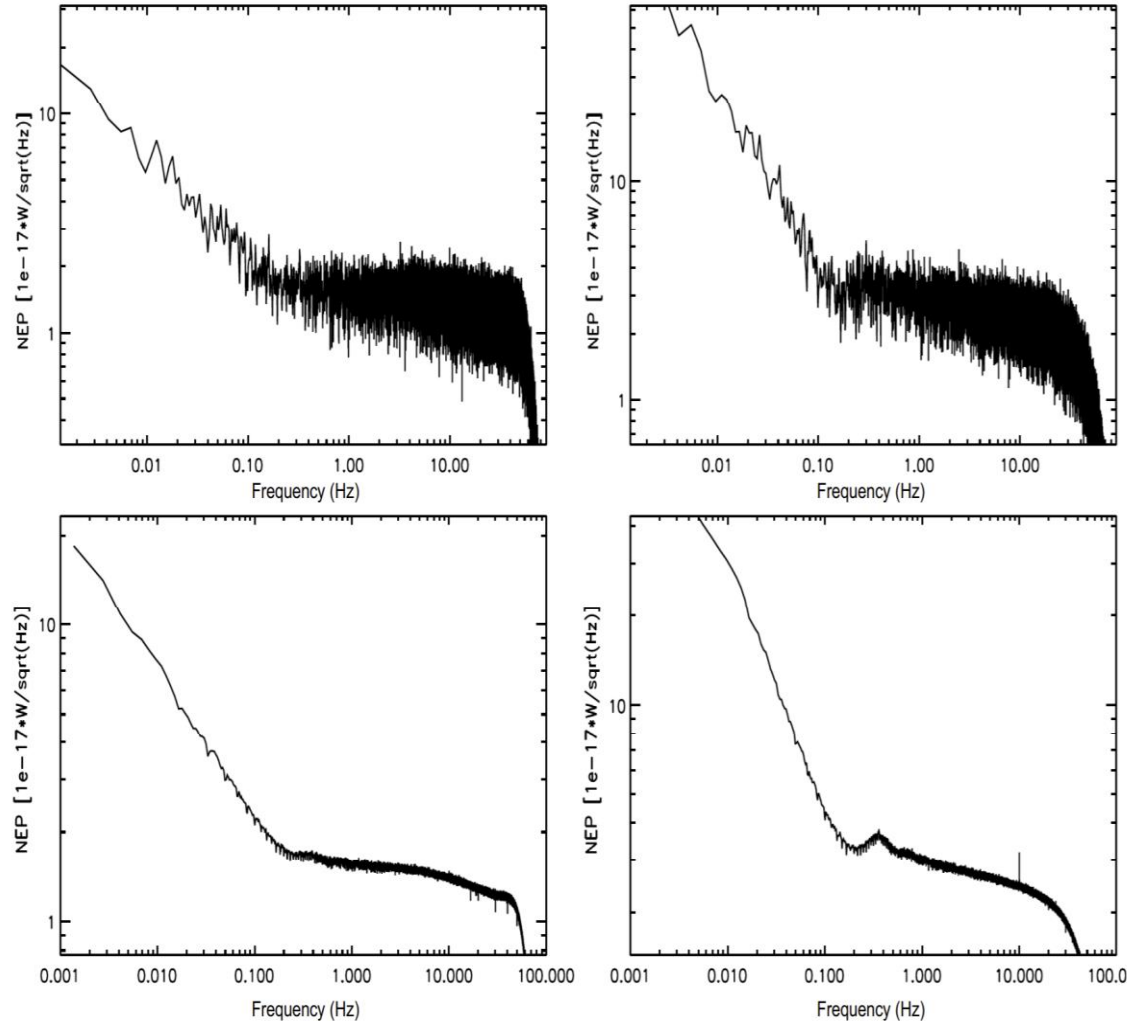


**Fig. 14.** Typical power spectrum amplitude of bolometers 143-5 and 545-2. For the upper panels, this is the power spectrum density of valid samples, after an average ring (the sky signal) has been subtracted from the TOI. Stacking of the result for 200 rings is shown in the lower panel. Here, the instrument time response is not deconvolved from the data.

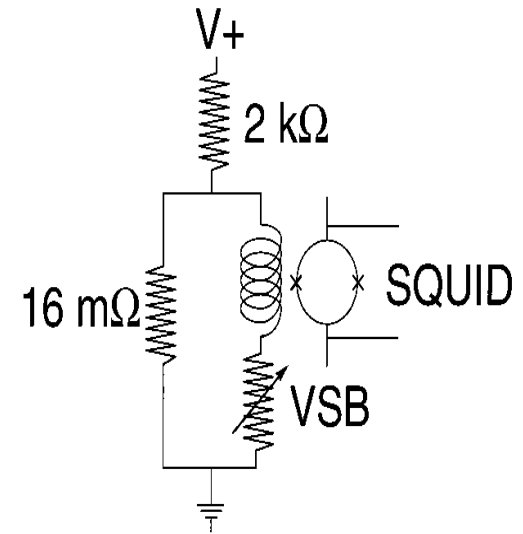
TES technology is best suited for large arrays

In a voltage-biased bolometer, a high value for  $\alpha$  (which is  $>0$  for TES) would induce a large change in the bias power when radiation hits the detector (electrothermal feedback)

One can feedback the bolometer so that its temperature is kept constant, and the bias power required to keep the temperature constant is monitored.

This method (extreme electrothermal feedback) results in a large reduction of the time constant and in the stabilization of the responsivity.

# Cryogenic Bolometers: TES



# Voltage-Biased Superconducting Bolometers

- Have very low R, so work better at constant voltage. Lets' write in detail the equations:

$$P + \frac{V_b^2}{R} = \bar{G}(T - T_o)$$

$$P + \delta P e^{i\omega t} + \frac{V_b^2}{R} + \delta \left[ \frac{V_b^2}{R} \right] = \bar{G}(T + \delta T e^{i(\omega t + \varphi)} - T_o) + \frac{dQ}{dt}$$

$$\Rightarrow \delta P e^{i\omega t} + \delta \left[ \frac{V_b^2}{R} \right] = \bar{G} \delta T e^{i(\omega t + \varphi)} + C \frac{d}{dt} [\delta T e^{i(\omega t + \varphi)}]$$

$$\delta P e^{i\omega t} + V_b^2 \frac{d}{dR} \left[ \frac{1}{R} \right] \frac{dR}{dT} \delta T e^{i(\omega t + \varphi)} = \bar{G} \delta T e^{i(\omega t + \varphi)} + C i \omega \delta T e^{i(\omega t + \varphi)}$$

$$\delta P - \frac{V_b^2}{R} \left[ \frac{T}{R} \frac{dR}{dT} \right] \frac{\delta T}{T} e^{i\varphi} = \bar{G} \delta T e^{i\varphi} + C i \omega \delta T e^{i\varphi}$$

$$\delta P = \left[ \frac{P\alpha}{T} + \bar{G} + C i \omega \right] \delta T e^{i\varphi} \Rightarrow \delta T = \frac{e^{-i\varphi}}{\frac{P\alpha}{T} + \bar{G} + C i \omega} \delta P$$



# Voltage-Biased Superconducting Bolometers

$$\delta P = \left[ \frac{P\alpha}{T} + \bar{G} + Ci\omega \right] \delta T e^{i\varphi} \Rightarrow \delta T = \frac{e^{-i\varphi}}{\frac{P\alpha}{T} + \bar{G} + Ci\omega} \delta P$$

- The effective thermal conductivity is

$$G_{eff} = \frac{P\alpha}{T} + \bar{G} + i\omega C$$

- The first part is the Electro-Thermal Feedback (ETF) part.
- When  $\delta P$  increases (a signal arrives)  $T$  increases; this increases the resistance which in turns decreases the bias power  $P_b = V_b^2/R$ . As a result the total power ( $P + P_b$ ) does not decrease as much, and the temperature does not change much.
- For a given incoming power, the ETF reduced the temperature change.
- It is the reverse of what happens in a semiconductor bolometer, where the negative  $\alpha$  produces a negative ETF, increasing the temperature change.
- But here we measure the bias *current* at constant voltage. The current needed to keep the bias more stable is increased by the ETF. So we define

$$L(\omega) = \frac{\frac{P\alpha}{T}}{\bar{G} + i\omega C} = \frac{\frac{P\alpha}{T\bar{G}}}{1 + i\omega \frac{C}{\bar{G}}} = \frac{L}{1 + i\omega\tau_o}$$

# Voltage-Biased Superconducting Bolometers

- The Responsivity is

$$\mathfrak{R} = \frac{\delta i_b}{\delta P} = \frac{\delta(V_b / R)}{\delta P} = -\frac{V_b \delta R}{R^2 \delta P} = -\frac{1}{V_b} \frac{V_b^2}{R} \frac{1}{R} \frac{\delta R}{\delta P} = -\frac{1}{V_b} \frac{P_b \alpha}{T} \frac{\delta T}{\delta P}$$

- And using

$$\delta T = \frac{e^{-i\varphi}}{\frac{P\alpha}{T} + \bar{G} + Ci\omega} \delta P \Rightarrow \frac{\delta T}{\delta P} = \frac{e^{-i\varphi}}{\frac{P\alpha}{T} + \bar{G} + Ci\omega} = \frac{e^{-i\varphi}}{\bar{G}(1+L+i\omega\tau_o)}$$

- We get

$$\mathfrak{R} = -\frac{1}{V_b} \frac{P_b \alpha}{T} \frac{\delta T}{\delta P} = -\frac{1}{V_b} \frac{P_b \alpha}{T} \frac{e^{-i\varphi}}{\bar{G}(1+L+i\omega\tau_o)} = -\frac{1}{V_b} \frac{L e^{-i\varphi}}{(1+L+i\omega\tau_o)}$$

- Defining

$$\tau = \frac{\tau_o}{L+1}$$

- We get

$$\mathfrak{R} e^{i\varphi} = -\frac{1}{V_b} \frac{L}{(1+L)} \frac{1}{1+i\omega\tau}$$

For large ETF ( $L \gg 1$ ):

- the time constant is reduced wrt the standard one by  $L+1$
- For slow signals ( $\omega \ll 1/\tau$ ) and large ETF the responsivity is simply  $-1/V_b$

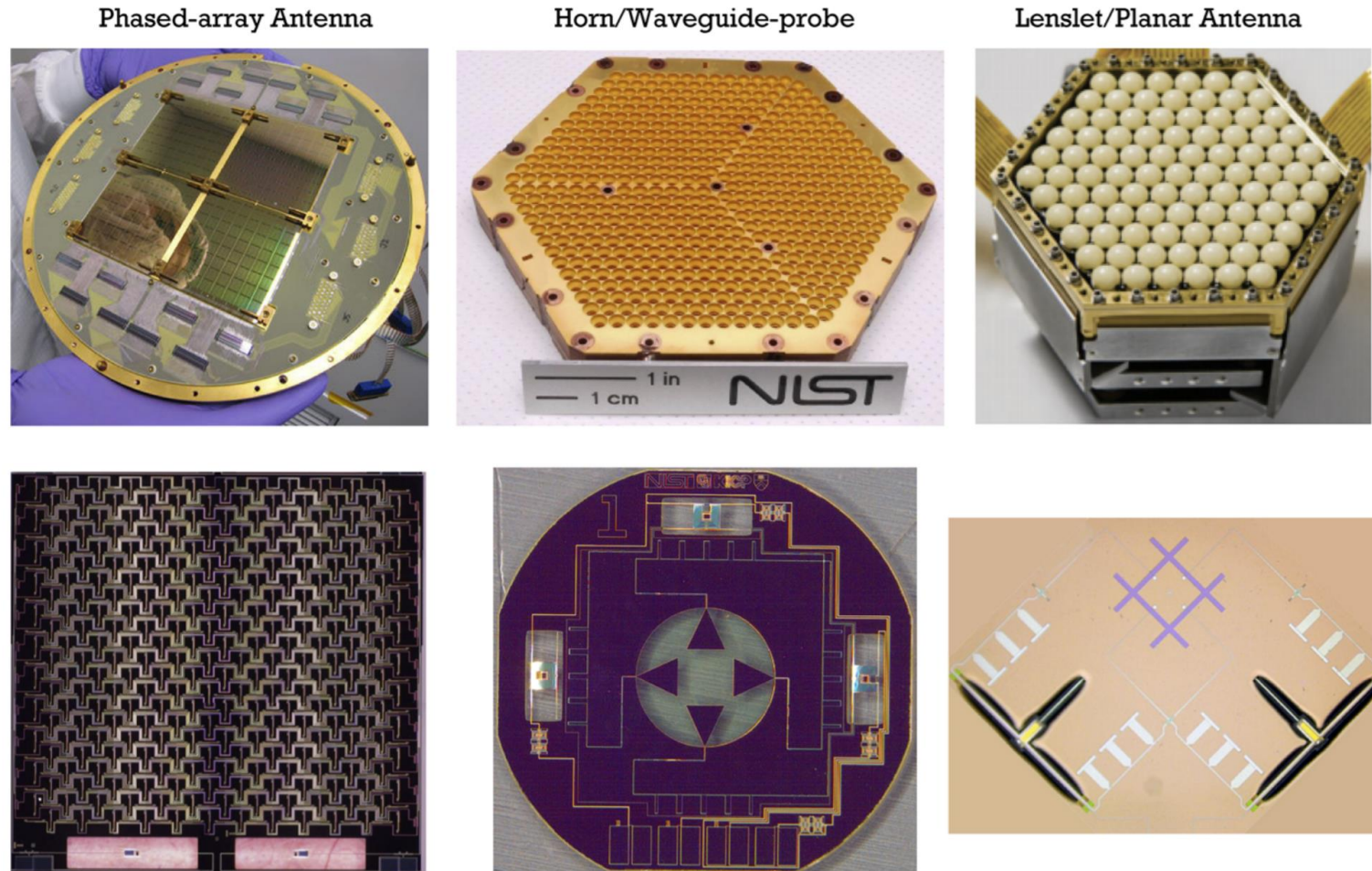


**Fig. 3** Superconducting ICs used for the CMB power spectrum measurements presented in Fig. 1. The top row shows the coupling technology, and the bottom shows the pixel IC. Left: Phased antenna arrays developed at Caltech/JPL [34,35]. In this architecture, the beam is formed on-chip by the phased array, and thus, a flat antireflection wafer serves as the only off-detector-wafer focal plane optical coupling component. Center: Feedhorn/waveguide-probe-coupled detectors using silicon feedhorns (pictured) have been developed at NIST [36]. An alternative probe-coupled detector design (not pictured) has been developed at NASA/Goddard [37]. Right: Lenslet/planar antenna arrays have been developed at UC, Berkeley [38]. In this case, the antenna gain is increased with an extended hemispherical lenslet (color figure online)

Antenna coupled multichroic pixels to increase the density of bolometers in the focal plane

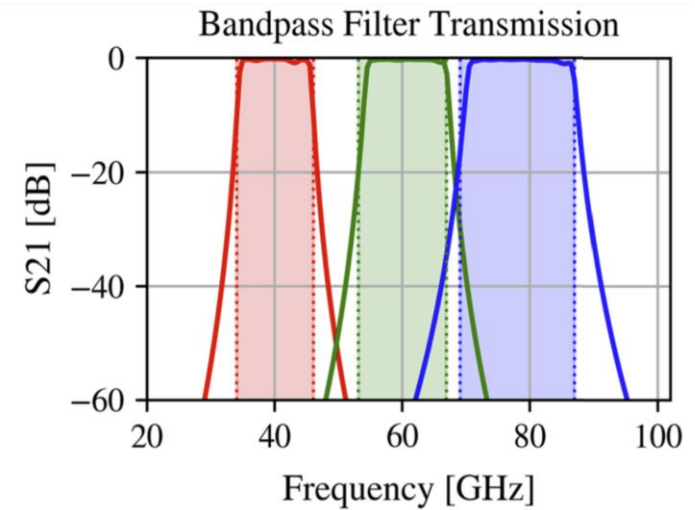
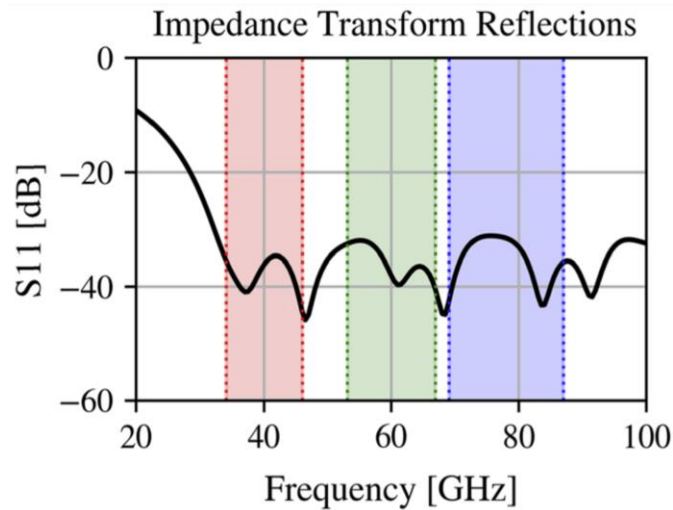


**Fig. 3** **a** LF-1 prototype pixel with sinuous antenna in the center, the microstrip transmission line is routed between antenna arms, bandpass filters with mitered stubs surround the antenna, and the bolometers appear as rectangles. **b** Antenna feedline coupling with line widths at the center of  $600 \pm 50$  nm. **c** The bolometer island with TES in the center, thermal ballast on the lower half of the island, readout wires routed to the lower right split the ballast, and antenna feedlines in the upper left and right lead to the load resistor above the TES (Color figure online)

*The alternative for large arrays :*

## *Kinetic Inductance Detectors (KIDs)*

### *Main characteristics:*

- ◆ Intrinsically multiplexable
- ◆ order of  $10^2$ - $10^3$  pixels read with a single coaxial cable
- ◆ *Extremely simple cold electronics:* one single LNA can be used for  $10^2$ - $10^3$  pixels. The rest of the readout is warm.
- ◆ *Ease of fabrication:* one single layer of material is needed.
- ◆ *Very flexible:* different materials and geometries can be chosen to tune detectors to specific needs.
- ◆ *Very resistant:* materials are all suitable for satellite and space missions.

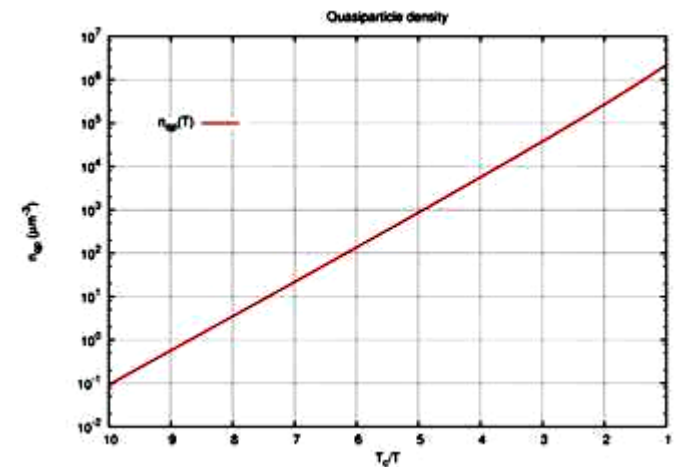
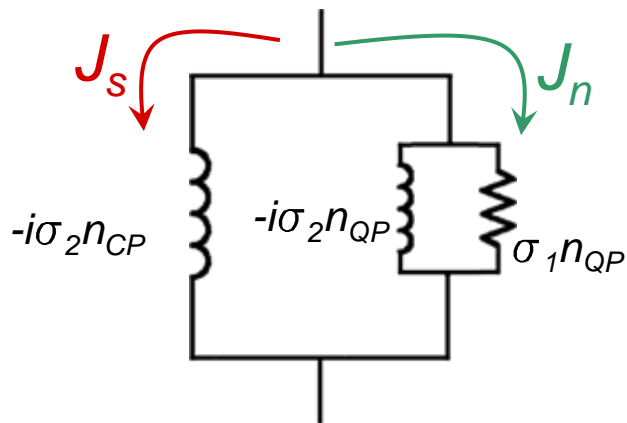
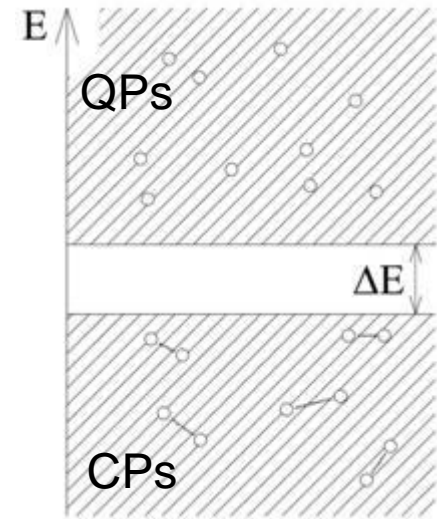
# KIDs working principle: meV photons can still break Cooper pairs

In a superconductor film below  $T_c$ , electrons can bind to form CPs with binding energy  $E=2\Delta = 3.5*k_bT_c$ .

The CPs have zero DC resistance, but the reactance is non-zero and has two distinct contribution  $\rightarrow$  *kinetic* and *magnetic L*.

The total conductivity of the material can be estimated using the *two-fluid model*

The values of  $\sigma_s$  and  $\sigma_n$  depend on the densities of QPs and CPs. By measuring them, we can get information on  $n_{qp}$ .

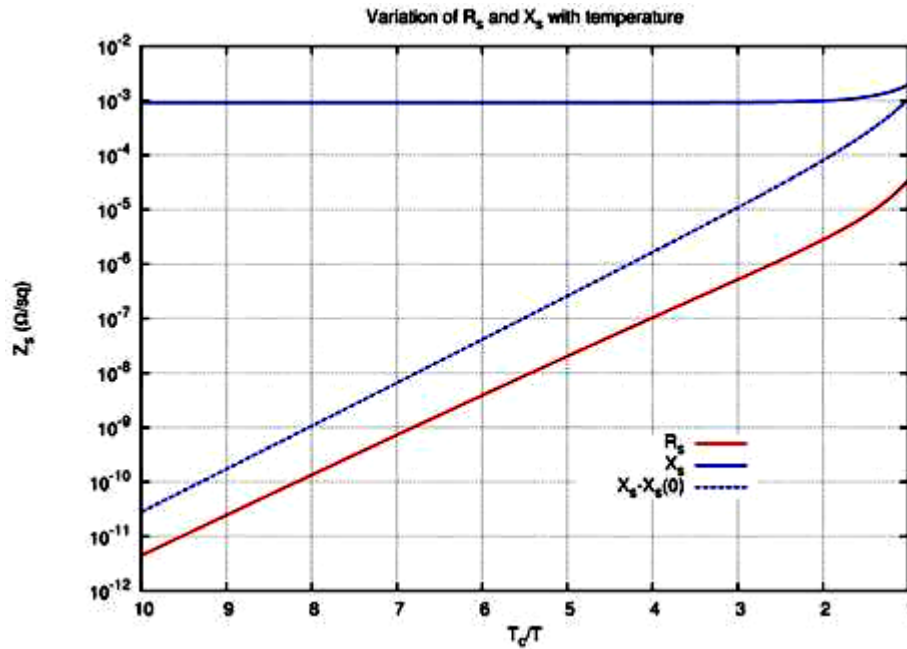


# A better theory...

A better estimate of  $\sigma_s$  and  $\sigma_n$  is obtained using the Mattis Bardeen integrals:

$$\frac{\sigma_2}{\sigma_n} = \frac{1}{\hbar\omega} \int_{\Delta-\hbar\omega}^{\Delta} d\epsilon \frac{[1 - 2f(\epsilon + \hbar\omega)] (\epsilon^2 + \Delta^2 + \hbar\omega\epsilon)}{\sqrt{\Delta^2 - \epsilon^2} \sqrt{(\epsilon + \hbar\omega)^2 - \Delta^2}}$$

$$\frac{\sigma_1}{\sigma_n} = \frac{2}{\hbar\omega} \int_{\Delta}^{\infty} d\epsilon \frac{[f(\epsilon) - f(\epsilon + \hbar\omega)] (\epsilon^2 + \Delta^2 + \hbar\omega\epsilon)}{\sqrt{\epsilon^2 - \Delta^2} \sqrt{(\epsilon + \hbar\omega)^2 - \Delta^2}}$$



Note that:

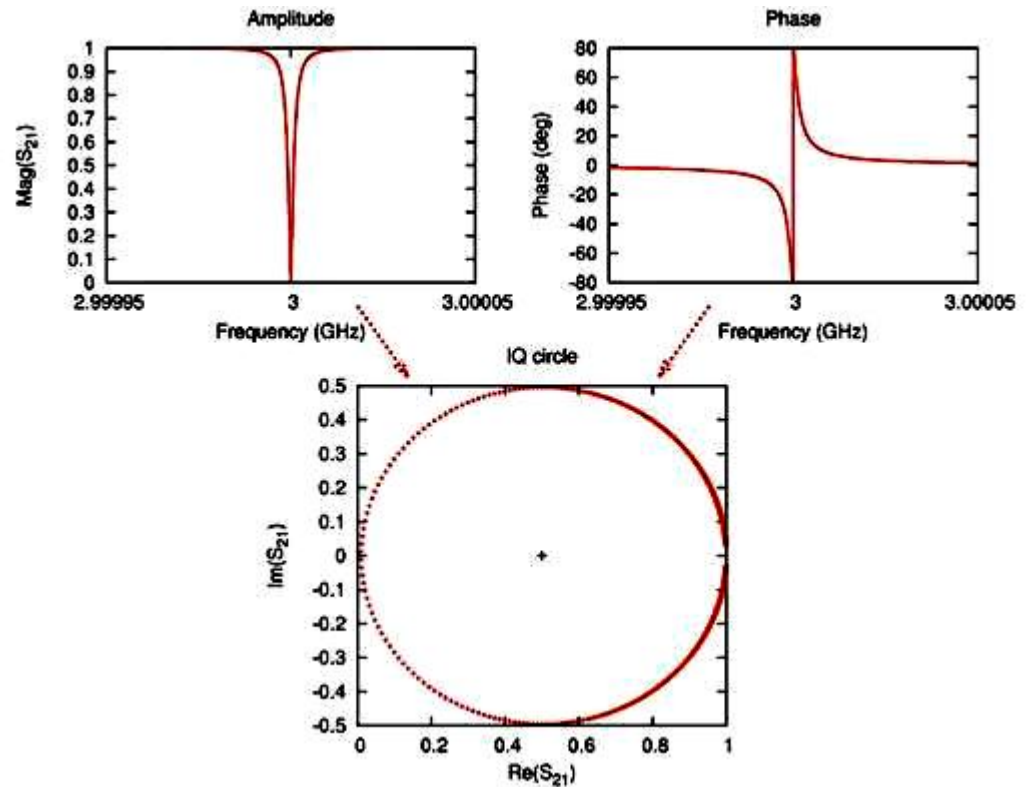
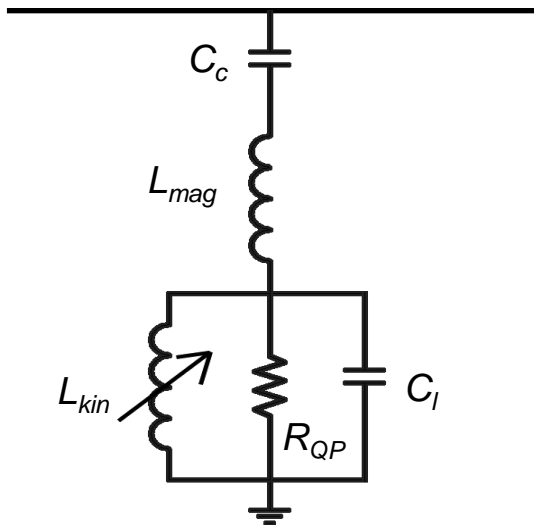
- $R_s$  decreases exponentially
- $X_s$  becomes constant
- $X_s / R_s$  grows exponentially

# How can we measure the small variations of $L_k$ ?

The superconductor can be inserted in a resonating circuit with extremely high Q, since:

$$Q \propto X_s / R_s$$

The resonator is extremely simple to do, and consists of a shorted length of superconducting line capacitively coupled to the feedline  $\longrightarrow$   $\lambda/4$  resonator



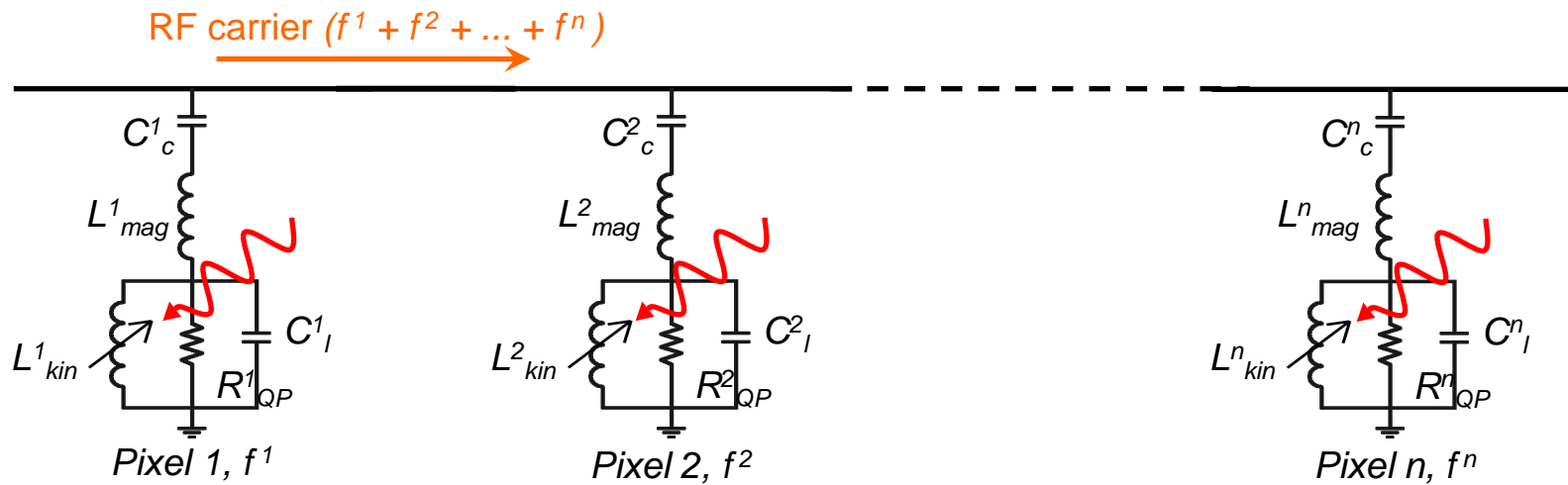


# Multiplexing

KIDs are *intrinsically* multiplexable:

- Unitary transmission off resonance
- Q values very large ( $\sim 10^5$ )

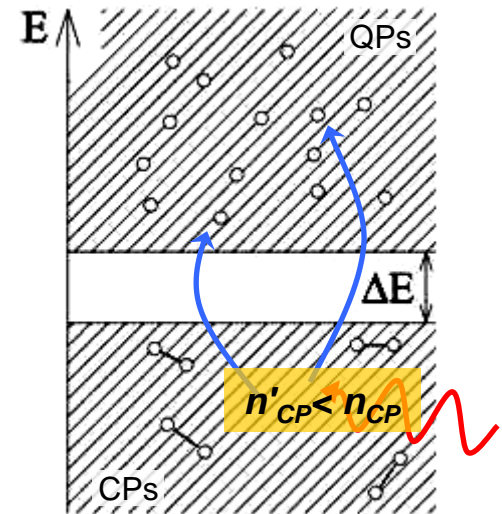
Each resonator acts at the same time as *detector* and *filter*



*One single amplifier needed!*

# How do we actually measure the incoming radiation?

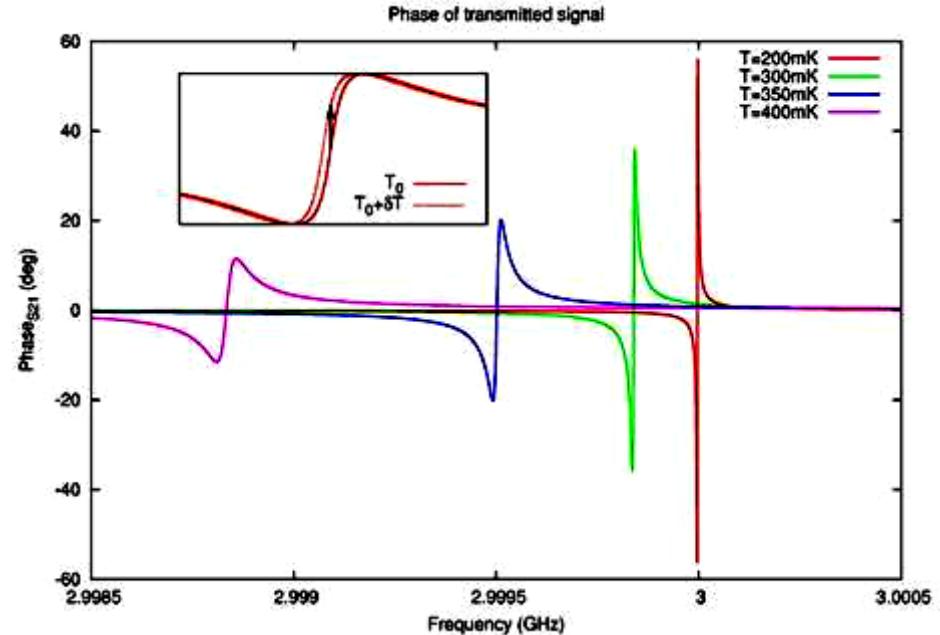
- Suppose a photon hits the detector
- If its energy is high enough ( $h\nu > 2\Delta E$ ) it can break CPs
- The density of CPs therefore changes
- This leads to a variation of  $L_{kin}$



The same effect as an increase of the temperature of the superconductor

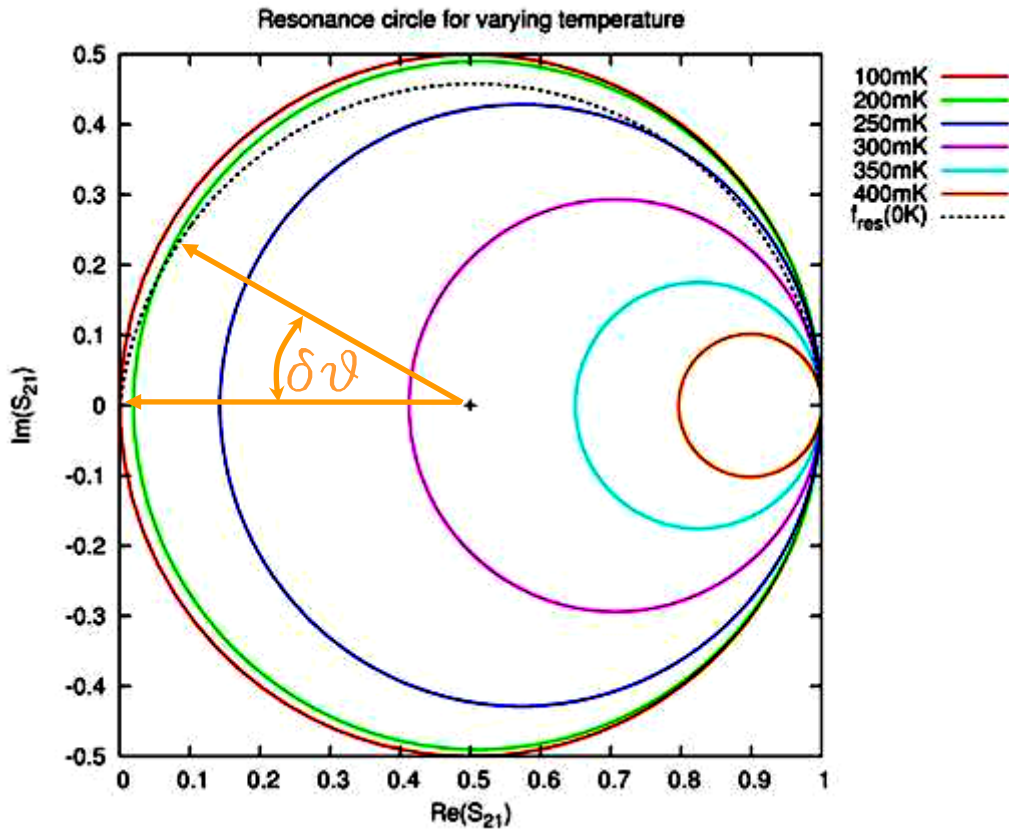
The readout is accomplished by monitoring the phase of the transmitted signal

$$f_0 \propto 1/\sqrt{L}$$



# Readout technique

Usually the phase is redefined and referred to the center of the resonance circle:



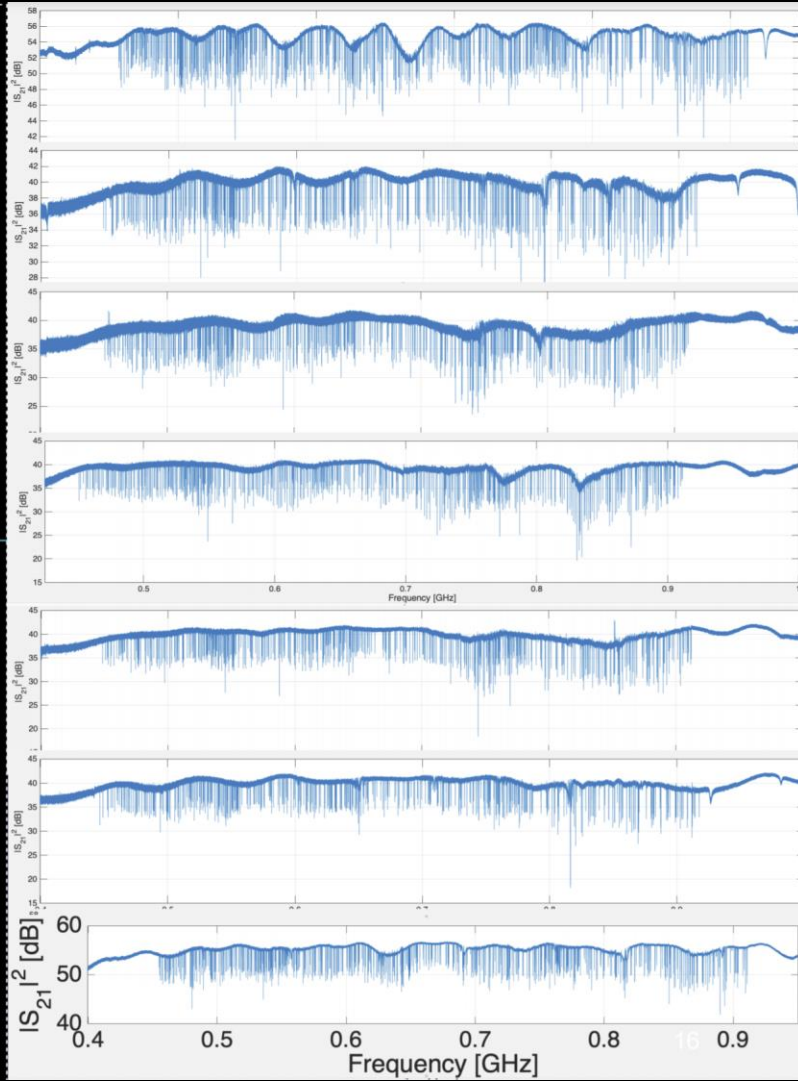
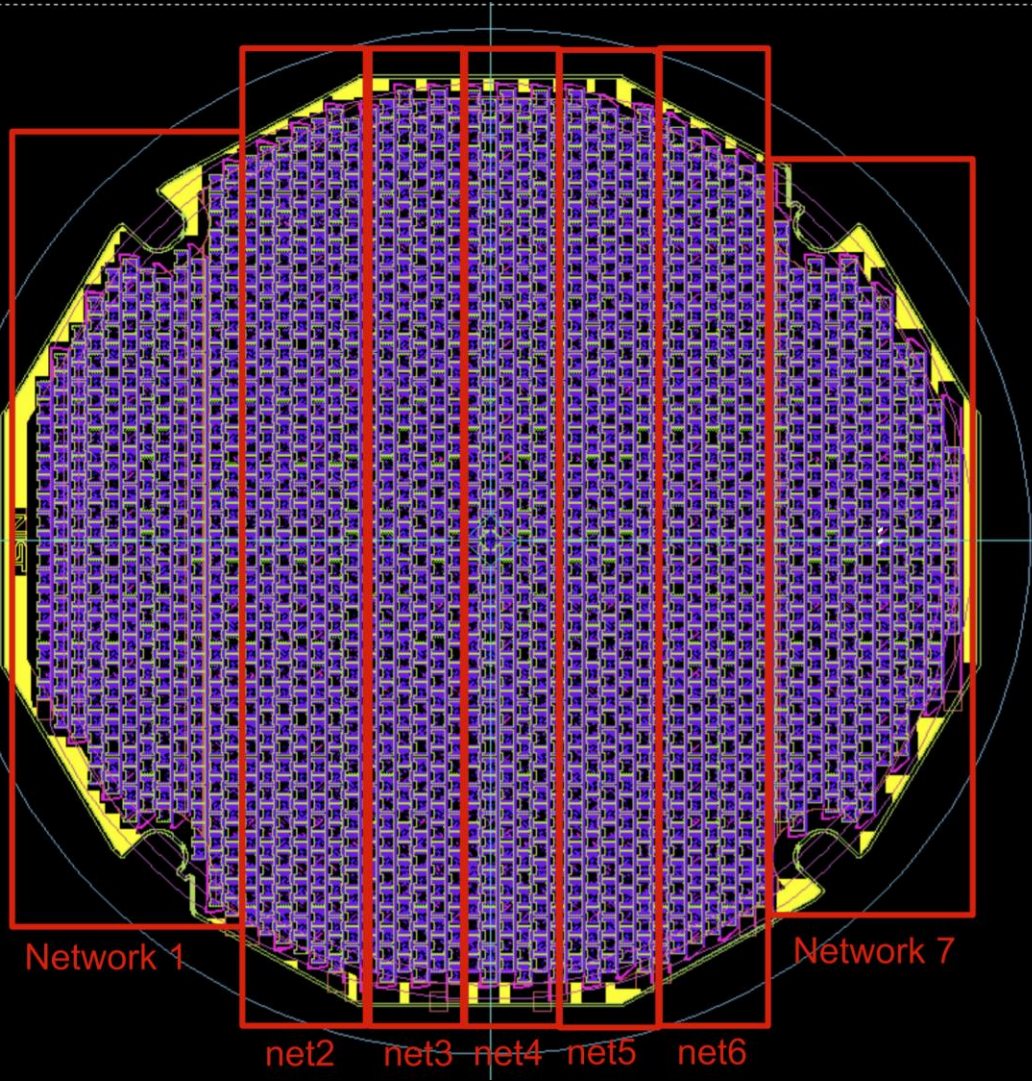
This kind of plots can give all the information regarding resonator parameters

It is also the basis for actual measurements of radiation

Remember that:

$$\frac{\delta \vartheta}{\delta T} \longleftrightarrow^{n_{QP}(T)} \frac{\delta \vartheta}{\delta n_{QP}}$$

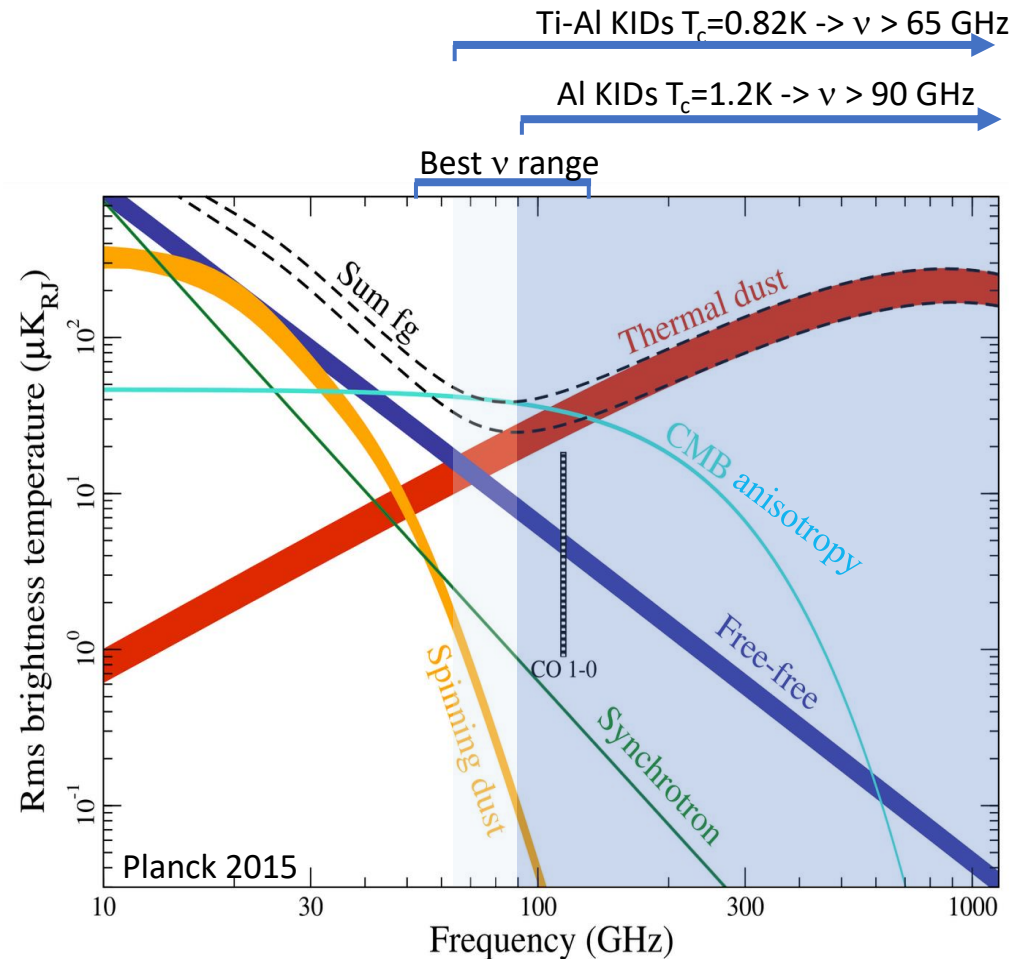
# Resonators can be arranged in large arrays



# KIDs for the CMB

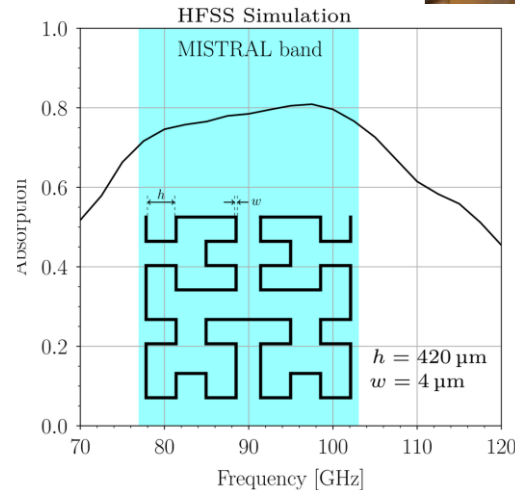
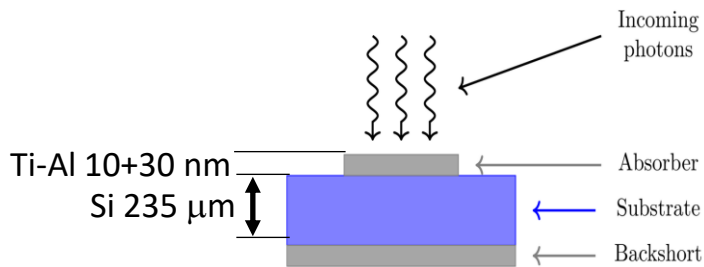
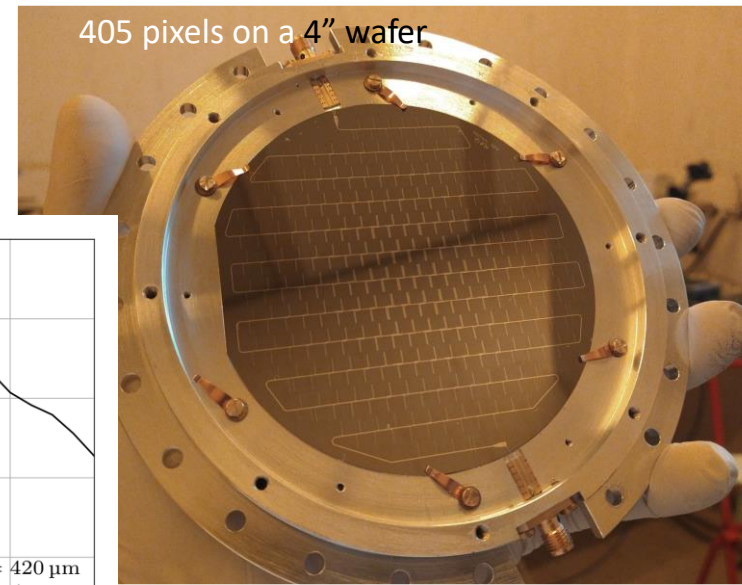
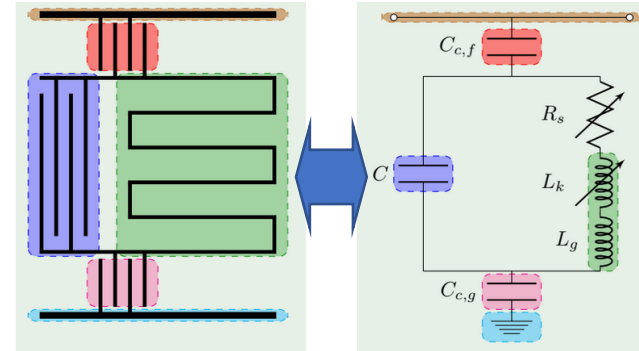
KIDs are currently used and/or under development for CMB-related science, in several ground-based and balloon-borne experiments:

- Ground-based: NIKA2 @IRAM, GroundBIRD, KISS, CONCERTO @APEX, MISTRAL @SRT, MUSCAT, ToITEC, CCAT-Prime and COSMO.
- Balloon-borne: OLIMPO, BLAST-TNG and EXCLAIM.
- Aluminum KIDs are well suited for mid-high frequencies.
- Low-frequencies coverage requires low  $T_c$  film material (e.g. Ti-Al) and low physical temperature of the sensor ( $T < 0.2 T_c$ ), or thermal KIDs.
- The latter are bolometers where the thermometer is a KID: the absorption function is separated from the detection function. At the cost of a slower response and a complex fabrication, one can relax the requirement of a very low operation temperature for low frequency detection. See e.g. L. Minutolo et al., IEEE Trans. Appl. Superconductivity, 31, 1-4 (2021)



# KIDs for the W-band: MISTRAL@SRT

- We have developed LEKIDs for the W-band (75-115 GHz). Due to the low-frequency, we used a Ti-Al bilayer superconducting film ( $T_c=0.82\text{K}$ )
- In the Lumped Elements Kinetic Inductance Detectors (LEKID) the inductor of the LC resonator is shaped and dimensioned to act also as the absorber of incoming photons.
- In particular, in MISTRAL and other receivers we have used a Hilbert shape for the inductor, optimized to efficiently and equally absorb W-band photons with both polarizations:



credit: G. Pettinari IFN-CNR

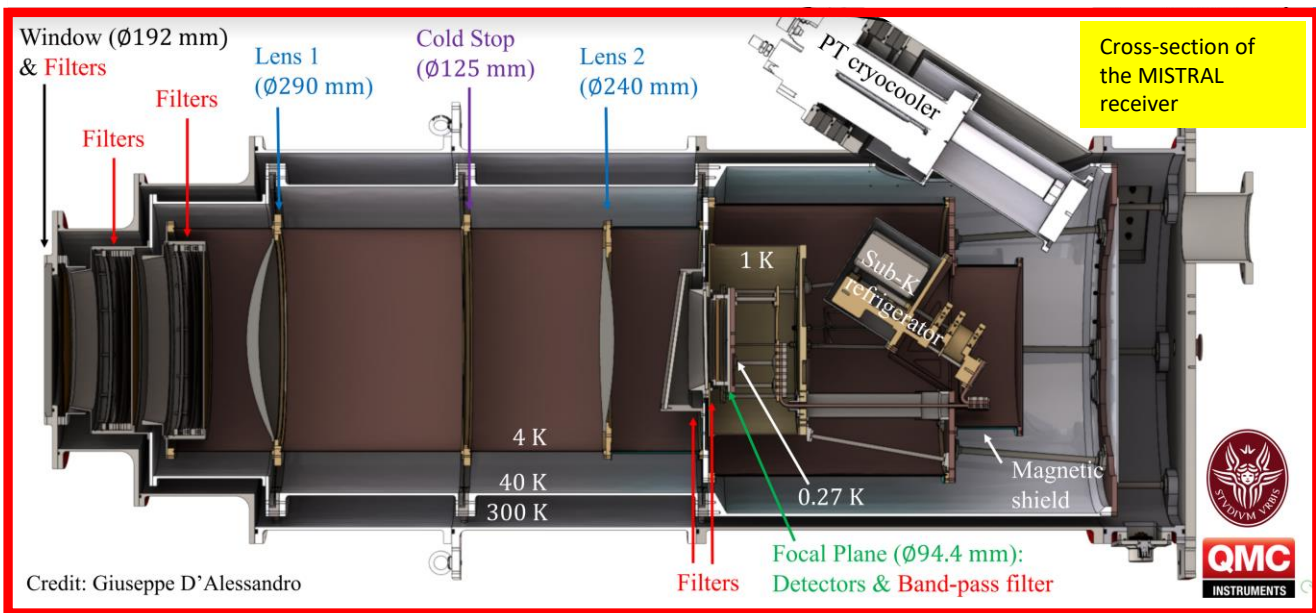
Courtesy: A. Paiella, Sapienza, see also:  
 Paiella A., et al., 2016, JLTP, 184, 97-102  
 A. Coppolecchia, A. Paiella, et al., 2020, JLTP, 199, 130-137  
 A. Paiella et al. "MISTRAL and its KIDs"; LTD19, 2021, JLTP in press

# KIDs for the W-band: MISTRAL@SRT

- This LEKID array is for the MISTRAL (*Millimetric Sardinia radio Telescope Receiver based on Array of Lumped element KIDs*) receiver at the Sardinia Radio Telescope, and is operated at 0.27 K in a custom cryogenic system, mounted on the rotating multi-receiver platform at the Gregorian focus of the telescope.
- The cryostat is based on a pulse-tube and a  $^3\text{He}$  evaporation sub-K refrigerator, and also includes the filters set, defining a 77-103 GHz bandwidth, the reimaging optics, and an absorbing cold stop to limit spillover radiation.
- The expected performance is photon-noise limited for  $T_n=30\text{K}$  in W-band.
- The receiver will be available to the community through observation proposals runs. The main scientific targets are the search for CMB Sunyaev-Zeldovich signals from galaxy clusters, the study of high frequency radio sources, and the study of the continuum emission of the interstellar medium.
- A polarization-sensitive extension with the addition of a polarization modulator is under study.



The Sardinia Radio Telescope



# KIDs arrays recently qualified in near space

## Kinetic Inductance Detectors for the OLIMPO experiment: in-flight operation and performance

S. Masi<sup>1,2</sup>, P. de Bernardis<sup>1,2</sup>, A. Paiella<sup>1,2</sup>, F. Piacentini<sup>1,2</sup>, L. Lamagna<sup>1,2</sup>, A. Coppolecchia<sup>1,2</sup>, P.A.R. Ade<sup>3</sup>, E.S. Battistelli<sup>1,2</sup>, M.G. Castellano<sup>4</sup>, I. Colantoni<sup>4,5</sup> + Show full author list

Published 1 July 2019 • © 2019 IOP Publishing Ltd and Sissa Medialab

[Journal of Cosmology and Astroparticle Physics](#), Volume 2019, July 2019

Citation S. Masi *et al* JCAP07(2019)003

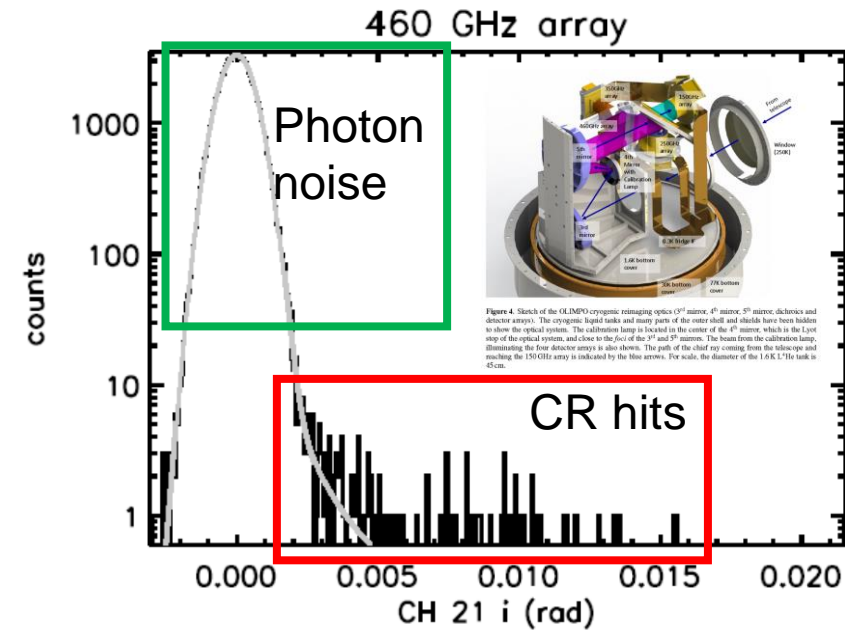
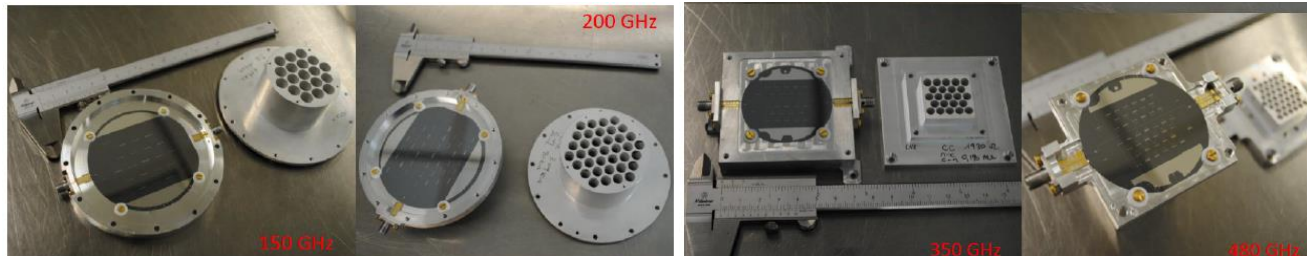
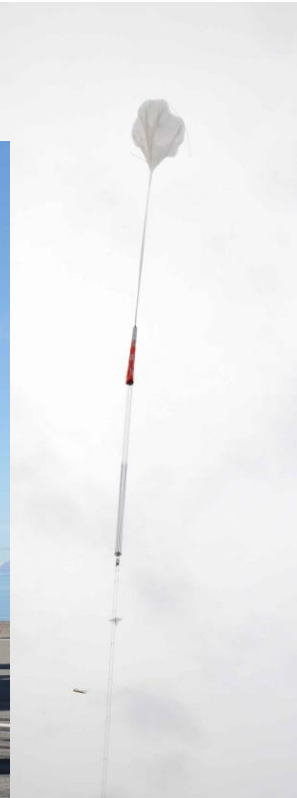


Figure 4. Sketch of the OLIMPO cryogenic retaining optics (9<sup>th</sup> mirror, 4<sup>th</sup> mirror, 5<sup>th</sup> mirror, dichroics and detector arrays). The cryogenic liquid tanks and many parts of the outer shell and shields have been hidden to show the optical system. The calibration lamp is located in the center of the 4<sup>th</sup> mirror, which is the 1<sup>st</sup> eye of the optical system, and close to the foot of the 3<sup>rd</sup> and 5<sup>th</sup> mirrors. The beam from the calibration lamp, illuminating the four detector arrays is also shown. The path of the chief ray coming from the telescope and reaching the 150 GHz array is indicated by the blue arrows. For scale, the diameter of the 1.6 K LHe tank is 45 cm.



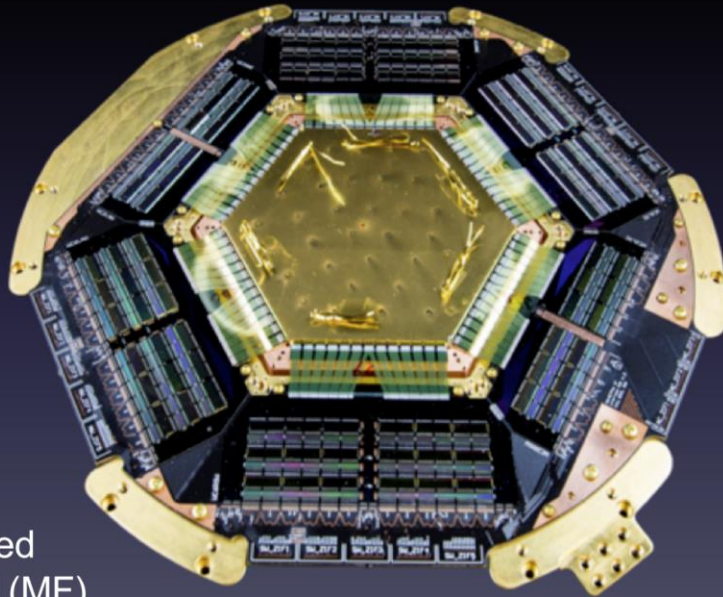


# Focal plane complexity comparison

## TES

Deployed TES ARRAY (~ 2000 Detectors)

- 1000's wire bonds
- 1000's SQUID amplifiers
- hundreds of additional SC components
- dozens of cables



Advanced  
ACTPoI (MF)

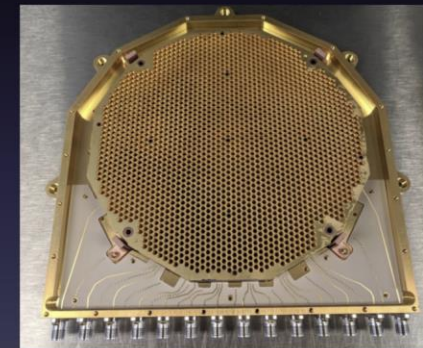
## MKID

Integrated readout

e.g. Toltec MKID (4000 detectors)

- 14 wire bonds
- 14 Coax cables
- 7 LNAs (at 4K stage)

(Shown at same scale)



Toltec 1.1 mm

Measurements of the  
spectrum (specific brightness)  
of the CMB

# Specific Brightness Measurements ?

- Let's see how we can use a bolometer or a KID, which are sensitive to all frequencies, to measure the specific brightness (the spectrum) of the cosmic microwave background.
- We couple the detector with a spectrometer, and in particular with a *Differential* Fourier Transform Spectrometer.
- But first of all, let's see which are the orders of magnitude of the observables and how they compare to the noise.

# Orders of magnitude

- The total CMB brightness is :

$$B(2.725K) = \int_0^{\infty} \frac{2h}{c^2} \frac{\nu^3}{e^x - 1} d\nu = 1.0 \times 10^{-10} W/cm^2 sr$$

- Over a band 120-170 GHz (one of the atmospheric «windows» where Earth's atmosphere is transparent, at least in dry, high-altitude sites) the integrated CMB brightness is :

$$B'(2.725K) = \int_{120GHz}^{170GHz} \frac{2h}{c^2} \frac{\nu^3}{e^x - 1} d\nu = 1.9 \times 10^{-11} W/cm^2 sr$$

- Typical throughput of a *single-mode* receiver in the same band is  $A\Omega \sim \lambda^2 \sim 0.05 cm^2 sr$ , with a typical detector efficiency of  $e=30\%$  and a typical atmospheric transmission of  $t=80\%$ ; so that the power collected is  $P = teA\Omega B' = 1.9 \times 10^{-13} W$

- With a detector NEP of  $\sim 10^{-17} W/\sqrt{Hz}$  the Signal to Noise ratio  $S/N$  for the measurements would be very high:

$$\frac{S}{N} = \frac{P}{\sigma_{\langle W \rangle_t}} = \frac{P\sqrt{t}}{NEP} = 19000\sqrt{t(s)}$$

- However, there are other important noise sources: fluctuations from the optics and the atmosphere, system instability .... Anyway, very *sensitive* measurements of CMB brightness are possible.

# Orders of magnitude

- Moreover, if we are interested to *spectral* measurements, we want to measure the brightness in many narrow bands, so that we can check e.g. if the CMB is a blackbody or if there are deviations (which would be very interesting for cosmology).

- Over a 1 GHz frequency bin e.g. around 140 GHz, the integrated CMB brightness is :

$$B''(2.725K) = \int_{139.5GHz}^{140.5GHz} \frac{2h}{c^2} \frac{v^3}{e^{x-1}} dv = 3.4 \times 10^{-13} W/cm^2 sr$$

- In this case, the power collected becomes  $P'' = teA\Omega B'' = 3.7 \times 10^{-15} W$

- With a detector NEP of  $\sim 10^{-17} W/\sqrt{Hz}$  the  $S/N$  for the measurement of this spectral bin would be much smaller than in the previous wide-band example, but still very good:

$$\frac{S}{N} = \frac{P''}{\sigma_{\langle W \rangle_t}} = \frac{P''\sqrt{t}}{NEP} = 920\sqrt{t(s)}$$

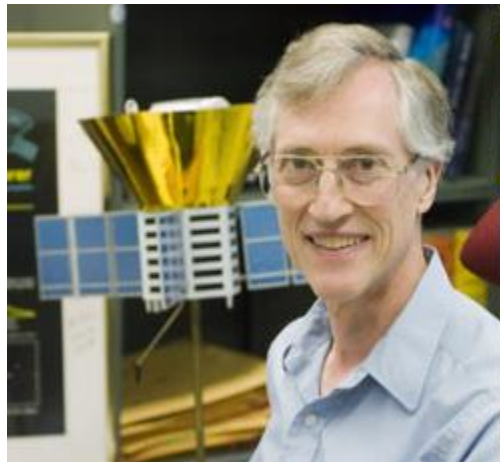
- In a dispersion instrument, like the diffraction-grating spectrometer, one measures sequentially all the 1 GHz spectral bins from say 30 GHz to 600 GHz. This requires a long measurement time to cover the entire spectral range of interest for the CMB.
- For this spectral range, a very competitive spectrometer is the Fourier Transform Spectrometer (FTS), where all the spectral bins are measured simultaneously, and, if detectors noise is dominating over photon noise, there is a measurement efficiency advantage. COBE-FIRAS (Nobel prize 2006) was a FTS with bolometers.



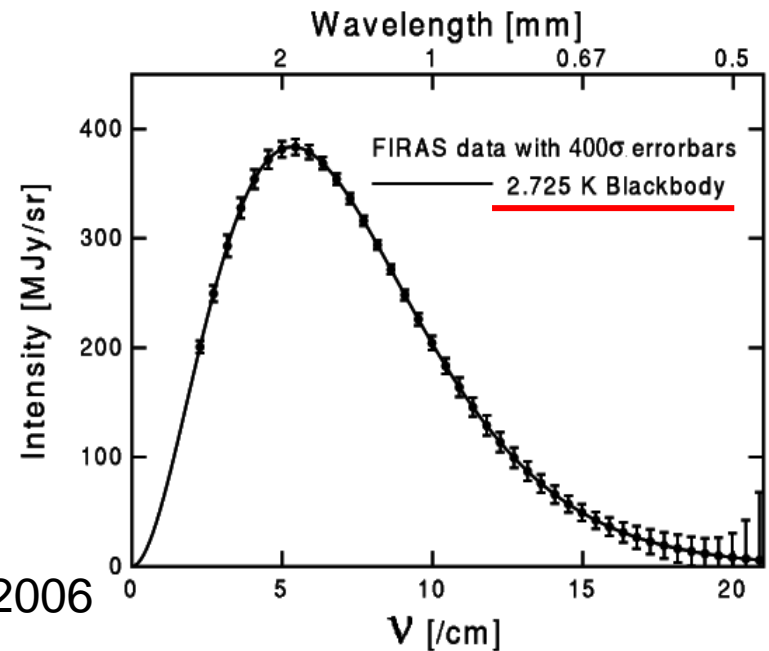
Arno Penzias and Robert Wilson (1965):  
*We get microwaves isotropically from every direction of the sky. It's the Cosmic Microwave Background.*  
 Nobel Prize in Physics, 1977

© 2004 Pearson Education, publishing as Addison Wesley.

F. Melchiorri et al. (high mountain, 1974),  
 .... P. Richards et al. (balloon, 1980) ... and then John Mather et al. (1992) with the FIRAS on the COBE satellite: these microwaves have **exactly** a blackbody spectrum



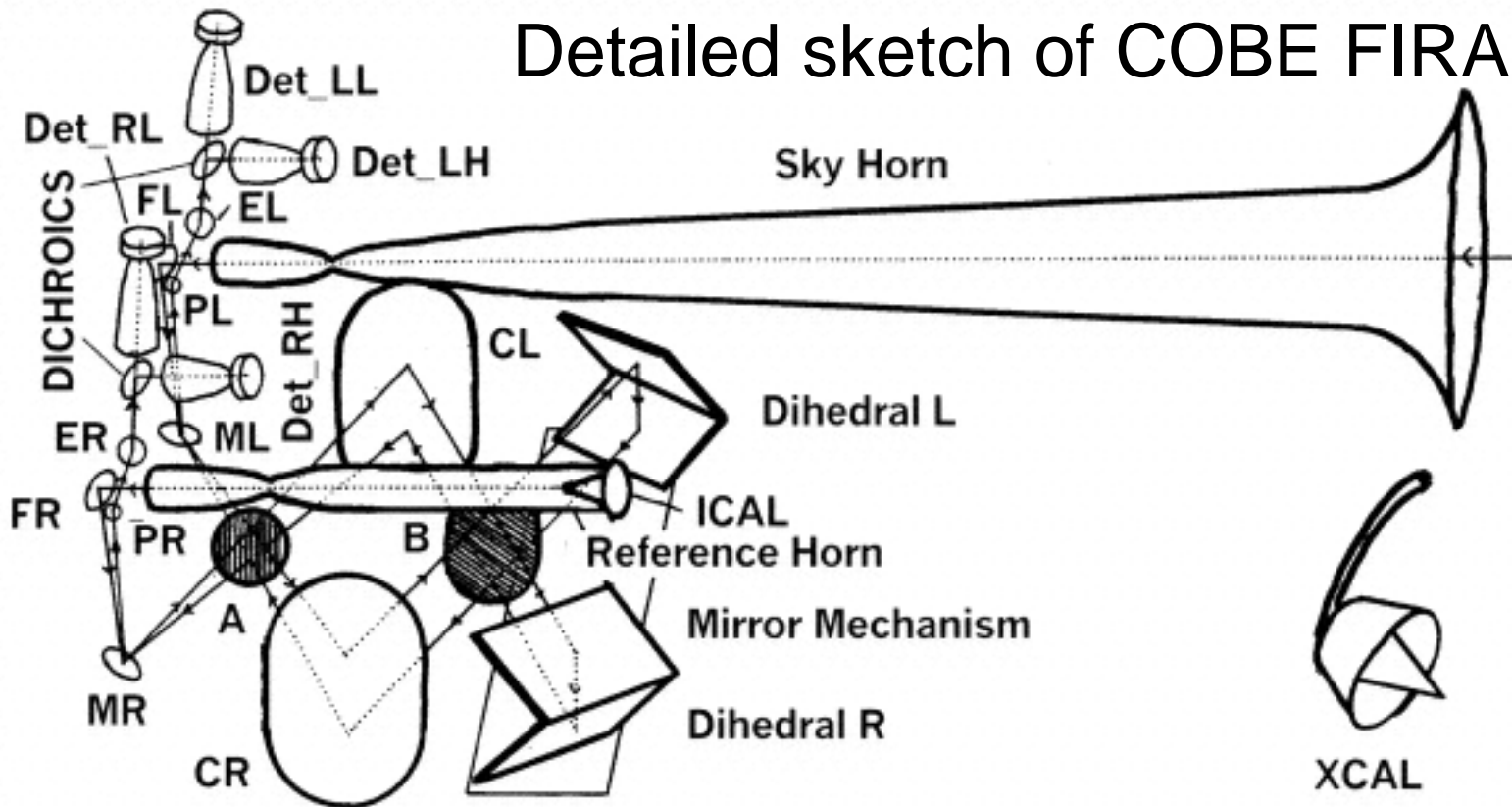
Nobel Prize in Physics, 2006



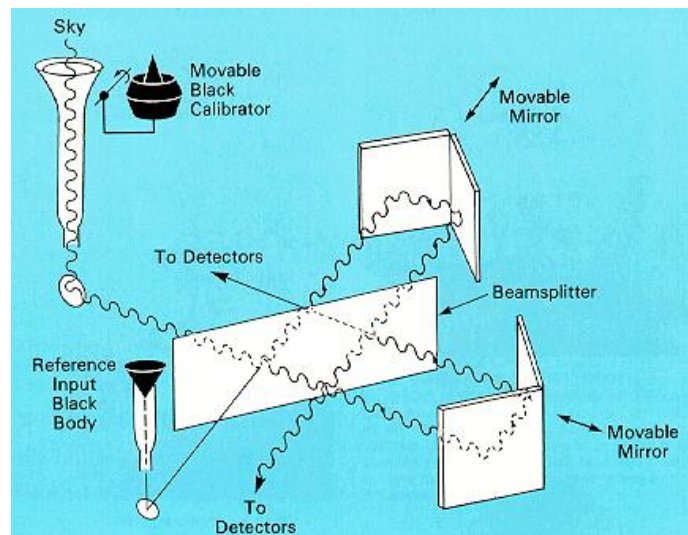
# COBE-FIRAS

- COBE-FIRAS was a particular Fourier-Transform Spectrometer (a Martin-Puplett interferometer, intrinsically differential) using cryogenic bolometers as detectors. It was placed in a 400 km orbit to avoid atmospheric emission.
- A zero instrument comparing the specific sky brightness to the brightness of an internal cryogenic blackbody
- The output was nulled (within detector noise) for  $T_{\text{ref}}=2.725$  K
- The brightness of the empty sky is a blackbody at the same temperature !
- The early universe was in thermal equilibrium at high Temperature.

# Detailed sketch of COBE FIRAS



## Block diagram of COBE FIRAS





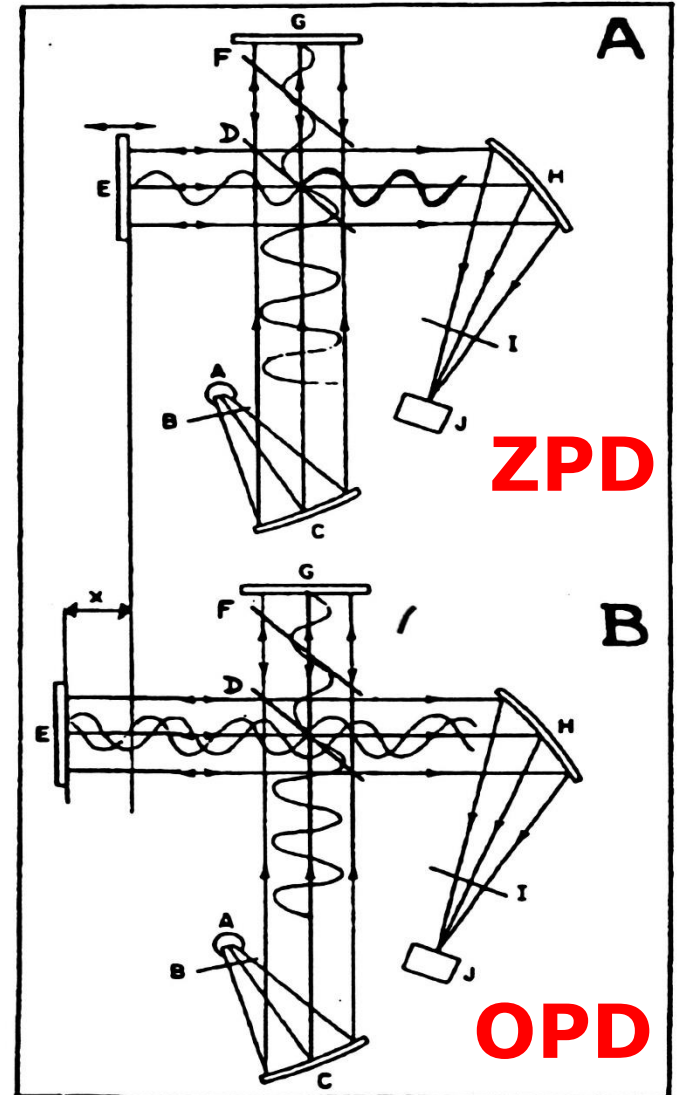
# Elementary theory of the FTS

- The OPD (optical path difference) is  $2x$ .
- For a perfectly monochromatic radiation with wavenumber  $s$  ( $=1/\lambda$ ) the resulting field on the detector will be

$$E(t) = E_o(\sigma)RT(\sigma) \cos(2\pi\sigma ct) + E_o(\sigma)RT(\sigma) \cos(2\pi\sigma ct + 4\pi\sigma x)$$

- Here  $RT$  is the efficiency of the beamsplitter (frequency dependent, in general)

A well-known FTS:  
The Michelson Interferometer



# Elementary theory of the FTS

$$E(t) = E_o(\sigma)RT(\sigma) \cos(2\pi\sigma ct) + E_o(\sigma)RT(\sigma) \cos(2\pi\sigma ct + 4\pi\sigma x)$$

- The power on the detector  $I(x)$  will be proportional to the mean square electrical field:

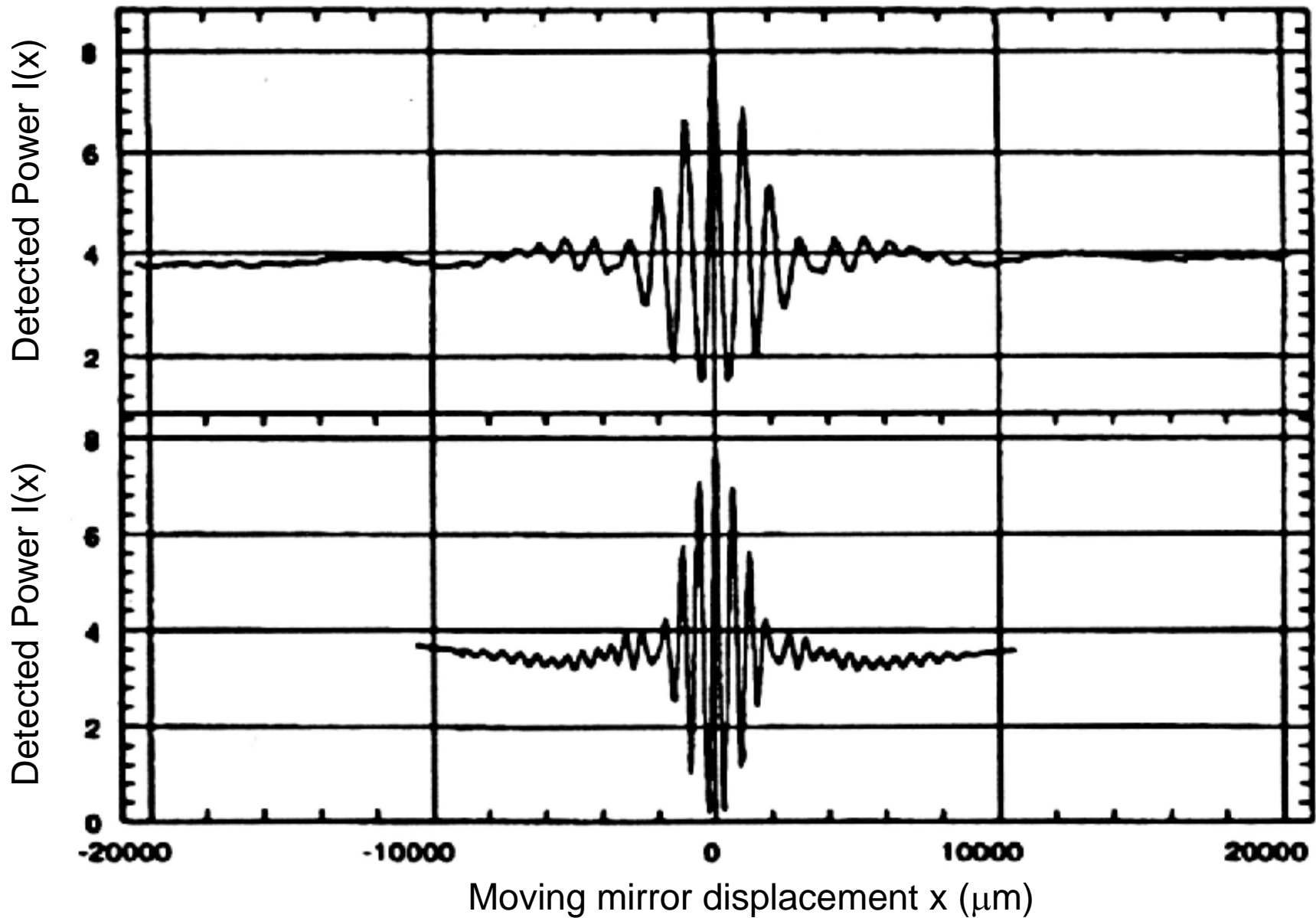
$$\begin{aligned} I(x) &\propto \langle E(t)^2 \rangle = \langle E(t)E^*(t) \rangle = \\ &= E_o^2(\sigma)rt(\sigma) \left[ e^{i2\pi\sigma ct} + e^{i2\pi\sigma ct} e^{i4\pi\sigma x} \right] \left[ e^{-i2\pi\sigma ct} + e^{-i2\pi\sigma ct} e^{-i4\pi\sigma x} \right] = \\ &= E_o^2(\sigma)rt(\sigma) \left[ 1 + e^{-i4\pi\sigma x} + e^{i4\pi\sigma x} + 1 \right] \\ &= E_o^2(\sigma)rt(\sigma) 2(1 + \cos 4\pi\sigma x) \end{aligned}$$

- So the interferogram is  $I(x) - \langle I \rangle = rt(\sigma) \cos(4\pi\sigma x)$
- If the input radiation is not monochromatic, and each wavenumber has amplitude  $S(\sigma)$ :

$$I(x) - \langle I \rangle = \int_0^{\infty} S(\sigma)rt(\sigma) \cos(4\pi\sigma x) d\sigma$$

The specific Brightness and the interferogram are related by a Fourier Transform

$$I(x) - \langle I \rangle = \int_0^{\infty} S(\sigma) r t(\sigma) \cos(4\pi\sigma x) d\sigma$$



# Elementary theory of the FTS

$$S(\sigma)rt(\sigma) = \int_{-\infty}^{\infty} (I(x) - \langle I \rangle) \cos(4\pi\sigma x) dx$$

- For obvious reasons we cannot extend  $x$  to infinity ! If the maximum displacement of the moving mirror is  $x_{\max}$ , all we can do is to compute:

$$S'(\sigma)rt(\sigma) = \int_{-x_{\max}}^{x_{\max}} (I(x) - \langle I \rangle) \cos(4\pi\sigma x) dx$$

- $S'$  is an approximation of the real spectrum  $S$
- The main difference is in the effective spectral resolution of the spectrometer, which for  $S'$  is limited to approx.  $1/(2x_{\max})$ .

# Spectral Resolution

- Consider a monochromatic line with wavenumber  $\sigma_o$  : the interferogram is

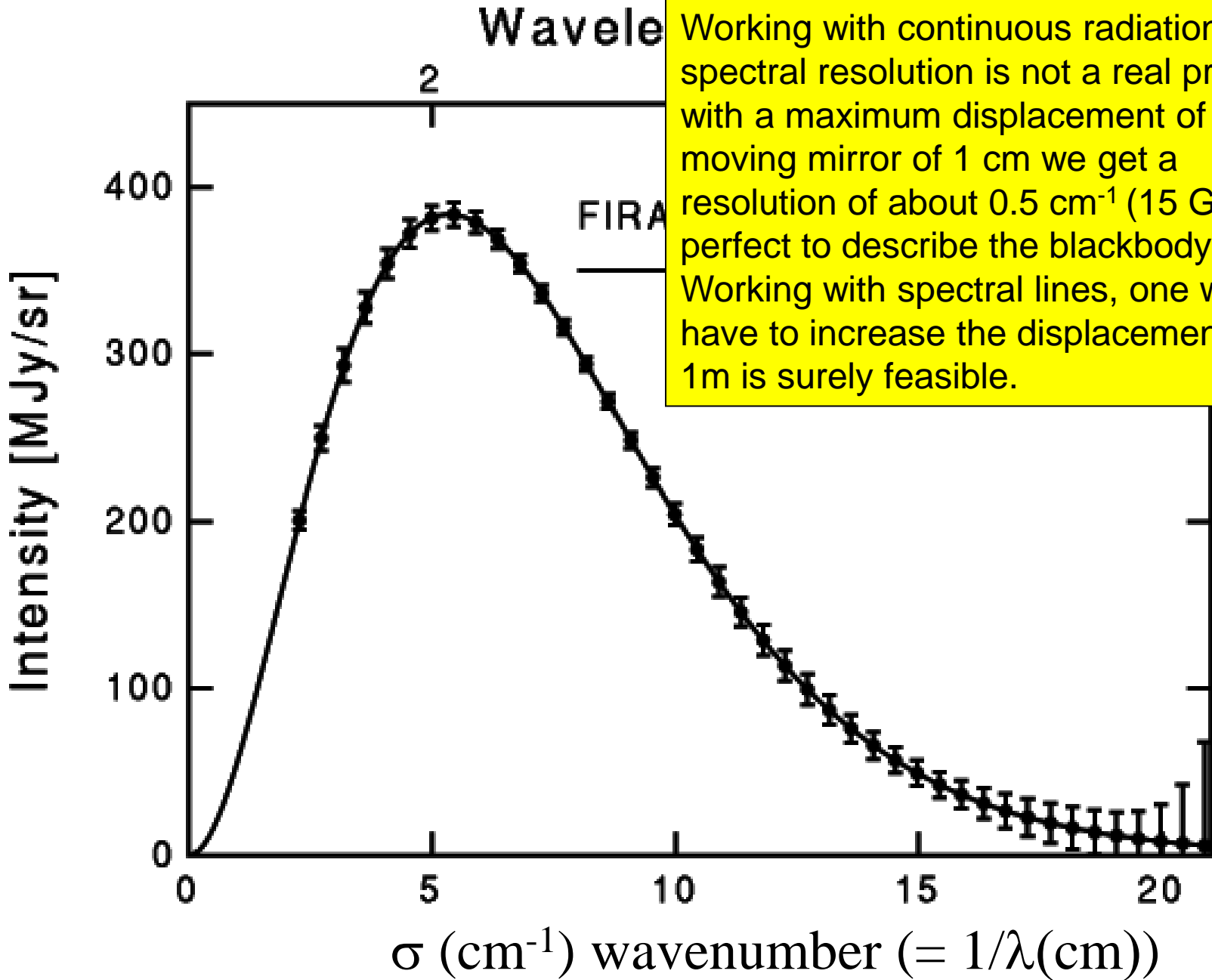
$$I(x) - \langle I \rangle = I_o \cos(4\pi\sigma_o x)$$

- The Fourier integral, limited to  $\pm x_{\max}$ , is:

$$S'(\sigma) = I_o \int_{-x_{\max}}^{x_{\max}} \cos(4\pi\sigma_o x) \cos(4\pi\sigma x) dx \quad \Rightarrow$$

$$S'(\sigma) = I_o x_{\max} \frac{\sin 4\pi(\sigma - \sigma_o)x_{\max}}{4\pi(\sigma - \sigma_o)x_{\max}}$$

- This is an approximation of the real  $S(\sigma)$  which would be a delta function centered in  $\sigma_o$  : in place of a delta, we get a sinc, with a half-width approx.  $1.23/(2x_{\max})$ .



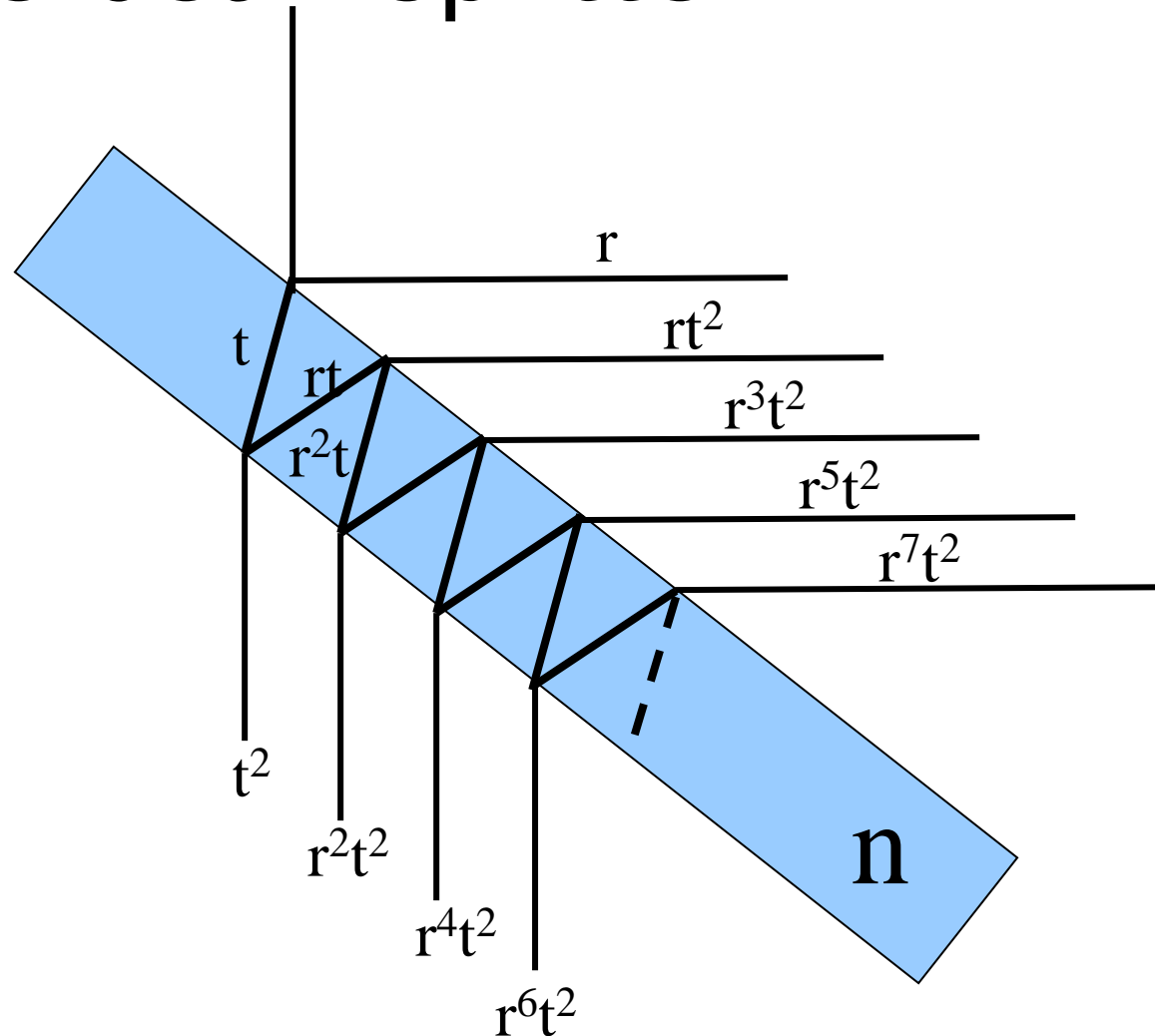
# Beamsplitter problems

$$S'(\sigma) \text{rt}(\sigma) = \int_{-x_{\max}}^{x_{\max}} (I(x) - \langle I \rangle) \cos(4\pi\sigma x) dx$$

- What we get is the input spectrum times the efficiency of the beamsplitter.
- If the latter goes to zero, we cannot retrieve the spectrum.
- So we need good beamplitters, ideally with  $\text{rt}=0.25$ , independent on frequency.

# the beamsplitter

- The simplest beamsplitter is a dielectric slab, with refraction index  $n$  and thickness  $t$ .
- Due to multiple reflections inside the slab, the transmitted and reflected fields can be computed as the sum of an infinite number of components with decreasing amplitude (a converging series) and increasing phase delay.



$$\delta = 4\pi n d \cos \theta' \sigma$$

$$E = E_o (-r \cos 2\pi\sigma ct + rt^2 \cos(2\pi\sigma ct + \delta) + r^3t^2 \cos(2\pi\sigma ct + 2\delta) + r^5t^2 \cos(2\pi\sigma ct + 3\delta) + \dots$$

From this, the efficiency  $rt(\sigma)$  is computed



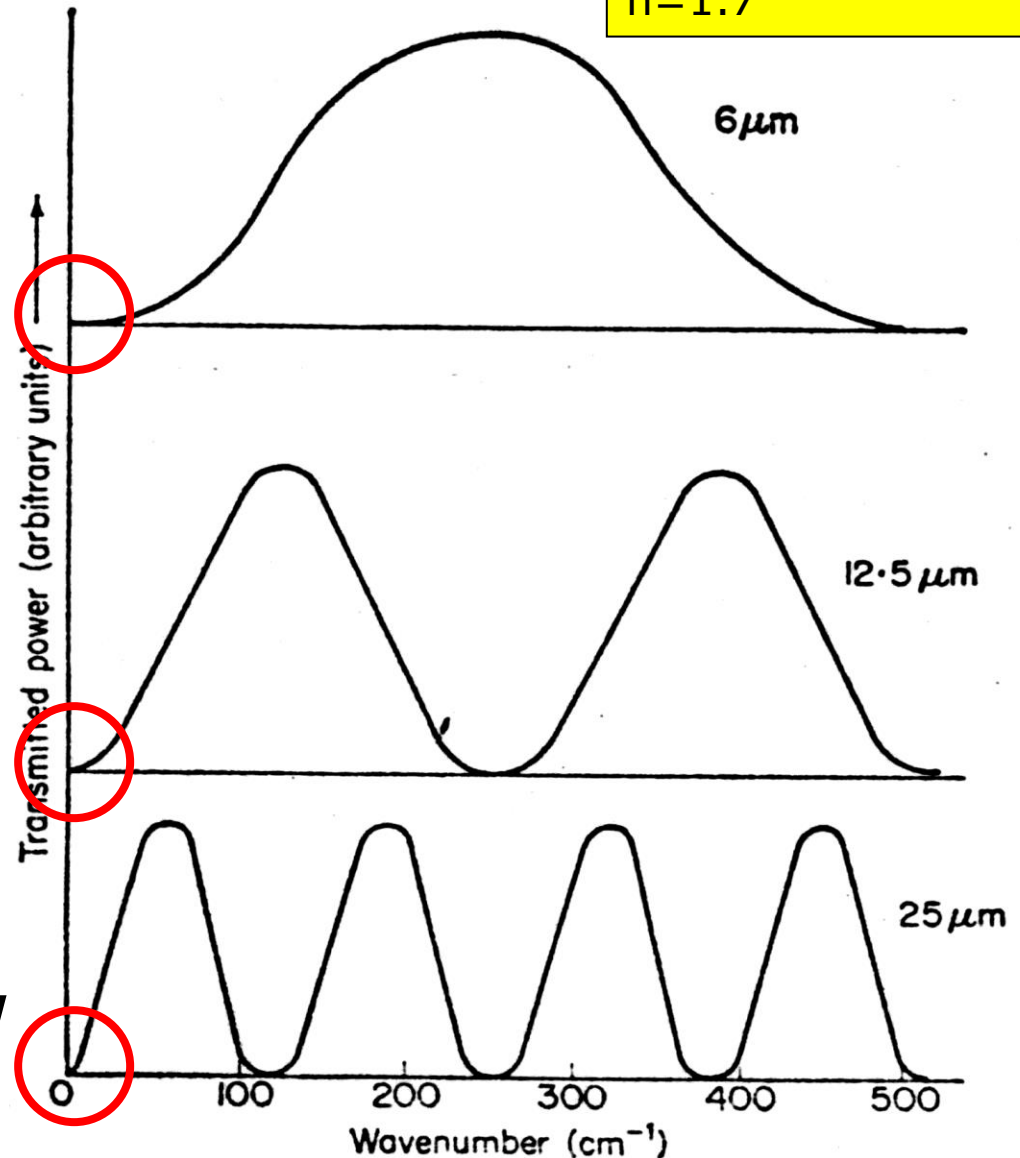
# the beamsplitter

Polyethylene  
Terephthalate  
(mylar or melinex)  
 $n=1.7$

- The efficiency is a periodic function with zeros at wavenumbers

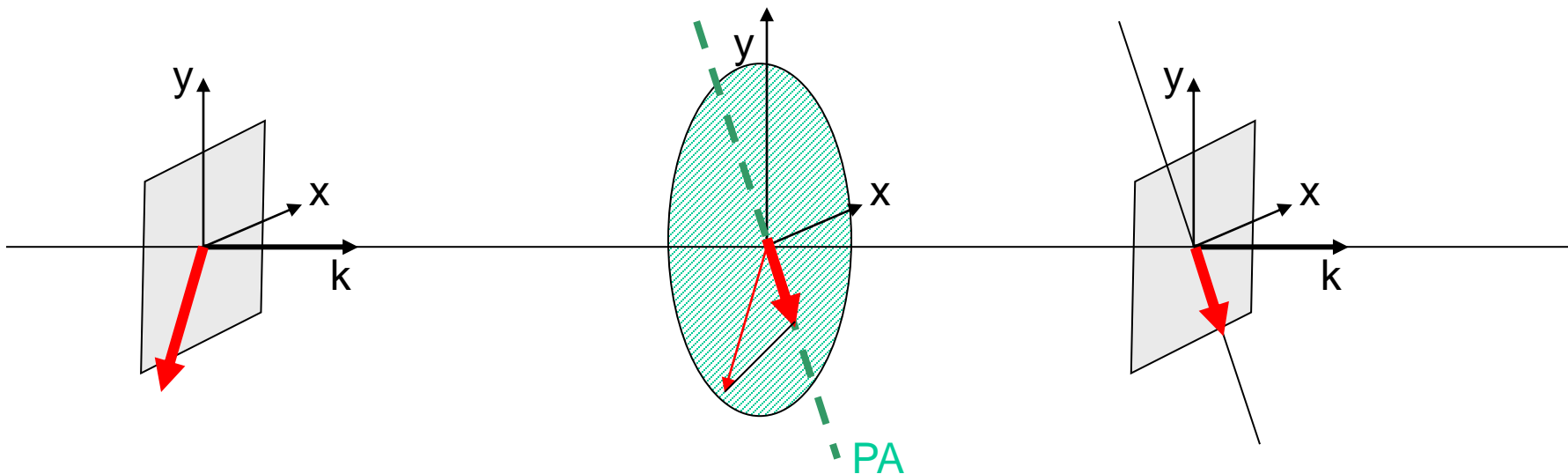
$$\sigma_m = \frac{m}{nd \cos \theta'}$$

- Whatever thickness and refraction index you select, this is not efficient at low frequencies.



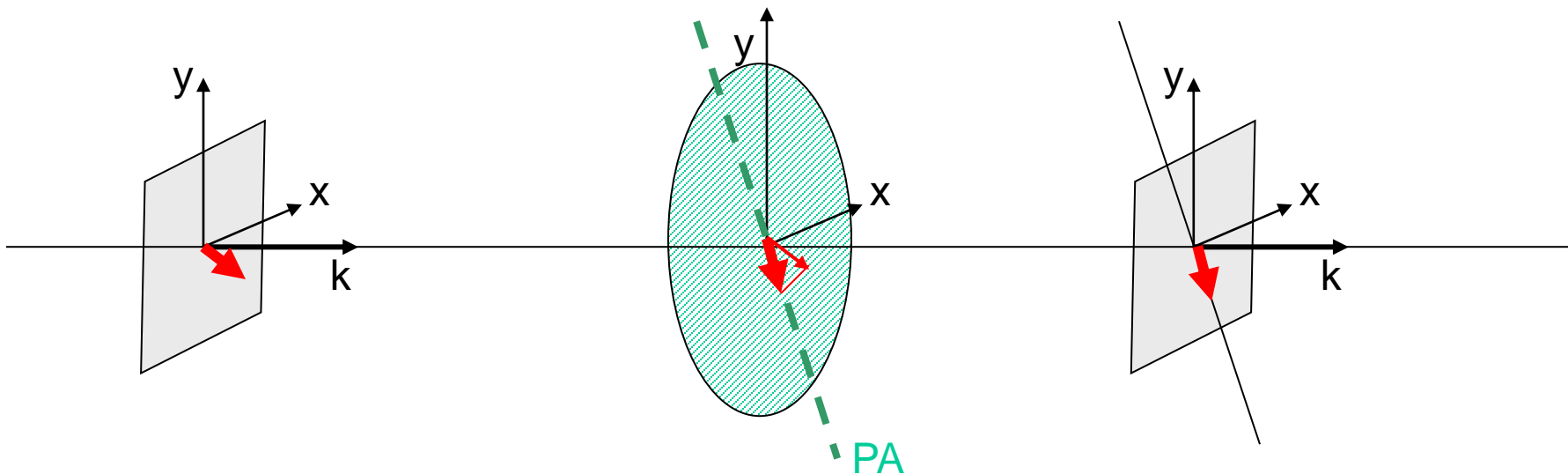
# Linear Polarizers

- Linear polarizers can be used as high efficiency achromatic beamsplitters at long wavelengths.
- A linear polarizer is an optical device transmitting only the projection of the E field of the EM wave parallel to a given direction, which is called the principal axis of the polarizer.
- Unpolarized radiation (where the E field direction in the wavefront is random) is transformed into linearly polarized radiation (where the E field direction is constant) when crossing a polarizer.



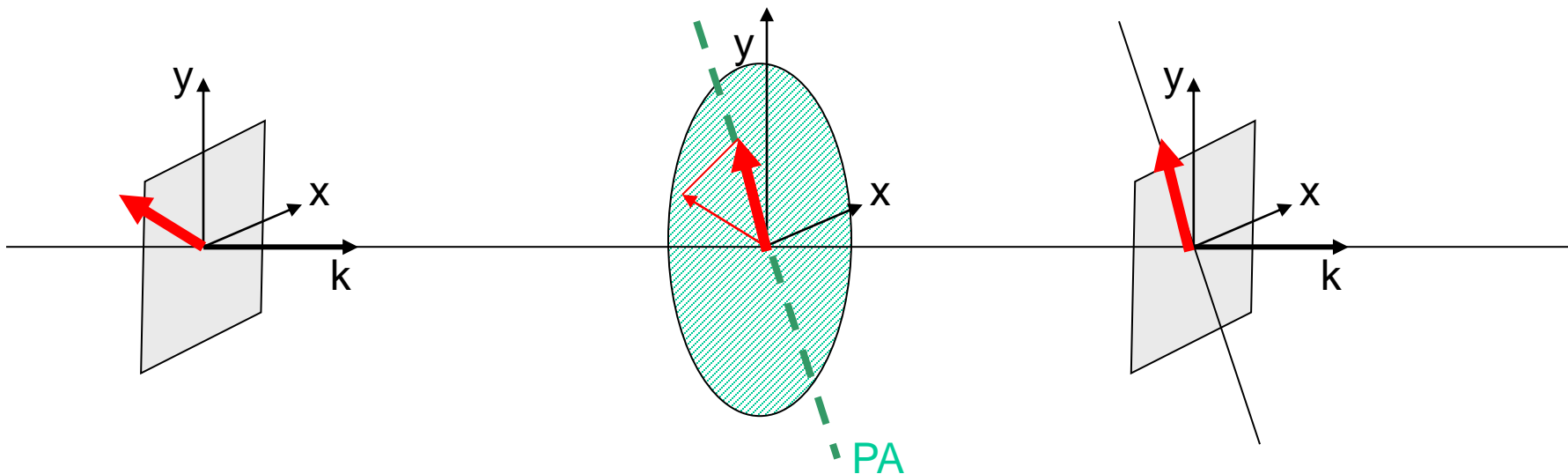
# Linear Polarizers

- Linear polarizers can be used as high efficiency achromatic beamsplitters at long wavelengths.
- A linear polarizer is an optical device transmitting only the projection of the E field of the EM wave parallel to a given direction, which is called the principal axis of the polarizer.
- Unpolarized radiation (where the E field direction in the wavefront is random) is transformed into linearly polarized radiation (where the E field direction is constant) when crossing a polarizer.



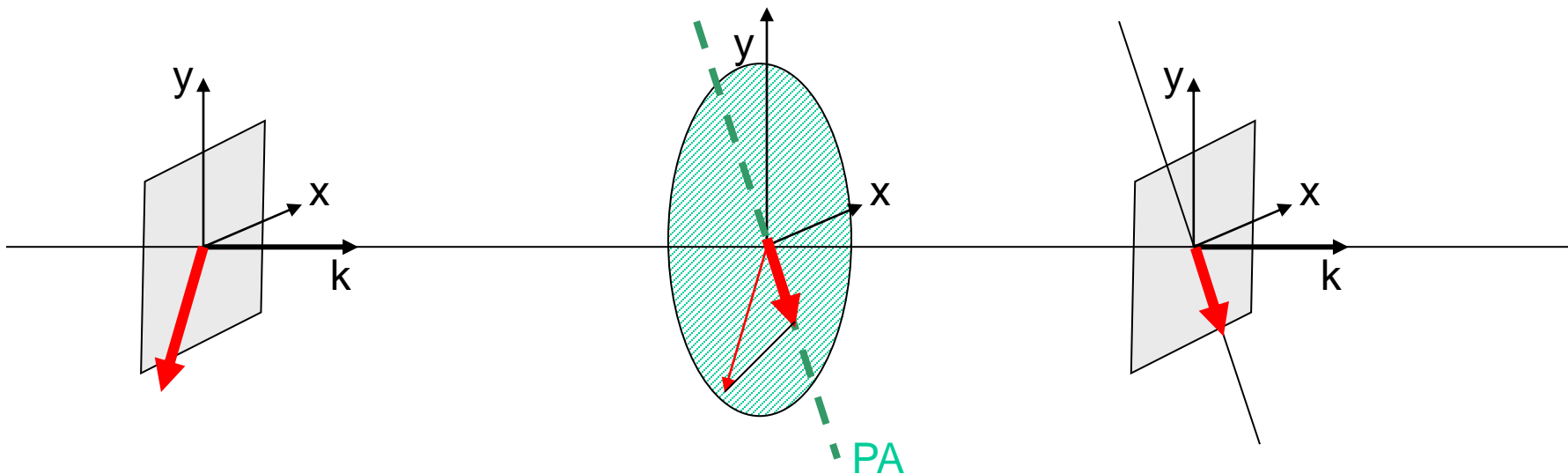
# Linear Polarizers

- Linear polarizers can be used as high efficiency achromatic beamsplitters at long wavelengths.
- A linear polarizer is an optical device transmitting only the projection of the E field of the EM wave parallel to a given direction, which is called the principal axis of the polarizer.
- Unpolarized radiation (where the E field direction in the wavefront is random) is transformed into linearly polarized radiation (where the E field direction is constant) when crossing a polarizer.



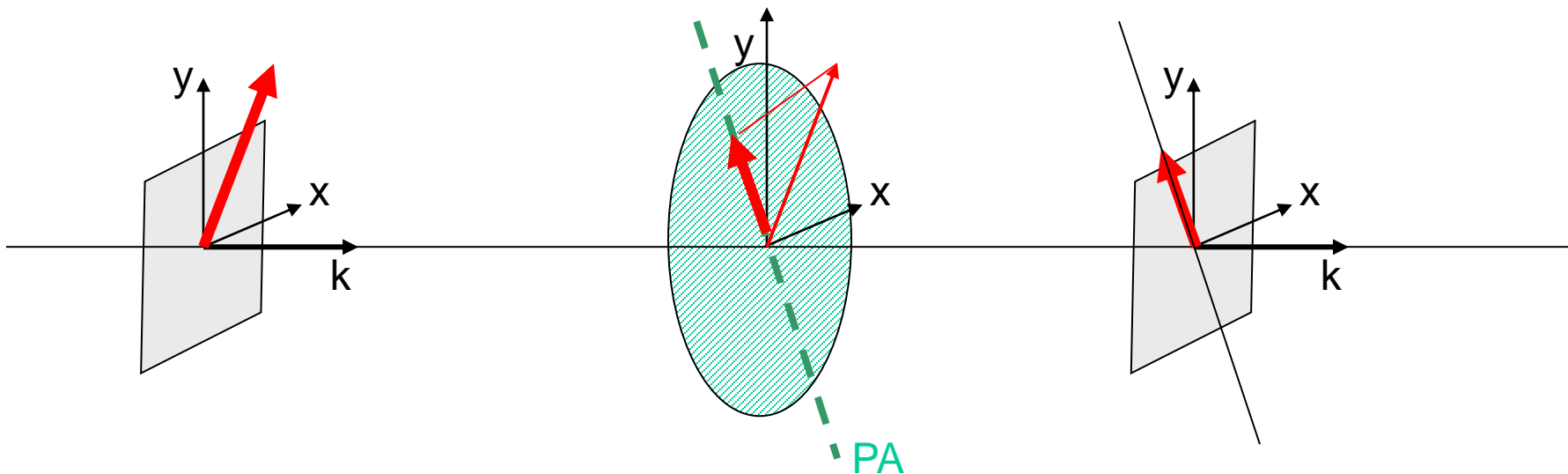
# Linear Polarizers

- Linear polarizers can be used as high efficiency achromatic beamsplitters at long wavelengths.
- A linear polarizer is an optical device transmitting only the projection of the E field of the EM wave parallel to a given direction, which is called the principal axis of the polarizer.
- Unpolarized radiation (where the E field direction in the wavefront is random) is transformed into linearly polarized radiation (where the E field direction is constant) when crossing a polarizer.



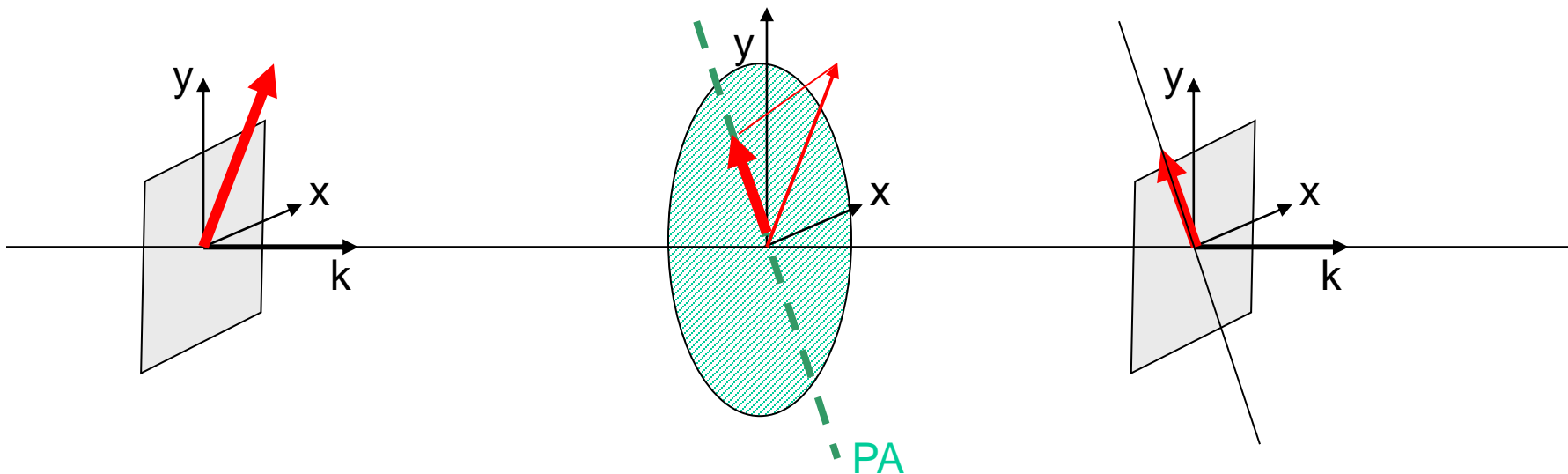
# Linear Polarizers

- Linear polarizers can be used as high efficiency achromatic beamsplitters at long wavelengths.
- A linear polarizer is an optical device transmitting only the projection of the E field of the EM wave parallel to a given direction, which is called the principal axis of the polarizer.
- Unpolarized radiation (where the E field direction in the wavefront is random) is transformed into linearly polarized radiation (where the E field direction is constant) when crossing a polarizer.



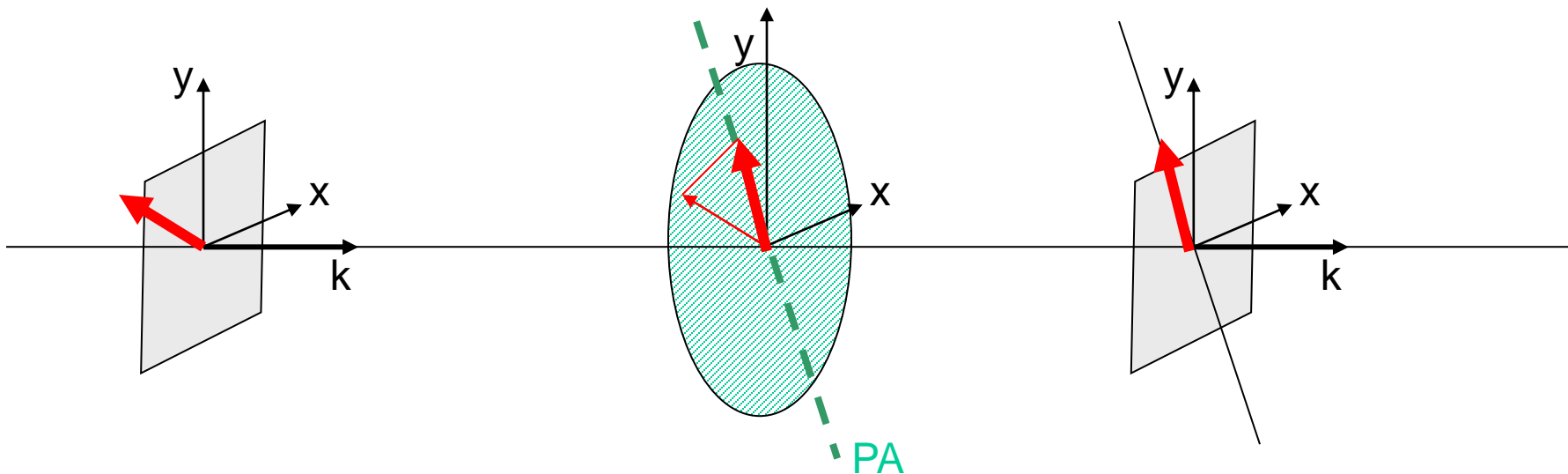
# Linear Polarizers

- Linear polarizers can be used as high efficiency achromatic beamsplitters at long wavelengths.
- A linear polarizer is an optical device transmitting only the projection of the E field of the EM wave parallel to a given direction, which is called the principal axis of the polarizer.
- Unpolarized radiation (where the E field direction in the wavefront is random) is transformed into linearly polarized radiation (where the E field direction is constant) when crossing a polarizer.



# Linear Polarizers

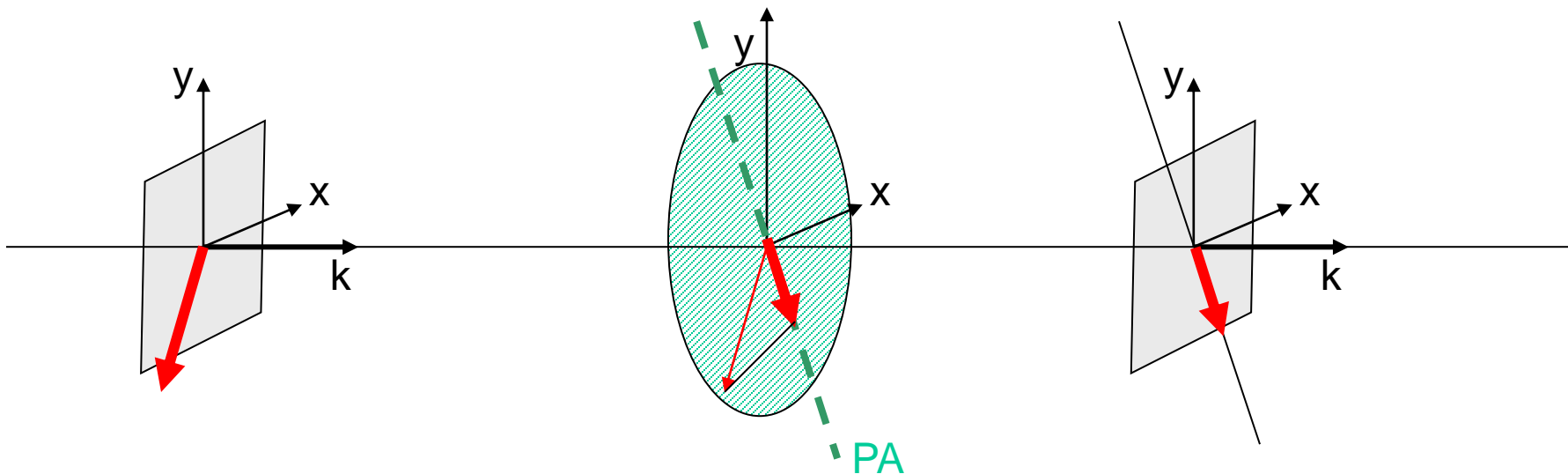
- Linear polarizers can be used as high efficiency achromatic beamsplitters at long wavelengths.
- A linear polarizer is an optical device transmitting only the projection of the E field of the EM wave parallel to a given direction, which is called the principal axis of the polarizer.
- Unpolarized radiation (where the E field direction in the wavefront is random) is transformed into linearly polarized radiation (where the E field direction is constant) when crossing a polarizer.





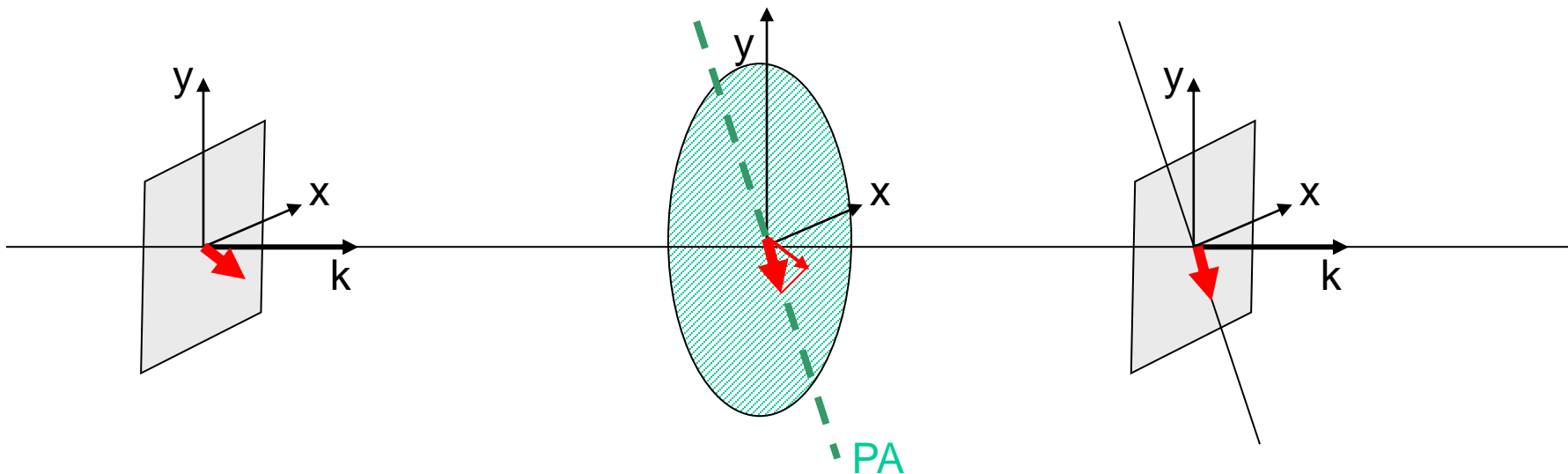
# Linear Polarizers

- Linear polarizers can be used as high efficiency achromatic beamsplitters at long wavelengths.
- A linear polarizer is an optical device transmitting only the projection of the E field of the EM wave parallel to a given direction, which is called the principal axis of the polarizer.
- Unpolarized radiation (where the E field direction in the wavefront is random) is transformed into linearly polarized radiation (where the E field direction is constant) when crossing a polarizer.



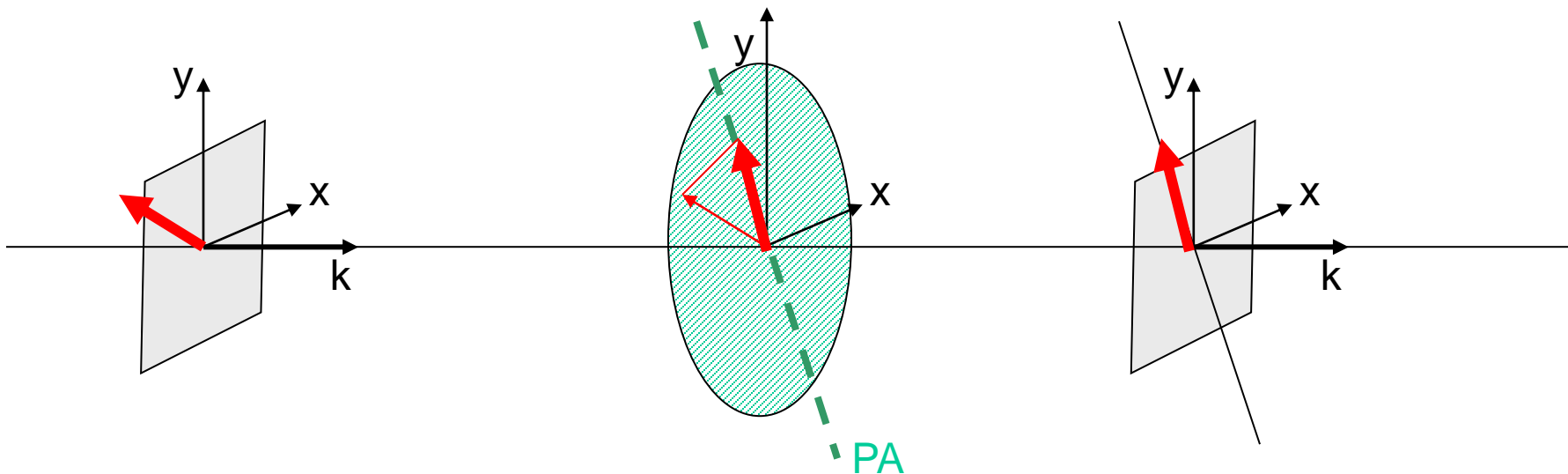
# Linear Polarizers

- Linear polarizers can be used as high efficiency achromatic beamsplitters at long wavelengths.
- A linear polarizer is an optical device transmitting only the projection of the E field of the EM wave parallel to a given direction, which is called the principal axis of the polarizer.
- Unpolarized radiation (where the E field direction in the wavefront is random) is transformed into linearly polarized radiation (where the E field direction is constant) when crossing a polarizer.



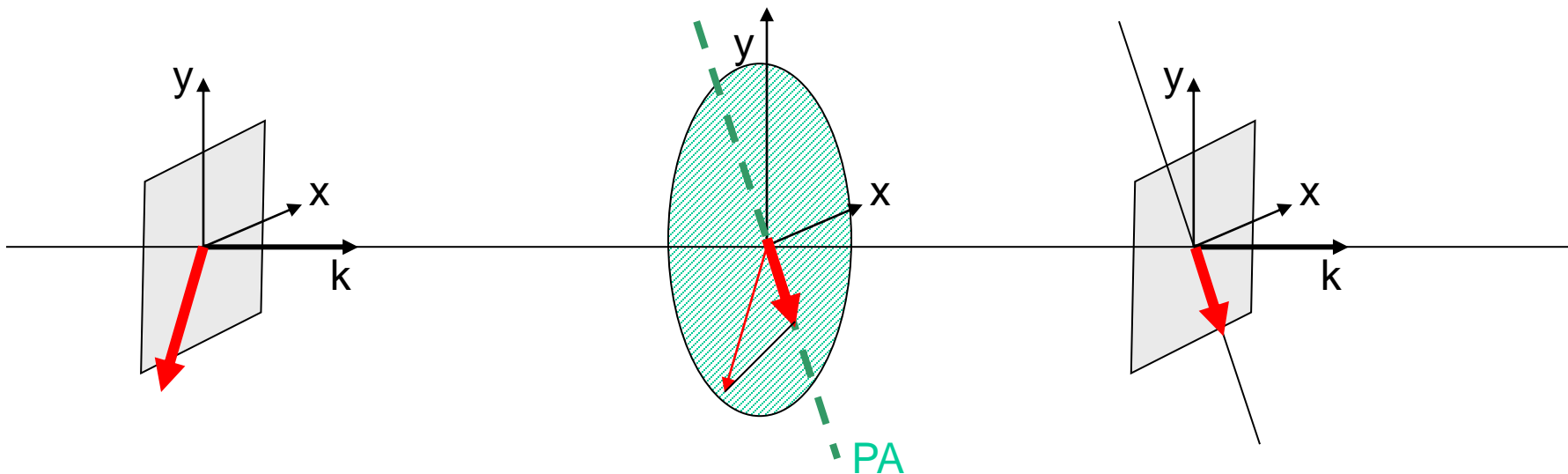
# Linear Polarizers

- Linear polarizers can be used as high efficiency achromatic beamsplitters at long wavelengths.
- A linear polarizer is an optical device transmitting only the projection of the E field of the EM wave parallel to a given direction, which is called the principal axis of the polarizer.
- Unpolarized radiation (where the E field direction in the wavefront is random) is transformed into linearly polarized radiation (where the E field direction is constant) when crossing a polarizer.



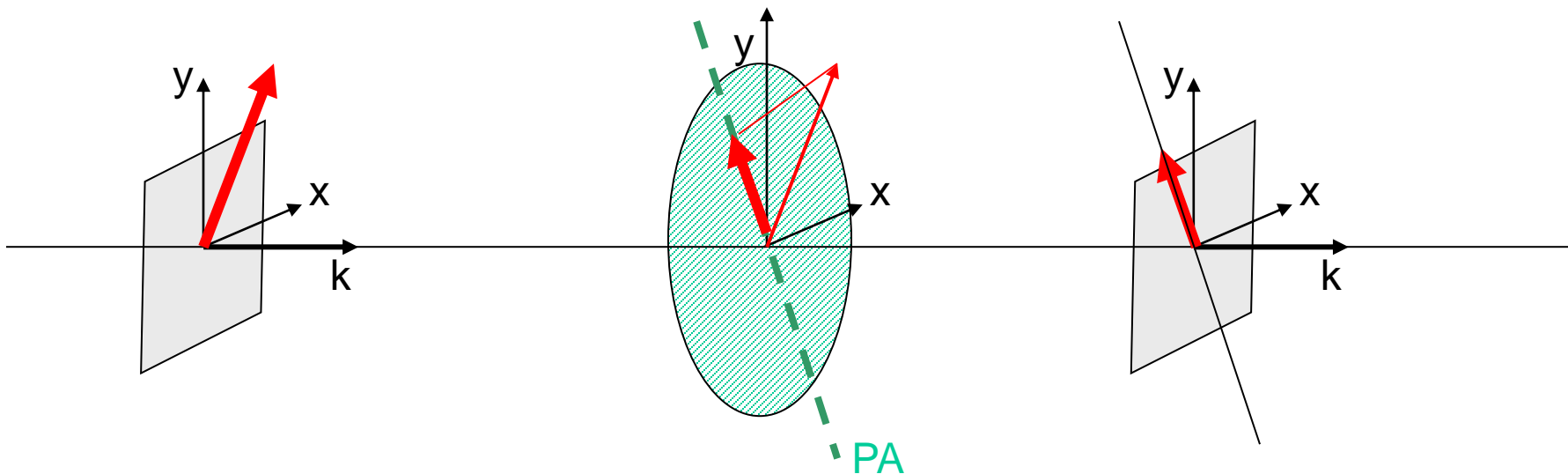
# Linear Polarizers

- Linear polarizers can be used as high efficiency achromatic beamsplitters at long wavelengths.
- A linear polarizer is an optical device transmitting only the projection of the E field of the EM wave parallel to a given direction, which is called the principal axis of the polarizer.
- Unpolarized radiation (where the E field direction in the wavefront is random) is transformed into linearly polarized radiation (where the E field direction is constant) when crossing a polarizer.



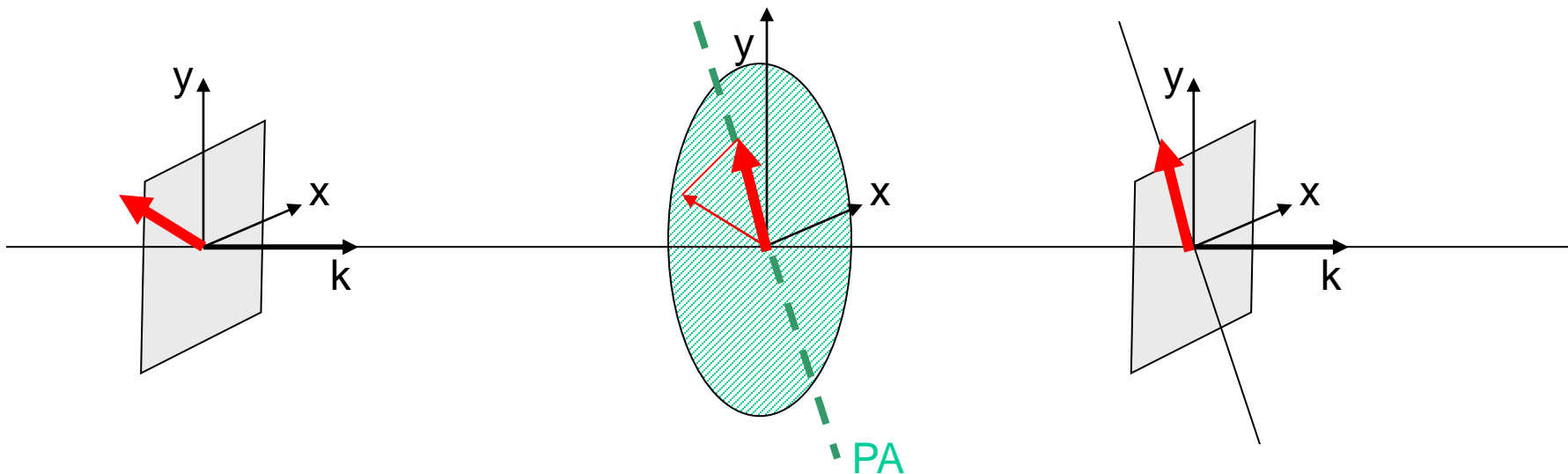
# Linear Polarizers

- Linear polarizers can be used as high efficiency achromatic beamsplitters at long wavelengths.
- A linear polarizer is an optical device transmitting only the projection of the E field of the EM wave parallel to a given direction, which is called the principal axis of the polarizer.
- Unpolarized radiation (where the E field direction in the wavefront is random) is transformed into linearly polarized radiation (where the E field direction is constant) when crossing a polarizer.



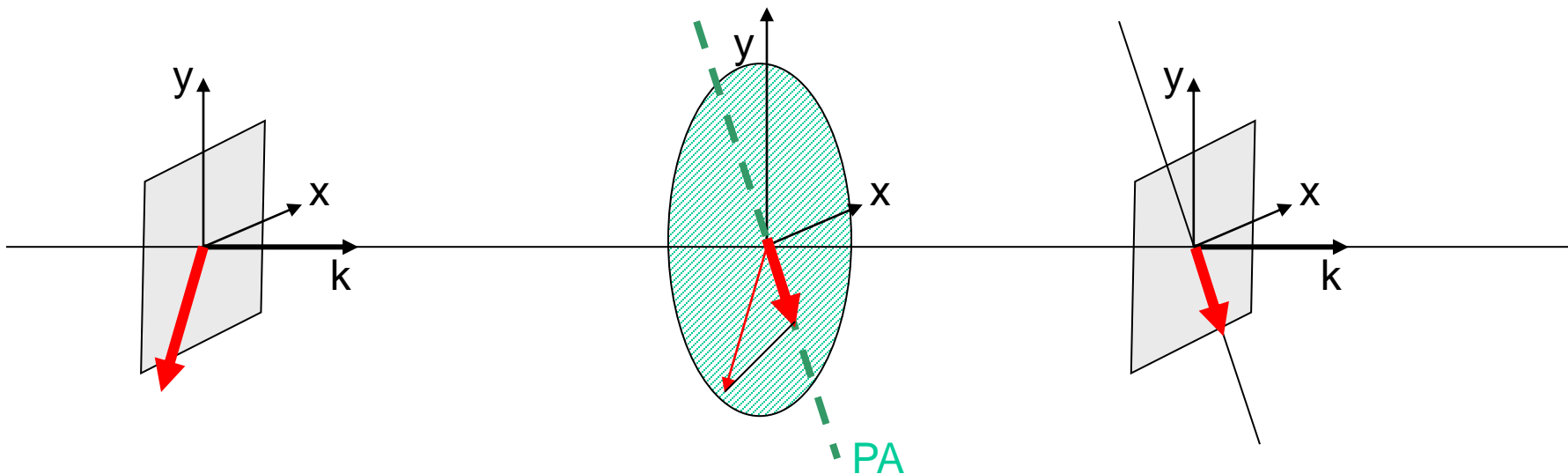
# Linear Polarizers

- Linear polarizers can be used as high efficiency achromatic beamsplitters at long wavelengths.
- A linear polarizer is an optical device transmitting only the projection of the E field of the EM wave parallel to a given direction, which is called the principal axis of the polarizer.
- Unpolarized radiation (where the E field direction in the wavefront is random) is transformed into linearly polarized radiation (where the E field direction is constant) when crossing a polarizer.



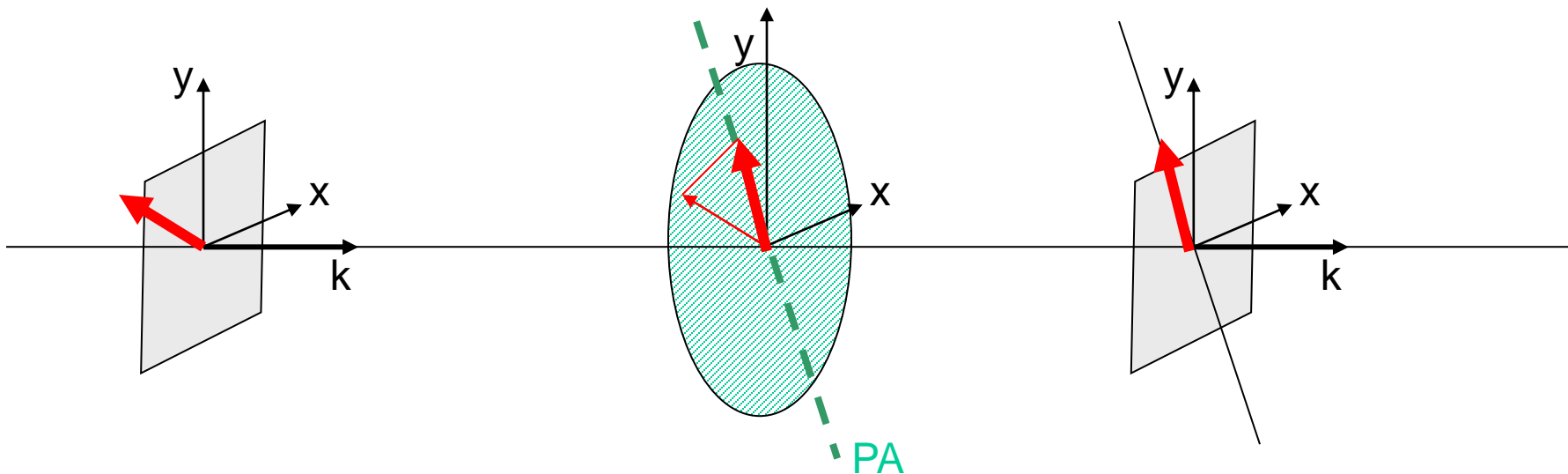
# Linear Polarizers

- Linear polarizers can be used as high efficiency achromatic beamsplitters at long wavelengths.
- A linear polarizer is an optical device transmitting only the projection of the E field of the EM wave parallel to a given direction, which is called the principal axis of the polarizer.
- Unpolarized radiation (where the E field direction in the wavefront is random) is transformed into linearly polarized radiation (where the E field direction is constant) when crossing a polarizer.



# Linear Polarizers

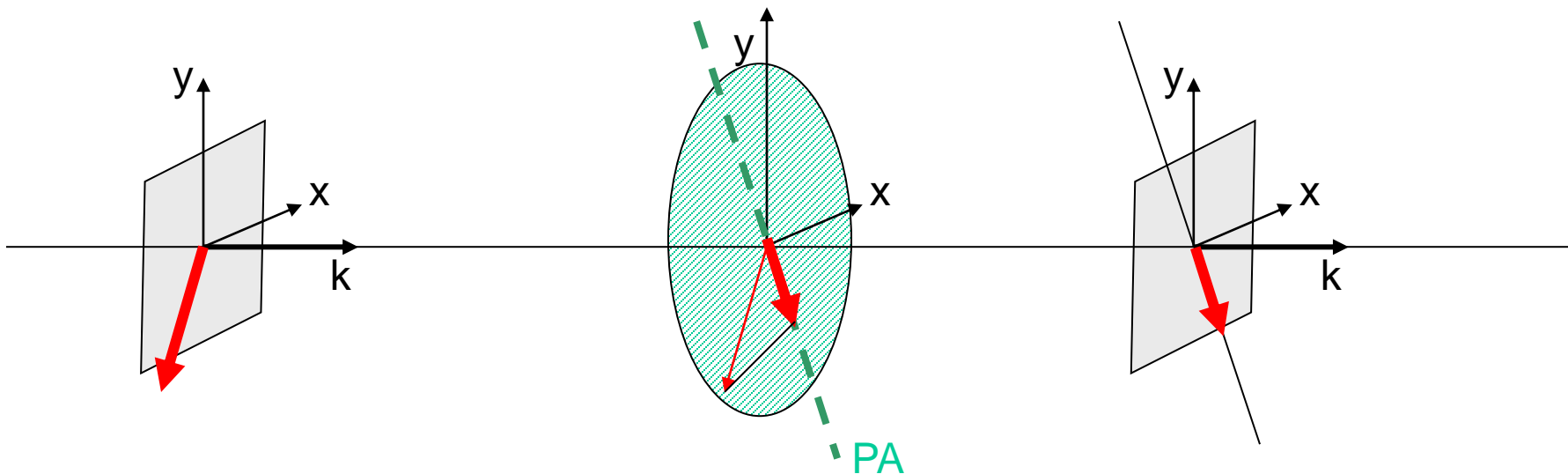
- Linear polarizers can be used as high efficiency achromatic beamsplitters at long wavelengths.
- A linear polarizer is an optical device transmitting only the projection of the E field of the EM wave parallel to a given direction, which is called the principal axis of the polarizer.
- Unpolarized radiation (where the E field direction in the wavefront is random) is transformed into linearly polarized radiation (where the E field direction is constant) when crossing a polarizer.





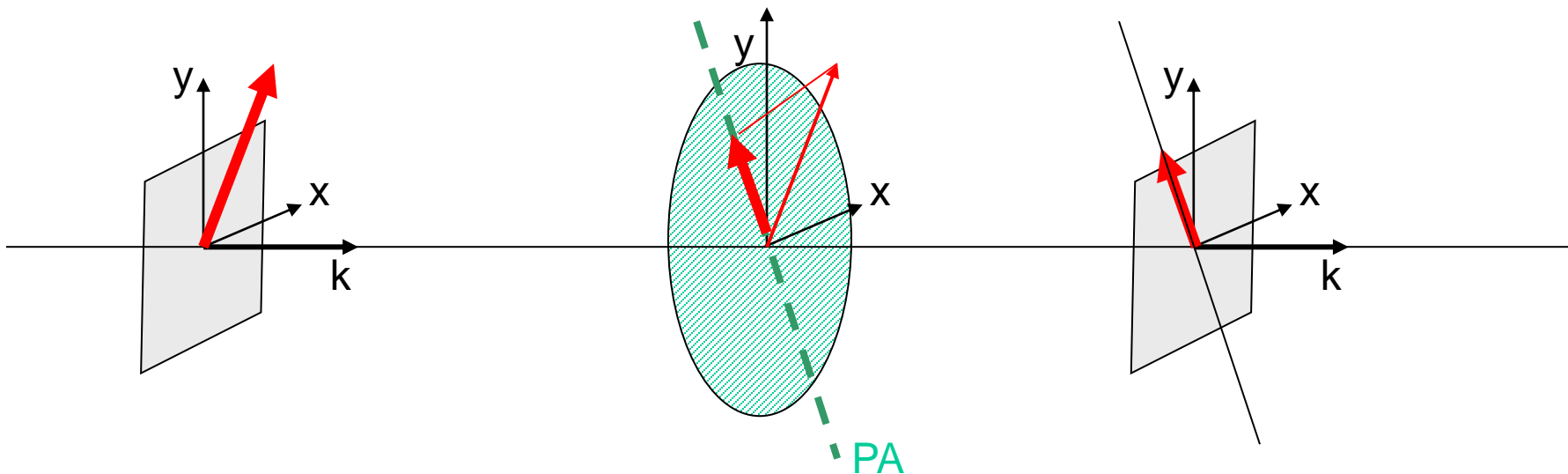
# Linear Polarizers

- Linear polarizers can be used as high efficiency achromatic beamsplitters at long wavelengths.
- A linear polarizer is an optical device transmitting only the projection of the E field of the EM wave parallel to a given direction, which is called the principal axis of the polarizer.
- Unpolarized radiation (where the E field direction in the wavefront is random) is transformed into linearly polarized radiation (where the E field direction is constant) when crossing a polarizer.



# Linear Polarizers

- Linear polarizers can be used as high efficiency achromatic beamsplitters at long wavelengths.
- A linear polarizer is an optical device transmitting only the projection of the E field of the EM wave parallel to a given direction, which is called the principal axis of the polarizer.
- Unpolarized radiation (where the E field direction in the wavefront is random) is transformed into linearly polarized radiation (where the E field direction is constant) when crossing a polarizer.

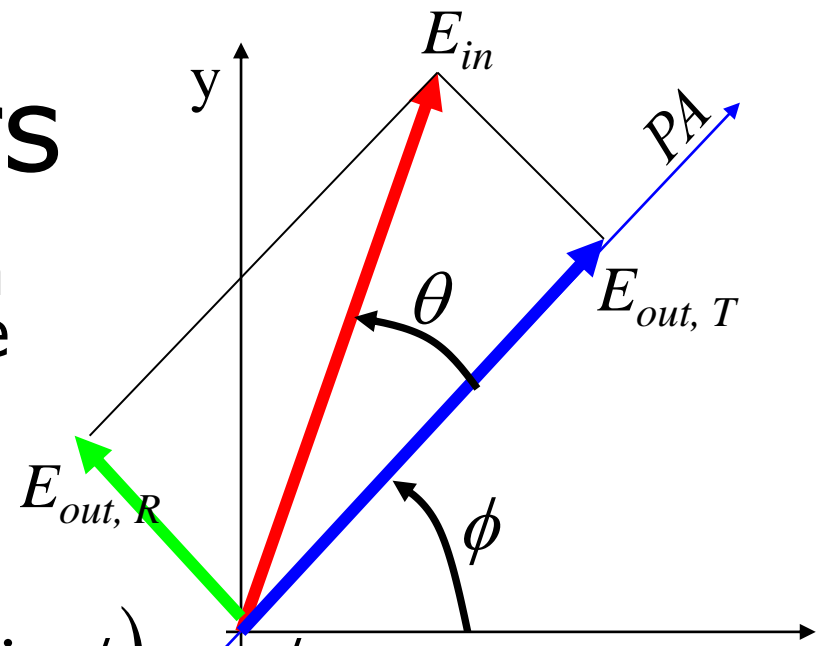


# Linear Polarizers

- The transmitted field  $E'$  can be computed projecting the incoming field  $E$  along the Principal Axis:

$$E_{par} = E_x \cos \phi + E_y \sin \phi$$

$$\begin{cases} E'_x = E_{par,x} = (E_x \cos \phi + E_y \sin \phi) \cos \phi \\ E'_y = E_{par,y} = (E_x \cos \phi + E_y \sin \phi) \sin \phi \end{cases}$$



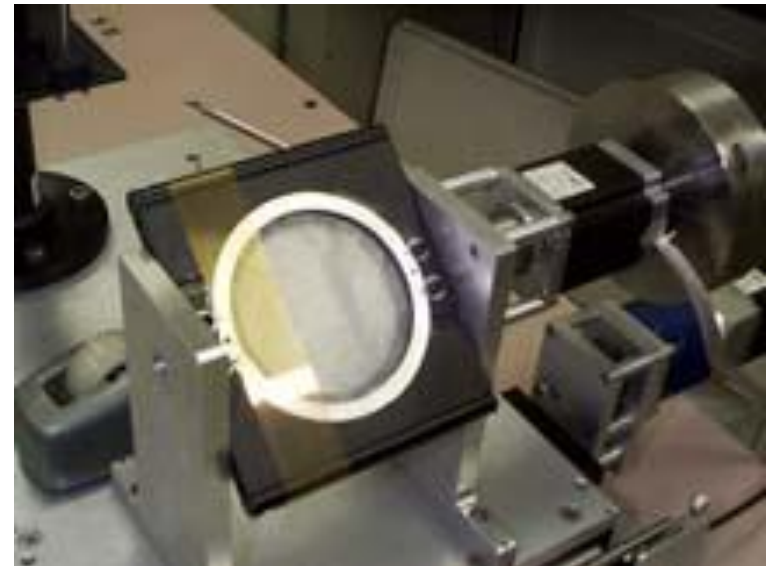
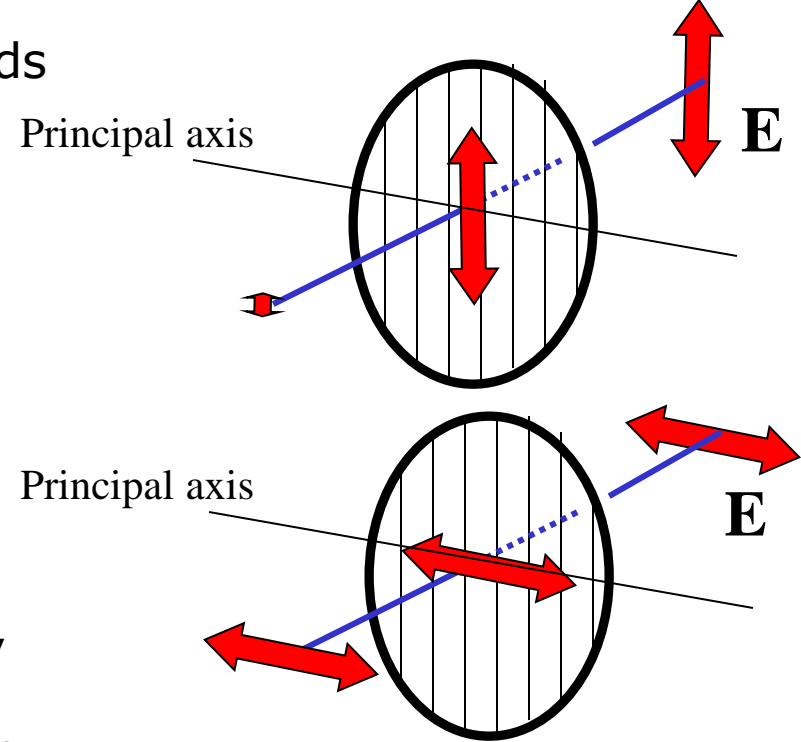
- The component of the incoming field orthogonal to the PA is either absorbed or reflected, depending on the particular polarizer used.

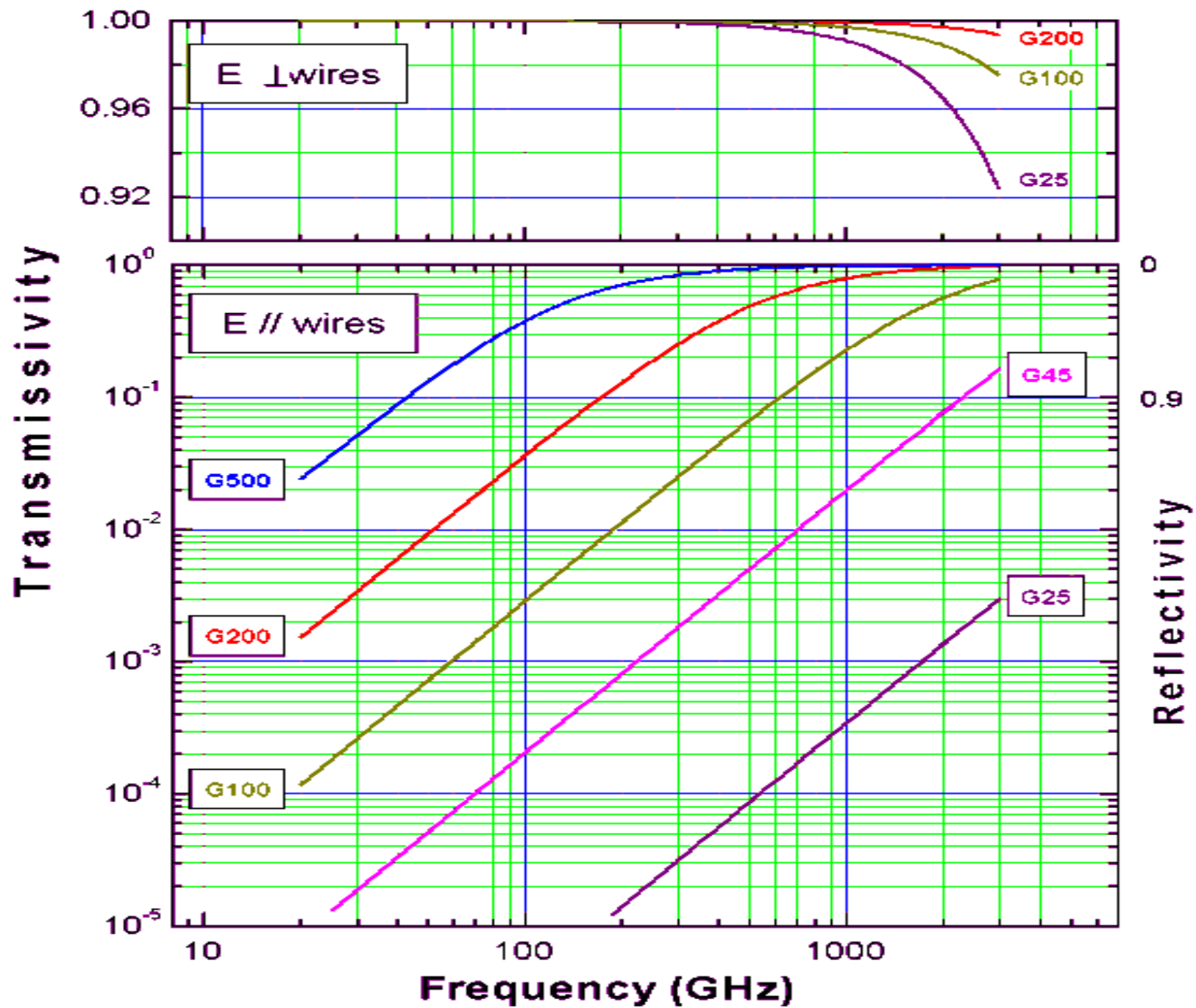
- Note that

$$I' = |E'|^2 = |E_{par}|^2 = |E|^2 \cos^2 \theta = I \cos^2 \theta \quad (\text{Malus law})$$

- So, for  $\theta=45^\circ$  incidence, half of the intensity is transmitted (and half is reflected or absorbed).

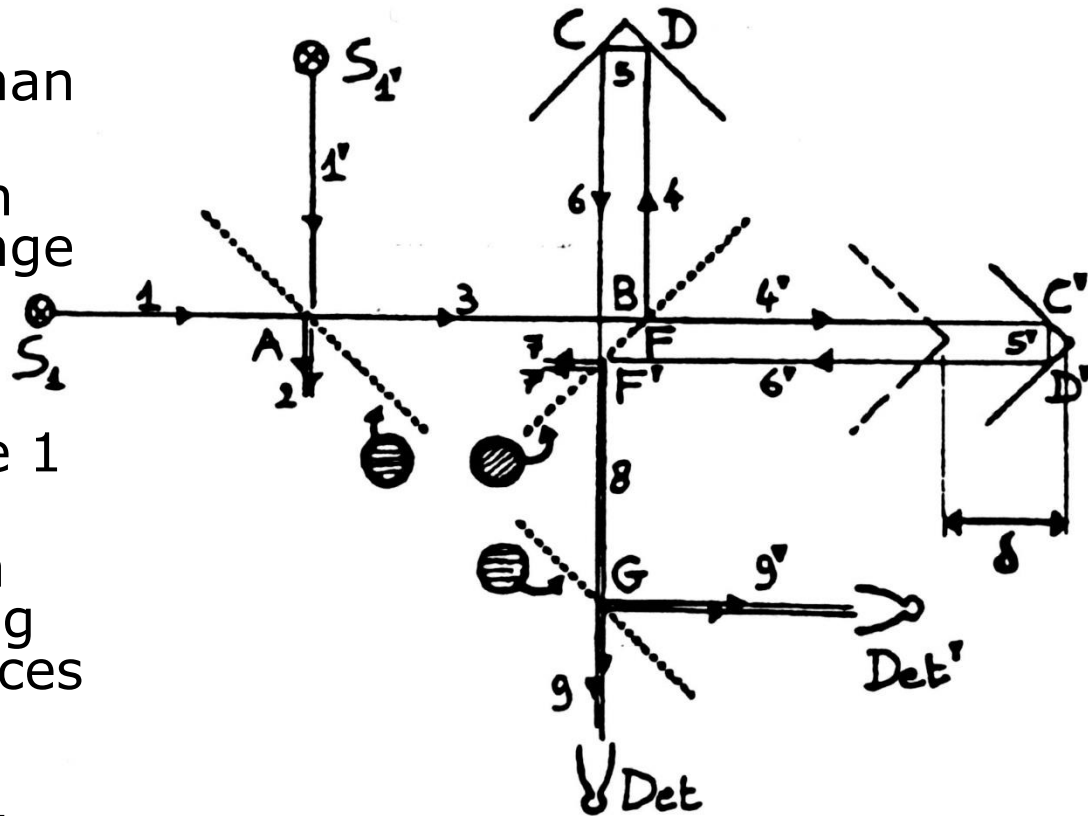
- At long wavelengths metallic wire grids act as ideal polarizers:
- Radiation with  $E$  parallel to the wires induces a current in the wires, so the polarizer acts as a metallic mirror: radiation is fully reflected and is not transmitted.
- Radiation with  $E$  orthogonal to the wires cannot induce a current in the wires, so it is transmitted.
- Radiation at a generic angle from the wires is partially transmitted (orthogonal component) and partially reflected (parallel component).
- If the spacing of the wires  $a$  and their diameter  $d$  are much less than the wavelength, the wire grid is very close to an ideal polarizer, with its principal axis orthogonal to the wires.
- Wire grid polarizers can be used as **ideal beamsplitters** for radiation at  $45^\circ$  wrt the wires: half of the intensity is transmitted, and half is reflected, without any wavelength dependence.
- Wire grids can be machined easily using a lathe and tungsten wire, which is available in long coils.





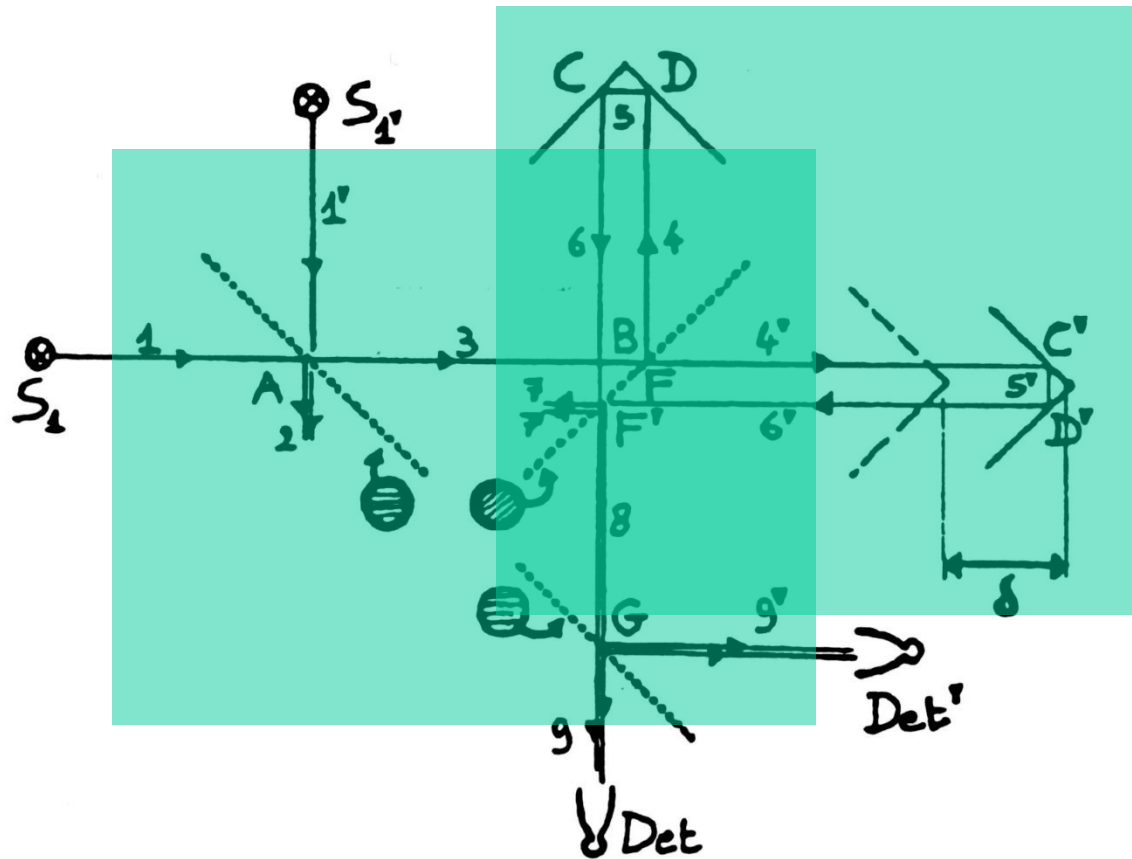
# Martin Puplett Interferometer

- In the Martin-Puplett configuration, radiation is prepared by the first polarizer, then is split by the second, and is recombined by the third.
- There are two sources. The beam from source  $1'$  is reflected one time more than the beam from source  $1$ .
- For each metallic reflection there is a  $180^\circ$  phase change of the electric field, so the detector will measure the difference in spectral brightness between source  $1$  and source  $1'$ .
- The instrument becomes a zero instrument, comparing the brightness of two sources (see later).
- In the case of FIRAS one source was the sky, the other one was an internal blackbody.



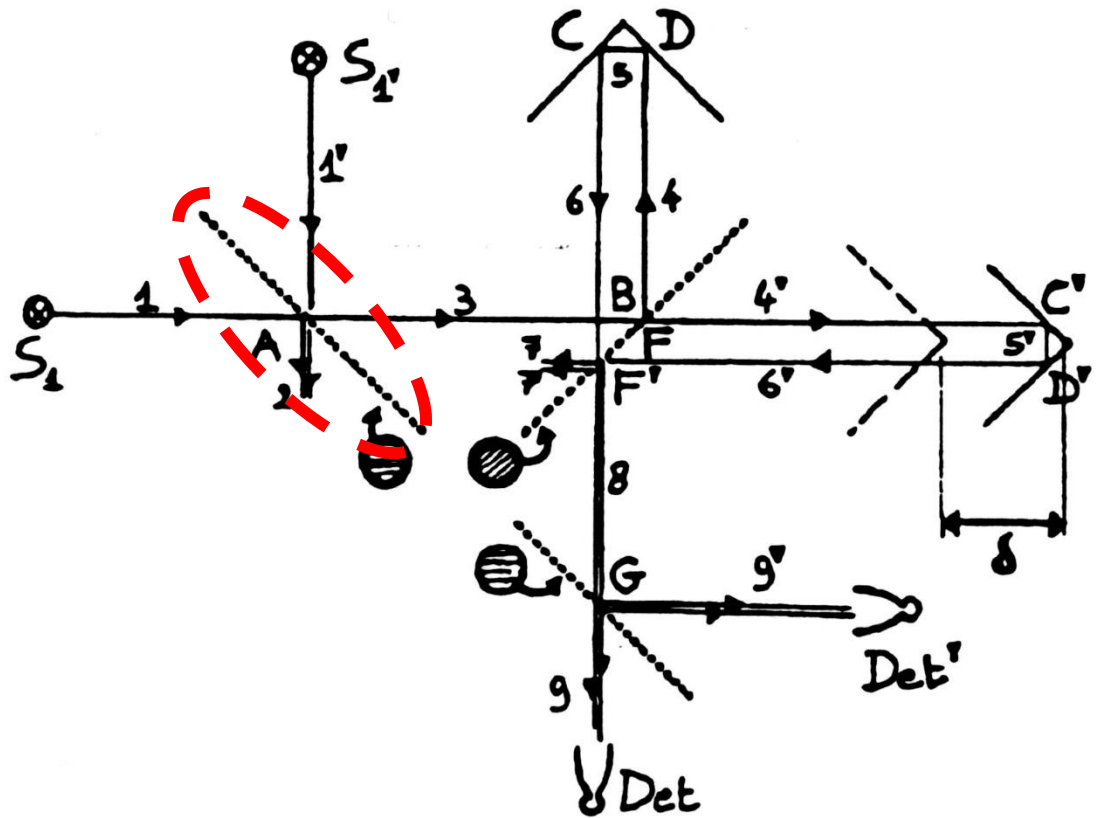
# Martin Puplett Interferometer

- Two input ports and two output ports.
- Uses two unpolarized sources, and two detectors sensitive to the power.
- Let's study the operation following the beams.



# Martin Puplett Interferometer

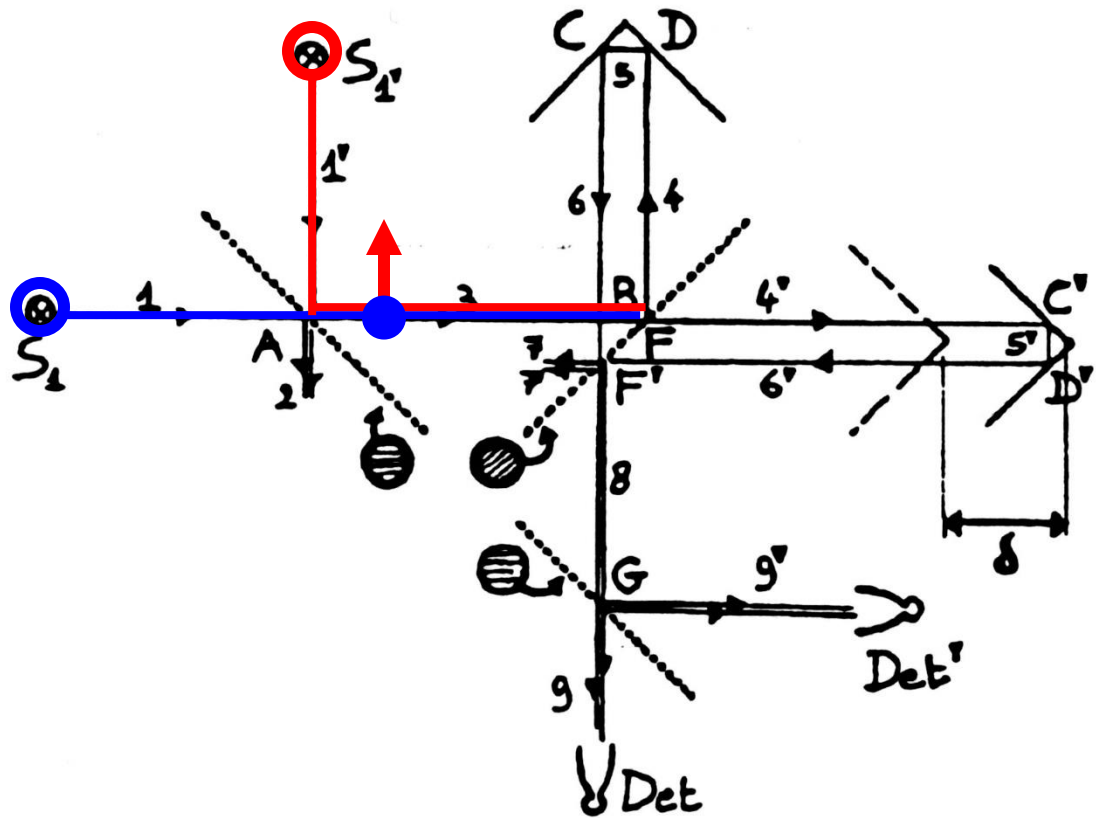
- The input polarizer A reflects radiation from source  $S_1$ , and transmits radiation from  $S_1$
- Assume that the polarizer wires are horizontal (main axis of the polarizer vertical)
- The beam at position 3 has a vertical component from  $S_1$  and a horizontal component from  $S_1$ ,





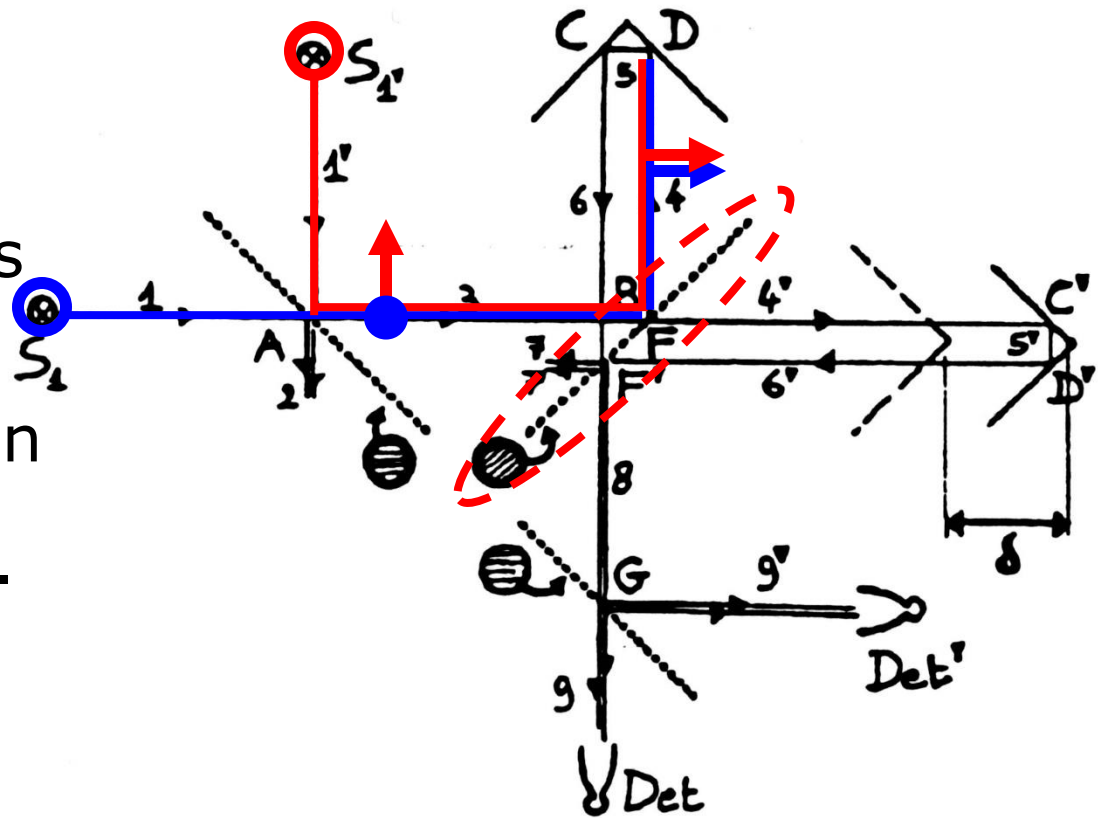
# Martin Puplett Interferometer

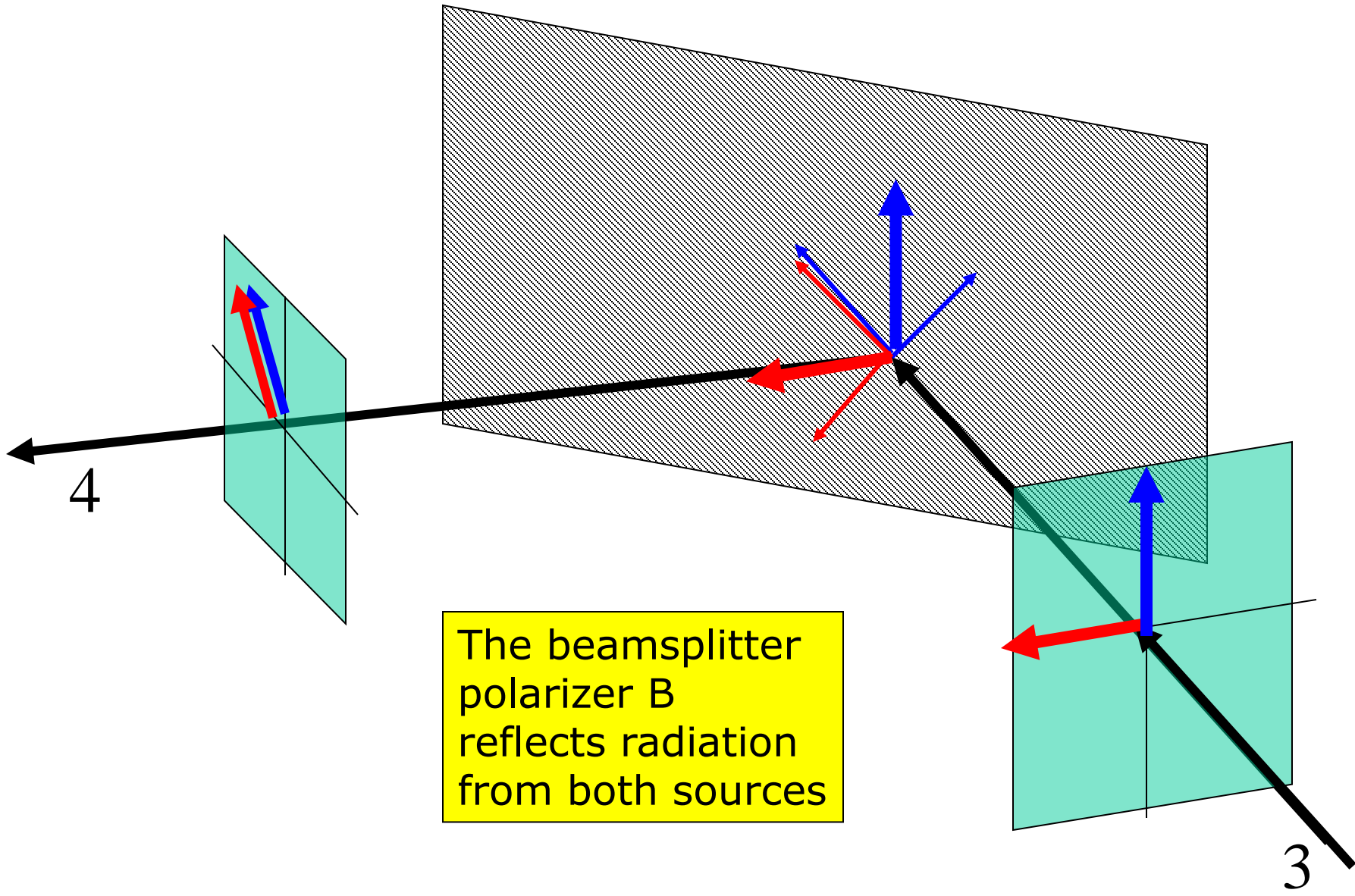
- The input polarizer A reflects radiation from source  $S_1$ , and transmits radiation from  $S_1$
- Assume that the polarizer wires are horizontal (main axis of the polarizer vertical)
- The beam at position 3 has a vertical component from  $S_1$  and a horizontal component from  $S_1$ ,



# Martin Puplett Interferometer

- The wires of the beamsplitter polarizer B are oriented to be seen by incoming radiation at  $45^\circ$  from the drawing plane.
- In this way, B reflects a fraction of the vertical component from  $\mathbf{S}_1$  and a fraction of the horizontal component from  $\mathbf{S}_1'$ .
- So beam 4 will be polarized at  $45^\circ$  and will consist of equal contributions from both  $\mathbf{S}_1$  e da  $\mathbf{S}_1'$ .

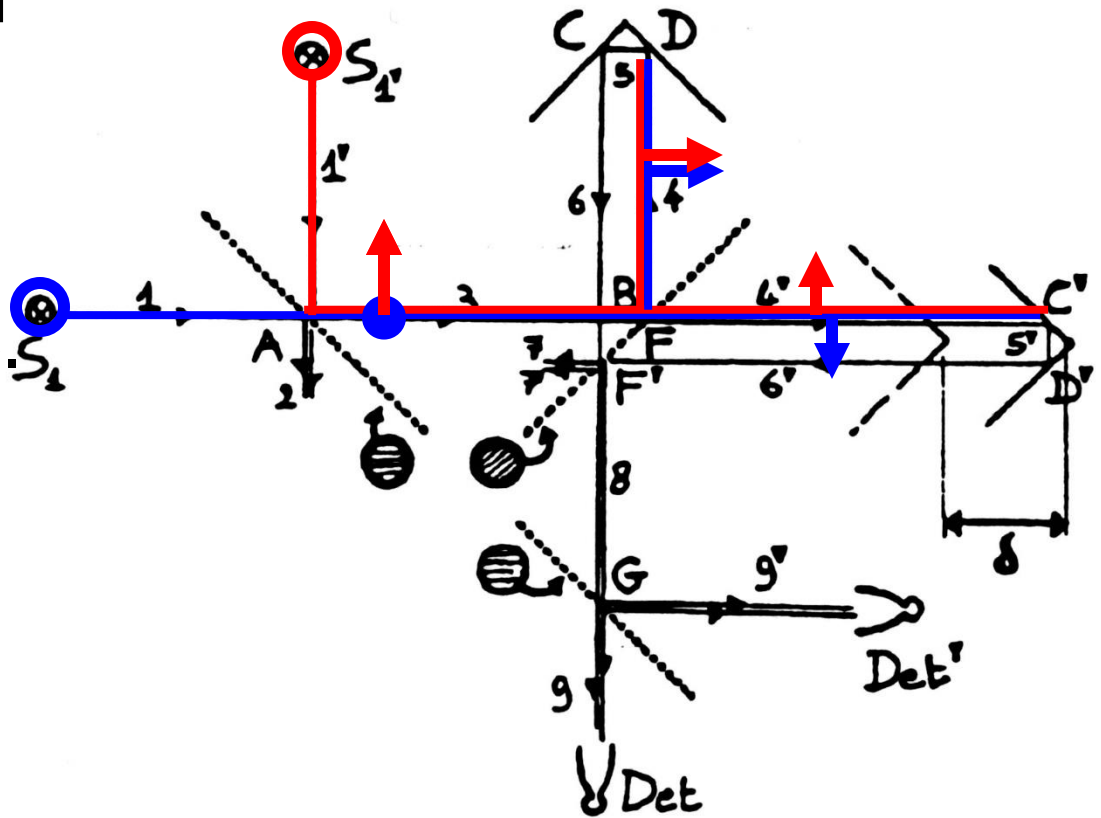




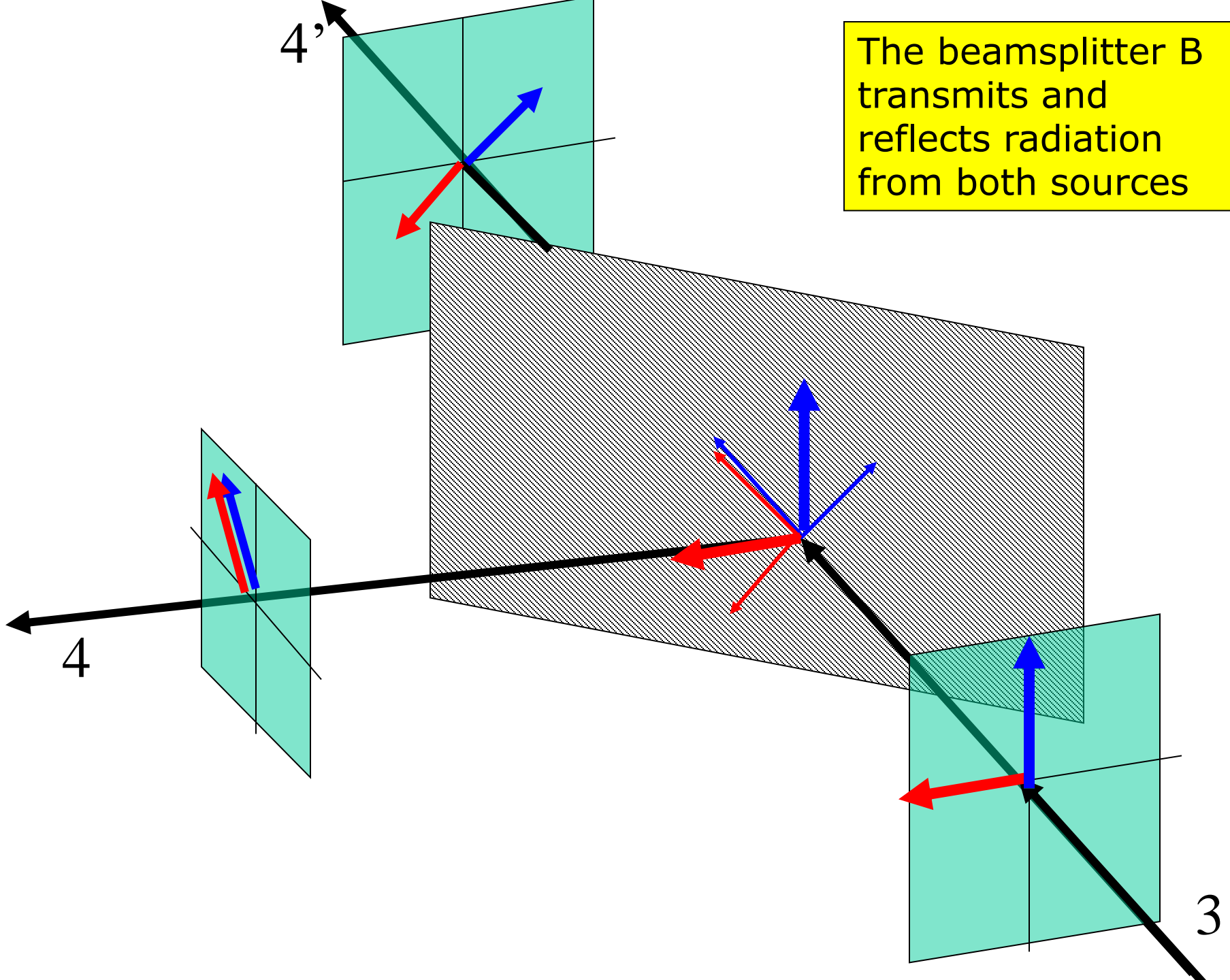
The beamsplitter polarizer B reflects radiation from both sources

# Martin Puplett Interferometer

- In addition, B **transmits** a fraction of the vertical component from  $\mathbf{S}_1$  and a fraction of the horizontal polarization from  $\mathbf{S}_{1'}$ .
- So beam 4' is polarized at  $45^\circ$  and consists of equal contributions from both  $\mathbf{S}_1$  and  $\mathbf{S}_{1'}$ .

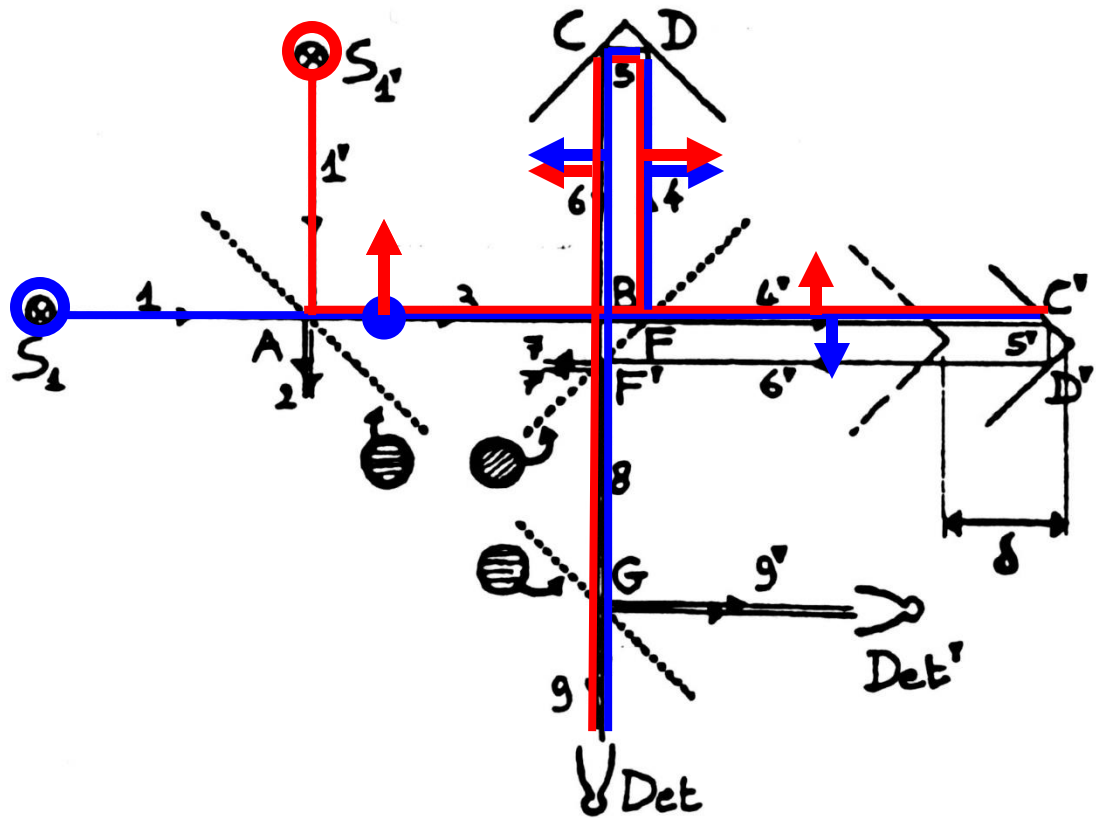


The beamsplitter B transmits and reflects radiation from both sources

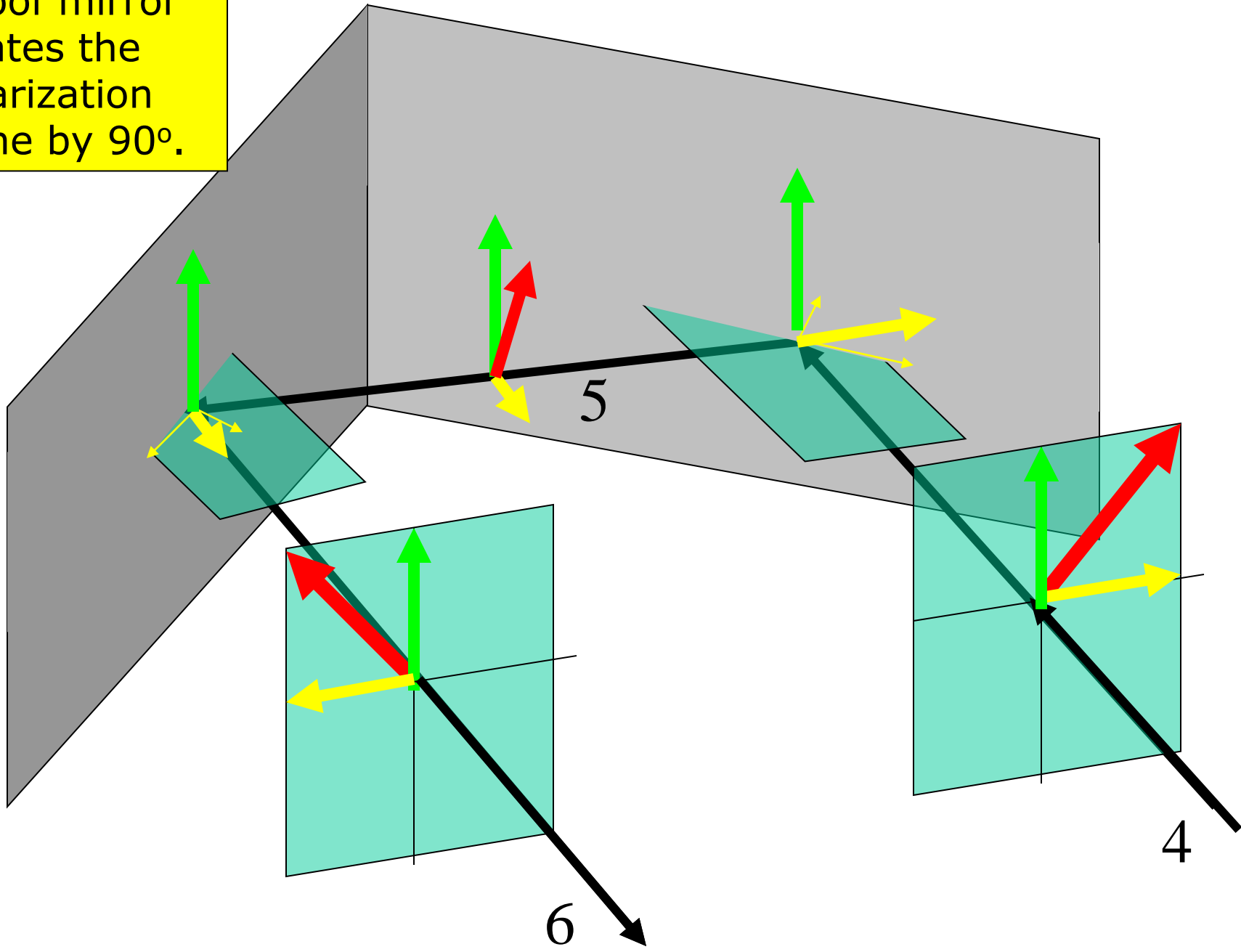


# Martin Puplett Interferometer

- The roof mirror CD reflects beam 4 into beam 6 back to the beamsplitter B.
- A roof mirror is used in place of a normal mirror because it rotates the polarization plane by  $90^\circ$ .
- In this way beam 6, which had been reflected by B, now is transmitted towards the detectors.

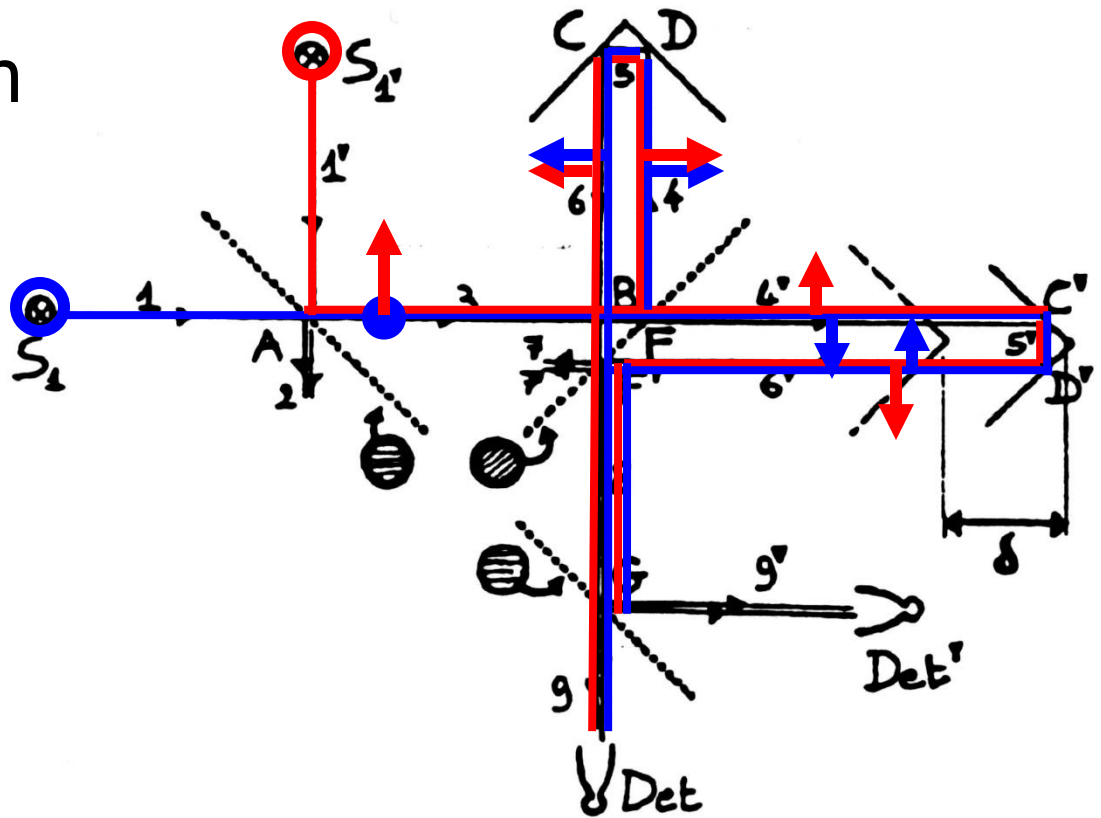


A roof mirror rotates the polarization plane by 90°.



# Martin Puplett Interferometer

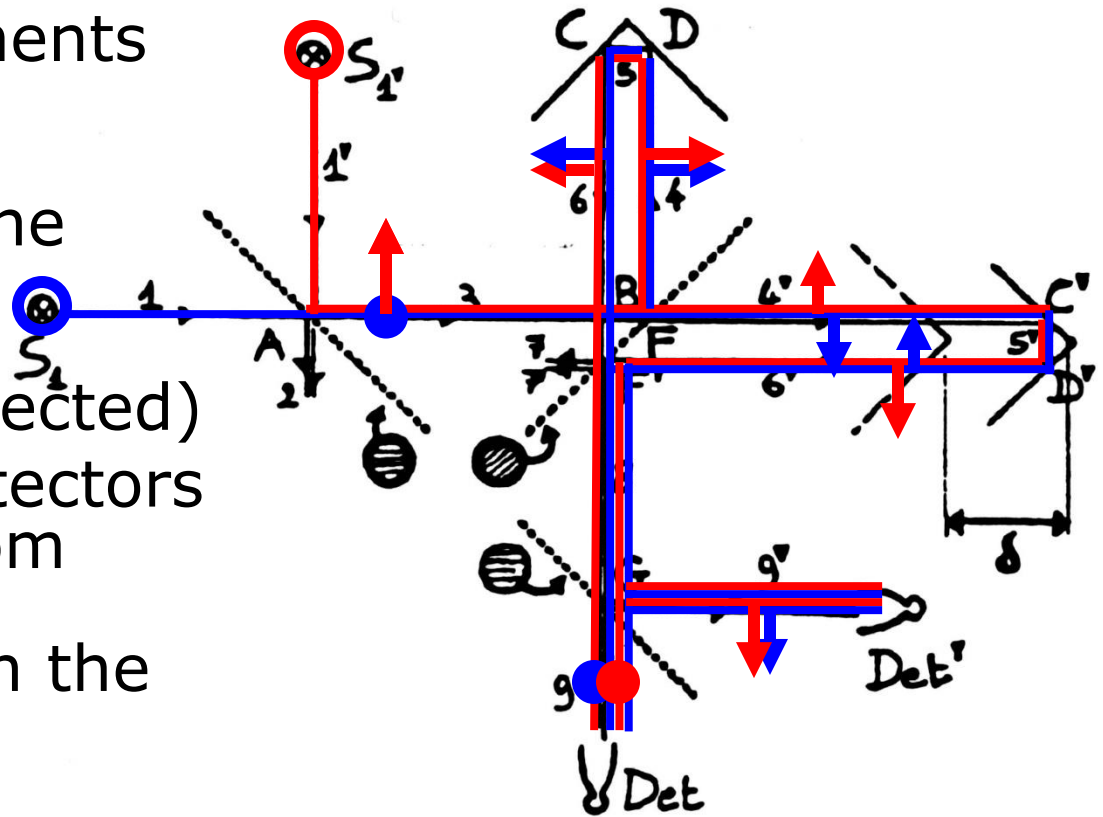
- In the same way the roof mirror  $C'D'$  reflects beam  $4'$  back towards the beamsplitter (as  $6'$ )
- The polarization plane is rotated by  $90^\circ$ , so that beam  $6'$ , which had been transmitted (as  $4'$ ) now is reflected towards the detectors.





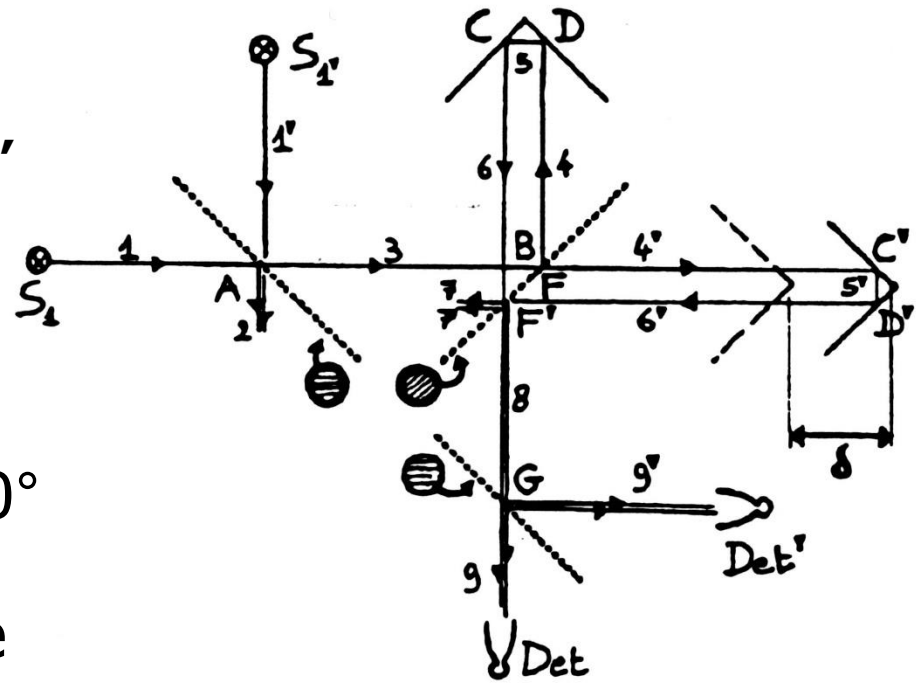
# Martin Puplett Interferometer

- The output polarizer G has wires parallel to the drawing plane.
- The rays coming from the beamsplitter, which are at  $45^\circ$ , have both horizontal and vertical components (coming from both sources) so they contribute to both the beams towards the detectors (both transmitted and reflected)
- In this way both detectors receive radiation from both sources, which passed through both the arms of the interferometer.



# Martin Puplett Interferometer

- The fundamental difference is that radiation from source  $S_{1'}$  underwent 4 reflections, while radiation from  $S_1$  underwent only 3 reflections. Since each reflection produces a  $180^\circ$  phase shift, the instrument measures the **diffence** between interferograms produced by  $S_{1'}$  and  $S_1$



# Quantitative treatment: uses Jones Calculus

- Jones matrices are used to describe linearly polarized radiation (Jones 1941)
- The interaction of the E field of the EM wave with an optical component is described by a 2x2 matrix:

$$\begin{pmatrix} E_{x,OUT} \\ E_{y,OUT} \end{pmatrix} = \begin{pmatrix} J_{11} & J_{12} \\ J_{21} & J_{22} \end{pmatrix} \begin{pmatrix} E_{x,IN} \\ E_{y,IN} \end{pmatrix}$$

- They work only for fully polarized radiation. For partially polarized radiation one can use Muller calculus (losing any phase information).

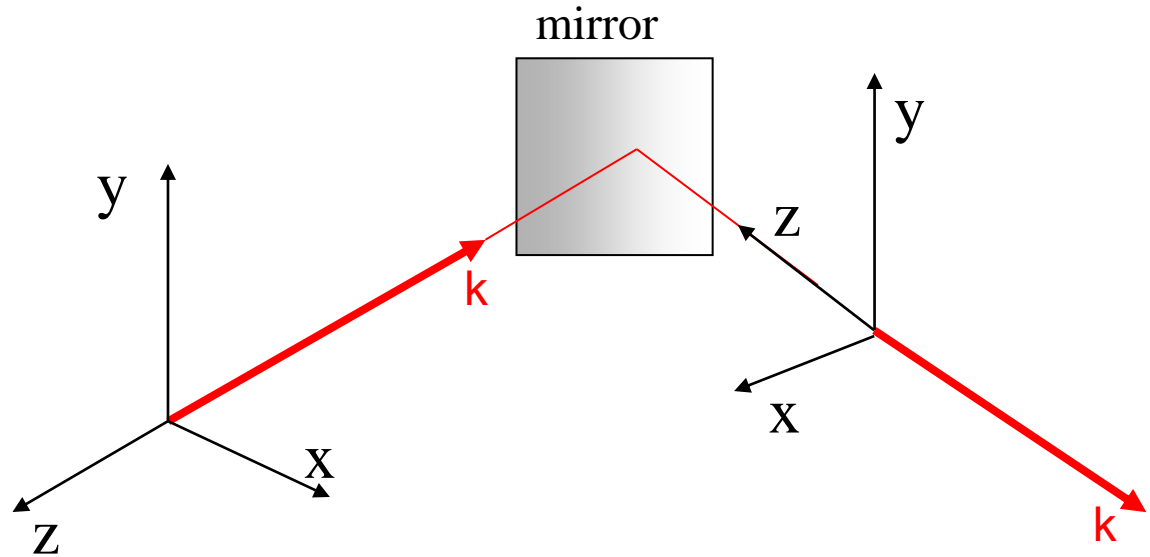
# E field

If  $E$  is the amplitude of the electric field of the EMW, it is represented as in the following examples:

- Linear polarization aligned along x axis  $E \begin{pmatrix} 1 \\ 0 \end{pmatrix}$
- Linear polarization aligned along y axis  $E \begin{pmatrix} 0 \\ 1 \end{pmatrix}$
- $45^\circ$  from x axis  $\frac{E}{\sqrt{2}} \begin{pmatrix} 1 \\ 1 \end{pmatrix}$
- $-45^\circ$  from x axis  $\frac{E}{\sqrt{2}} \begin{pmatrix} 1 \\ -1 \end{pmatrix}$
- Circular polarization (right)  $\frac{E}{\sqrt{2}} \begin{pmatrix} 1 \\ -i \end{pmatrix}$
- Circular polarization (left)  $\frac{E}{\sqrt{2}} \begin{pmatrix} 1 \\ i \end{pmatrix}$

# Reference system

- Comoving with the light beam :



## Mirrors

- Ideal single mirror, orthogonal to  $xz$  plane:
- Ideal roof mirror, orthogonal to  $xz$  plane:

$$M = \begin{pmatrix} 1 & 0 \\ 0 & -1 \end{pmatrix}$$

$$RM = \begin{pmatrix} 1 & 0 \\ 0 & -1 \end{pmatrix} \begin{pmatrix} 1 & 0 \\ 0 & -1 \end{pmatrix} = \begin{pmatrix} 1 & 0 \\ 0 & 1 \end{pmatrix}$$

# Linear polarizers

- Transmission :  
Polarizer with horizontal  
principal axis:  $\begin{pmatrix} 1 & 0 \\ 0 & 0 \end{pmatrix}$

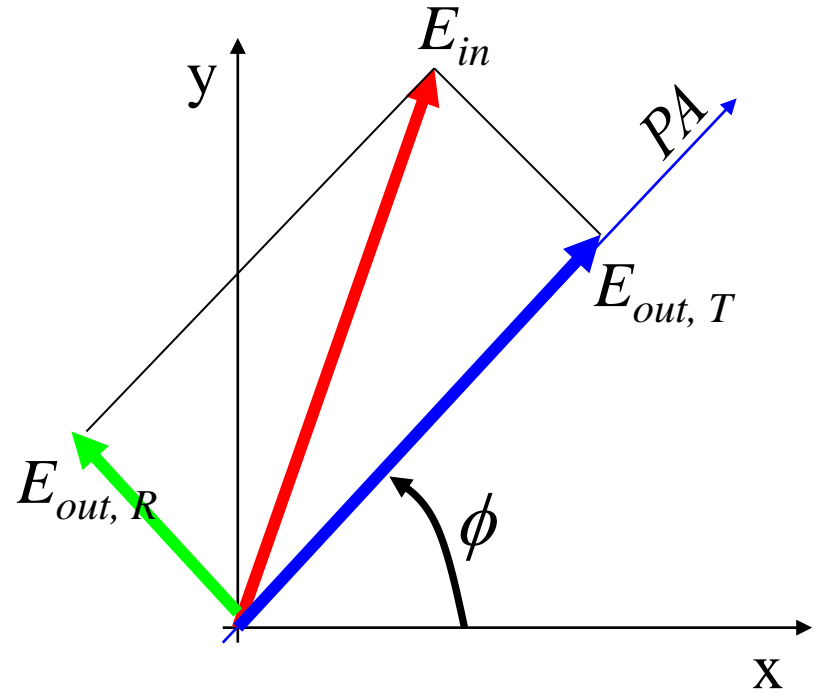
- Transmission :  
Polarizer with vertical  
principal axis:  $\begin{pmatrix} 0 & 0 \\ 0 & 1 \end{pmatrix}$

- Transmission :  
Polarizer with principal  
axis at angle  $\phi$  from x  
axis

$$P_t(\phi) = \begin{pmatrix} \cos^2 \phi & \cos \phi \sin \phi \\ \cos \phi \sin \phi & \sin^2 \phi \end{pmatrix}$$

- Reflection : Polarizer  
with principal axis at  
angle  $\phi$  from x axis

$$P_r(\phi) = \begin{pmatrix} \sin^2 \phi & -\cos \phi \sin \phi \\ \cos \phi \sin \phi & -\cos^2 \phi \end{pmatrix}$$



# Delay

- Introduced by an optical path difference  $\delta=4\pi\sigma x$  : this is common for both polarizations, so

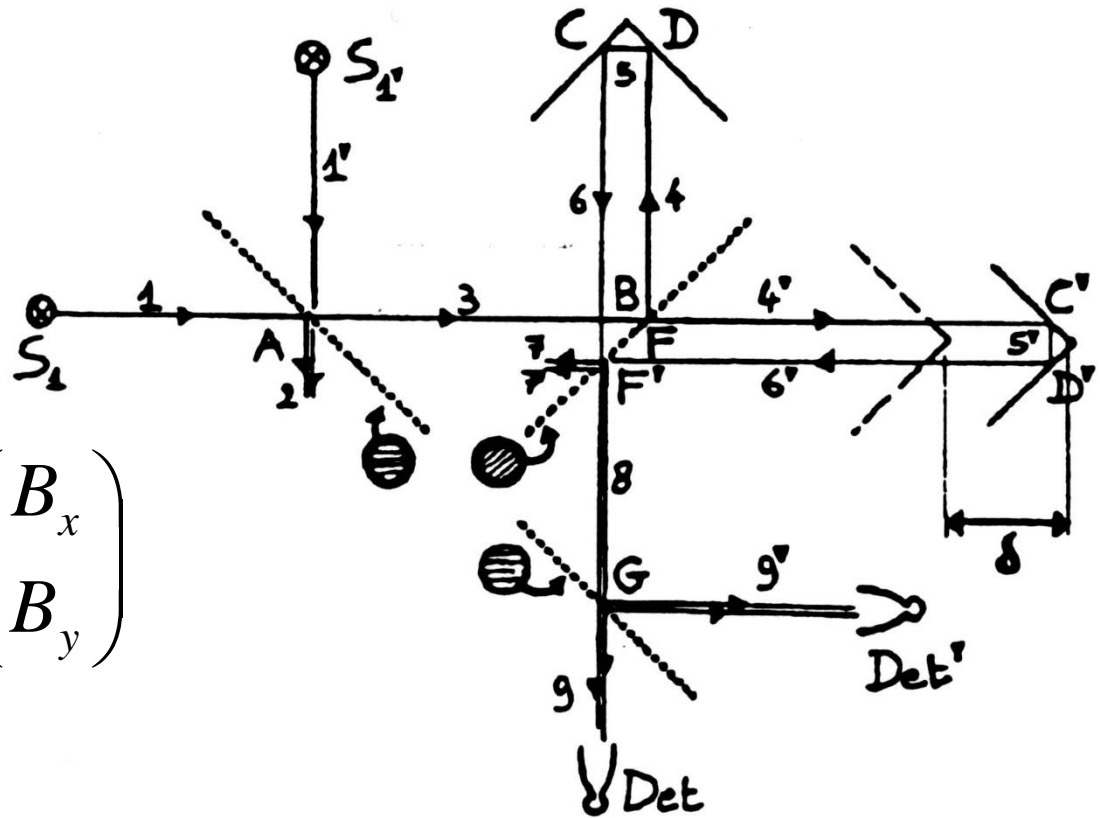
$$D(\delta) = \begin{pmatrix} e^{i\delta} & 0 \\ 0 & e^{i\delta} \end{pmatrix}$$

- The two sources  $S_1$  and  $S'_1$ , are described by Jones vectors

$$S_1 = \begin{pmatrix} A_x \\ A_y \end{pmatrix} \quad S'_1 = \begin{pmatrix} B_x \\ B_y \end{pmatrix}$$

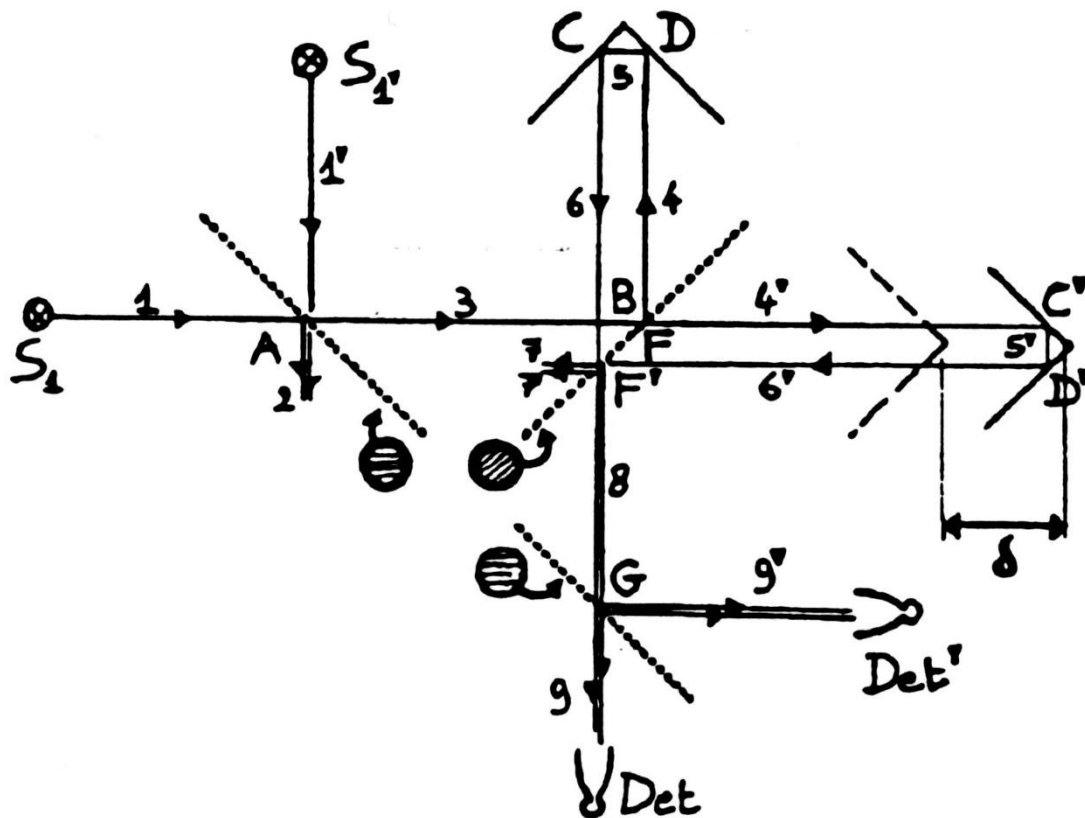
- beam 3, after the input polarizer (with horizontal principal axis), is

$$S_3 = P_t(0)S_1 + P_r(0)S'_1 = \begin{pmatrix} A_x \\ -B_y \end{pmatrix}$$





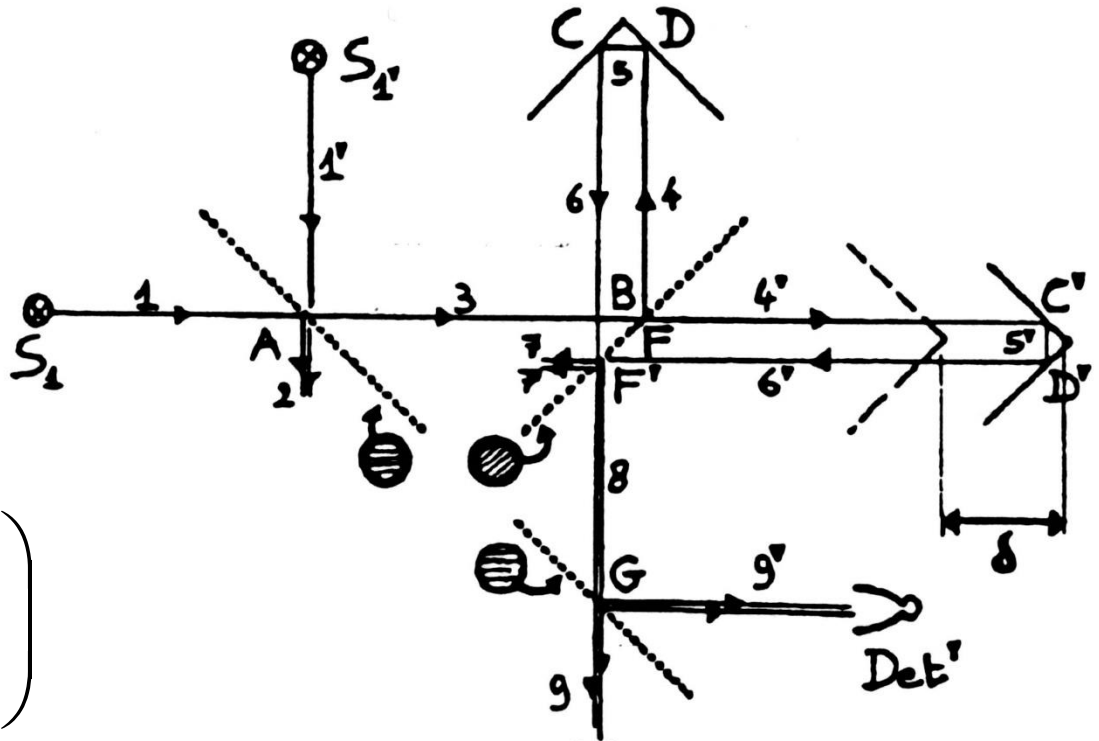
- beam 4 (reflected by the beamsplitter) and beam 4' (transmitted by the beamsplitter) will be:



$$S_4 = P_r(\pi/4)S_3 = \frac{1}{2} \begin{pmatrix} 1 & -1 \\ 1 & -1 \end{pmatrix} \begin{pmatrix} A_x \\ -B_y \end{pmatrix} = \frac{1}{2} \begin{pmatrix} A_x + B_y \\ A_x + B_y \end{pmatrix}$$

$$S_4' = P_t(\pi/4)S_3 = \frac{1}{2} \begin{pmatrix} 1 & 1 \\ 1 & 1 \end{pmatrix} \begin{pmatrix} A_x \\ -B_y \end{pmatrix} = \frac{1}{2} \begin{pmatrix} A_x - B_y \\ A_x - B_y \end{pmatrix}$$

- Since roof mirrors are represented by unity matrix, we have also



$$S_6 = S_4 = \frac{1}{2} \begin{pmatrix} A_x + B_y \\ A_x + B_y \end{pmatrix}$$

$$S'_6 = DS'_4 = D \frac{1}{2} \begin{pmatrix} A_x - B_y \\ A_x - B_y \end{pmatrix} = \frac{1}{2} \begin{pmatrix} (A_x - B_y) e^{i\delta} \\ (A_x - B_y) e^{i\delta} \end{pmatrix}$$

- $S_6$  is transmitted by the beamsplitter, while  $S'_6$  is reflected, so

$$S_8 = P_t(\pi/4)S_6 + P_r(3\pi/4)S'_6 = \frac{1}{2} \begin{pmatrix} 1 & 1 \\ 1 & 1 \end{pmatrix} S_6 + \frac{1}{2} \begin{pmatrix} 1 & 1 \\ -1 & -1 \end{pmatrix} S'_6$$

$$S_8 = P_t(\pi/4)S_6 + P_r(3\pi/4)S'_6 = \frac{1}{2} \begin{pmatrix} 1 & 1 \\ 1 & 1 \end{pmatrix} S_6 + \frac{1}{2} \begin{pmatrix} 1 & 1 \\ -1 & -1 \end{pmatrix} S'_6$$

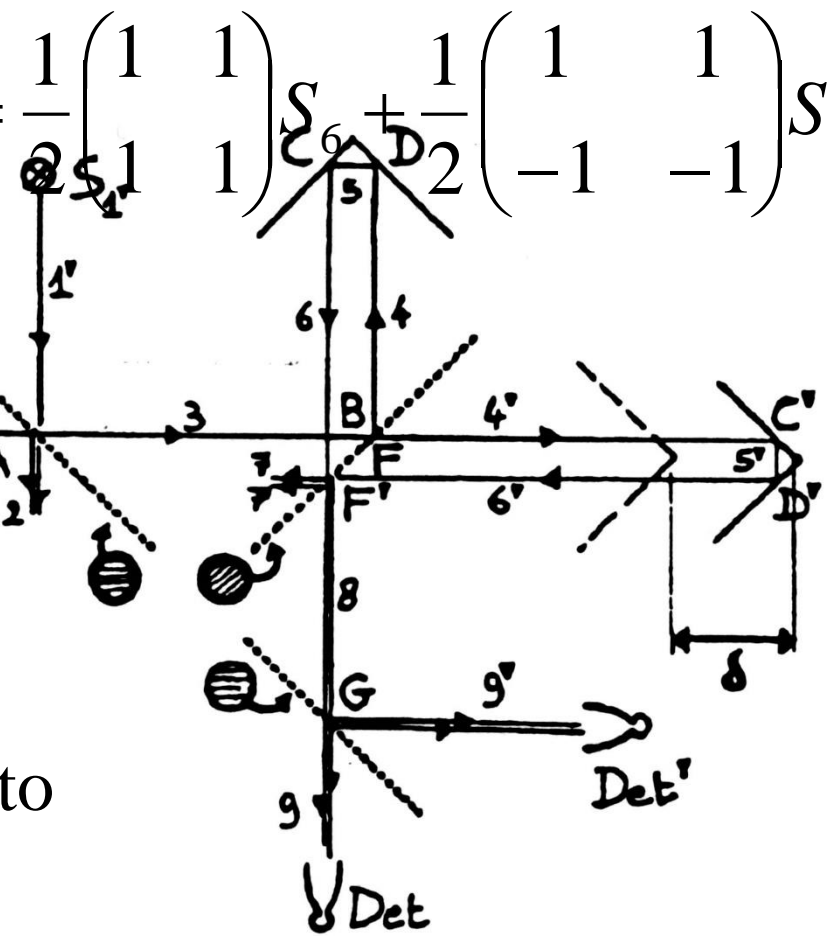
• So

$$S_8 = \frac{1}{2} \begin{pmatrix} A_x(e^{i\delta} + 1) - B_y(e^{i\delta} - 1) \\ -A_x(e^{i\delta} - 1) + B_y(e^{i\delta} + 1) \end{pmatrix}$$

• After the interaction with the output beamsplitter the beams to the detectors are

$$S_9 = P_t(0)S_8 = \frac{1}{2} \begin{pmatrix} A_x(e^{i\delta} + 1) - B_y(e^{i\delta} - 1) \\ 0 \end{pmatrix}$$

$$S'_9 = P_r(0)S_8 = \frac{1}{2} \begin{pmatrix} 0 \\ A_x(e^{i\delta} - 1) - B_y(e^{i\delta} + 1) \end{pmatrix}$$



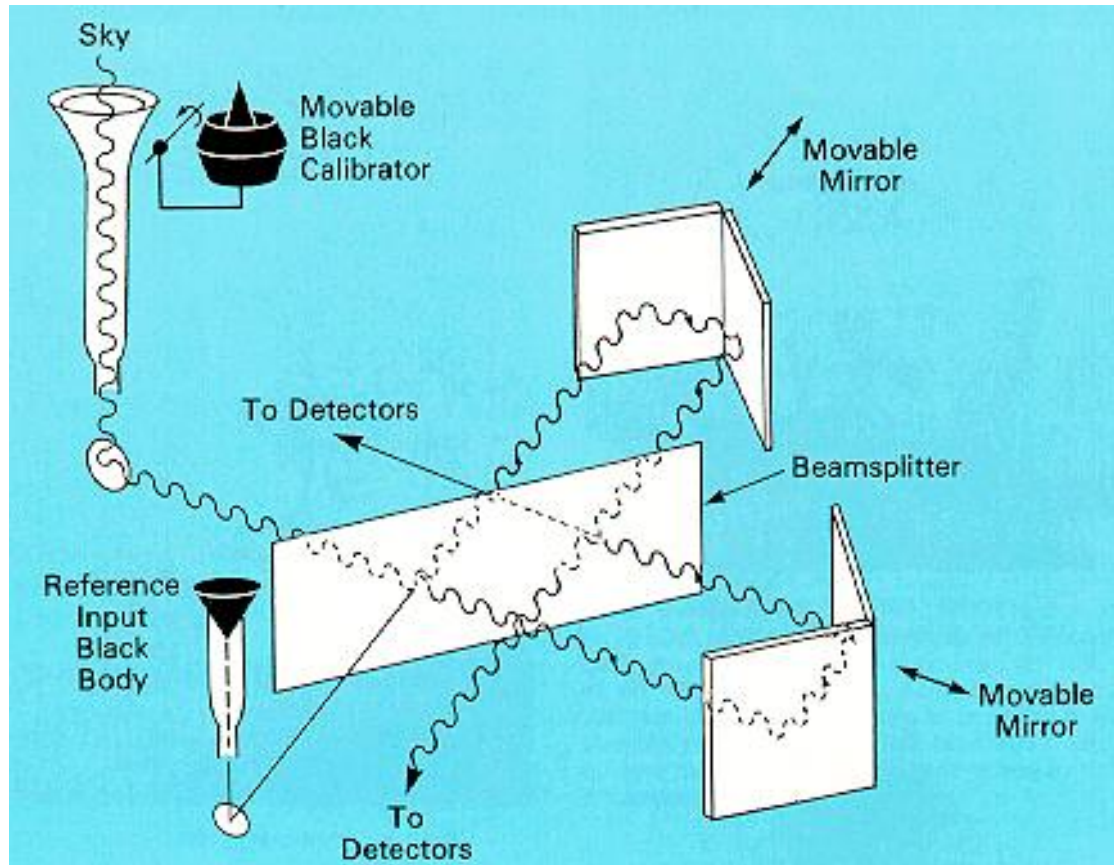
- Now we can compute the power on the detectors:

$$I = E_x E_x^* + E_y E_y^* \quad \rightarrow$$

$$I_9 = \frac{1}{2} [A_x^2 (1 + \cos \delta) + B_y^2 (1 - \cos \delta)] = \frac{A_x^2 + B_y^2}{2} + \frac{A_x^2 - B_y^2}{2} \cos \delta$$

$$I'_9 = \frac{1}{2} [A_x^2 (1 - \cos \delta) + B_y^2 (1 + \cos \delta)] = \frac{A_x^2 + B_y^2}{2} - \frac{A_x^2 - B_y^2}{2} \cos \delta$$

- Both detectors measure a **constant intensity** (equal to half of the sum of the intensities from the two sources), **plus a modulated intensity** (modulated by the optical path difference), whose amplitude is the **difference** of the spectra from the two sources.
- **The interferogram is zero if the two sources have the same spectrum.**

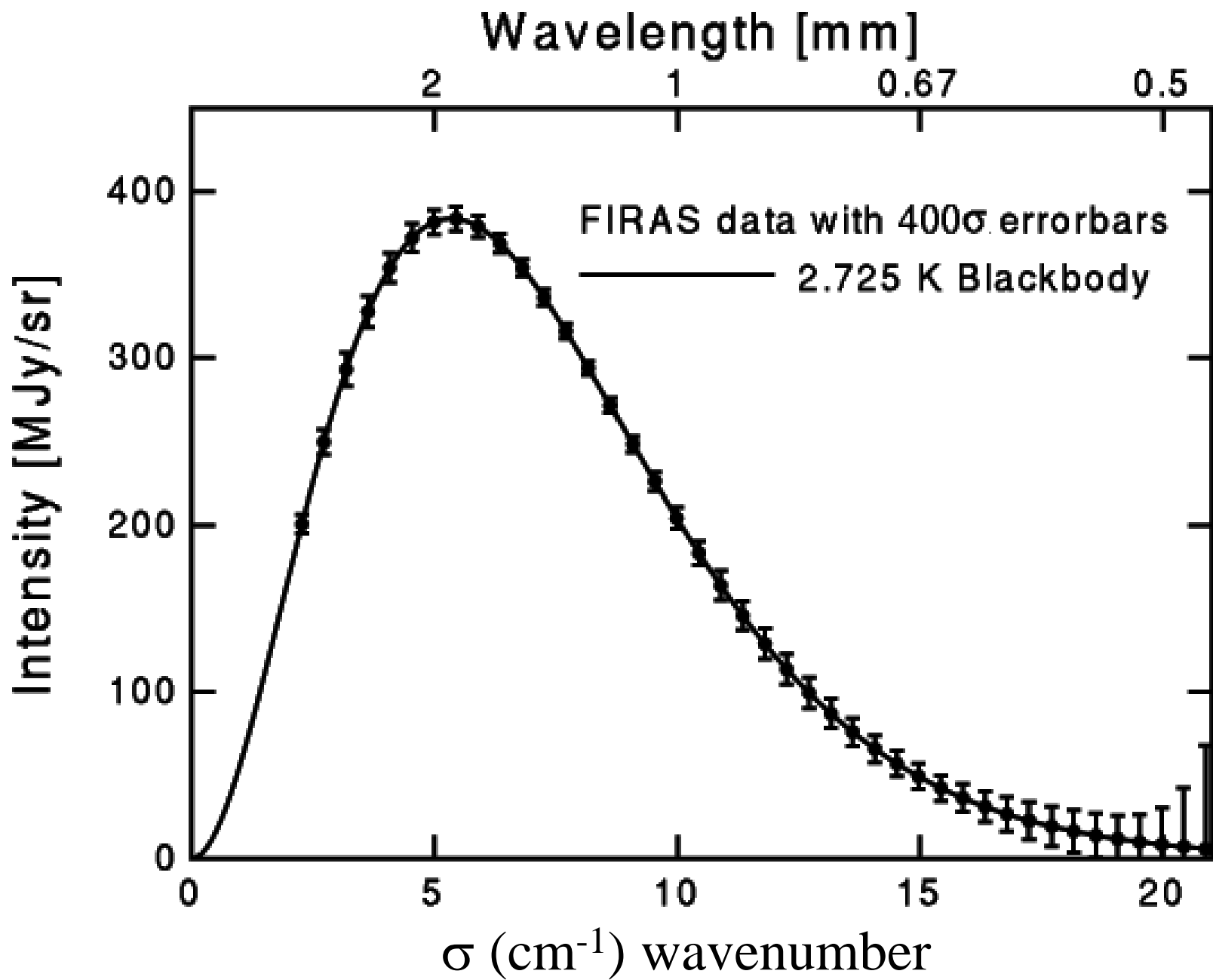


$$I_{SKY}(x) = C \int_0^{\infty} [S_{SKY}(\sigma) - S_{REF}(\sigma)] rt(\sigma) \{1 + \cos[4\pi\sigma x]\} d\sigma$$

$$I_{CAL}(x) = C \int_0^{\infty} [S_{CAL}(\sigma) - S_{REF}(\sigma)] rt(\sigma) \{1 + \cos[4\pi\sigma x]\} d\sigma$$

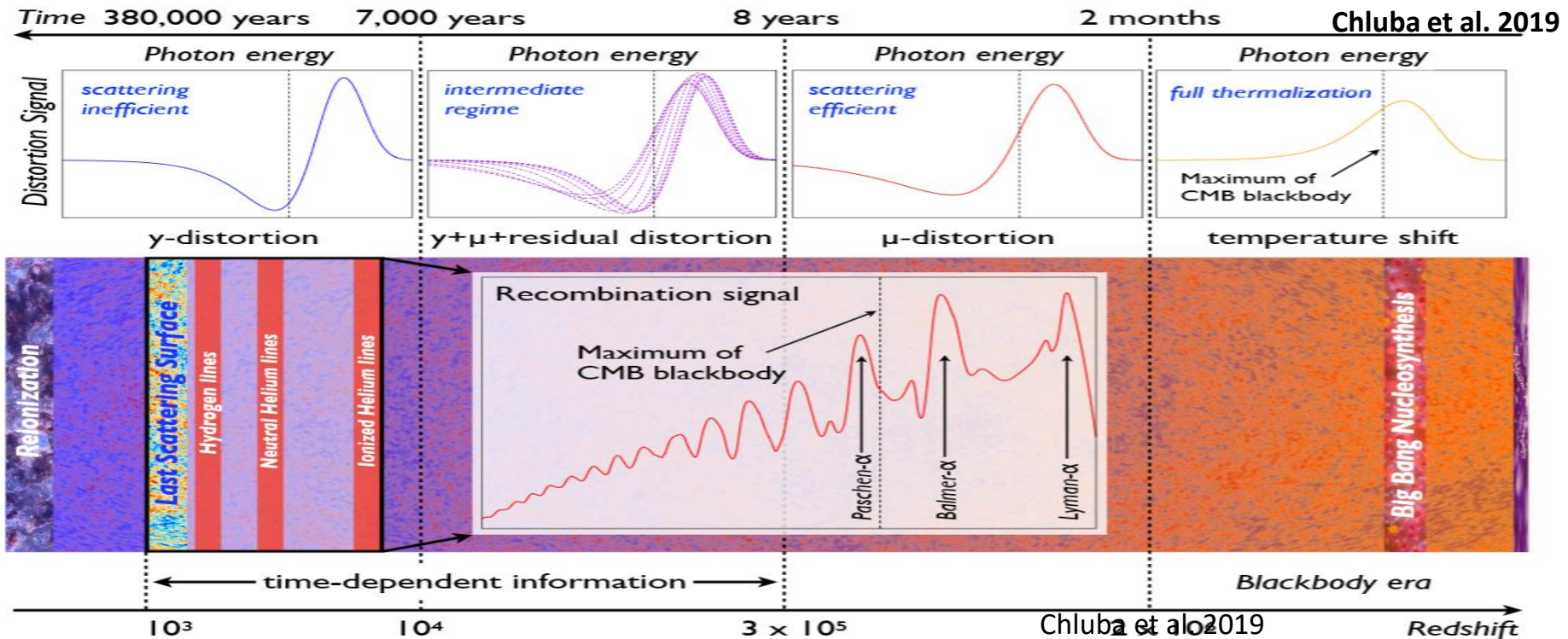
# FIRAS

- The FIRAS guys were able to change the temperature of the internal blackbody until the interferograms were flat zero.
- This is a null measurement, which is much more sensitive than an absolute one: (one can boost the gain without saturating !).
- This means that the difference between the spectrum of the sky and the spectrum of a blackbody is zero, i.e. **the spectrum of the sky is a blackbody with the same temperature as the internal reference blackbody.**
- This also means that the internal blackbody is a real blackbody: it is unlikely that the sky can have the same deviation from the Planck law as the source built in the laboratory.



# Spectral Distortions of the CMB

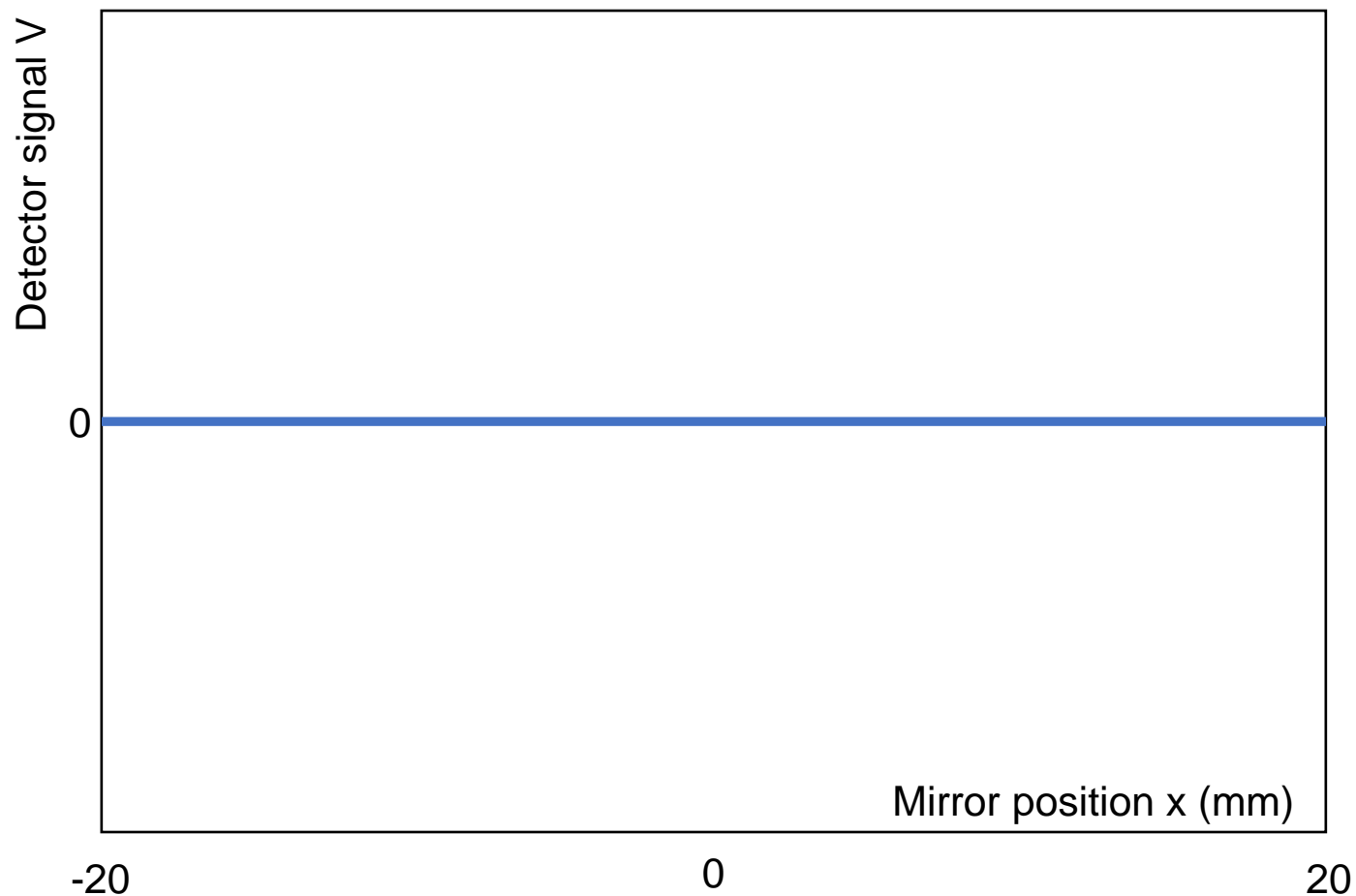
- CMB spectral distortions are expected at a level just below current upper limits, i.e. **0.01% of the peak brightness** of the CMB [COBE – FIRAS; Mather et al. (1990) Ap.J.L. **354** 37, Fixsen et al. (1996) Ap.J. **473** 576) >20 years ago !].
- This search represents a research path orthogonal and synergic to CMB polarization studies, promising to shed light on:
  - Cosmic Reionization
  - Physics of recombination
  - Dark matter & Energy releases in the primeval fireball
  - Very Early Universe and Cosmic Inflation
  - ... much more





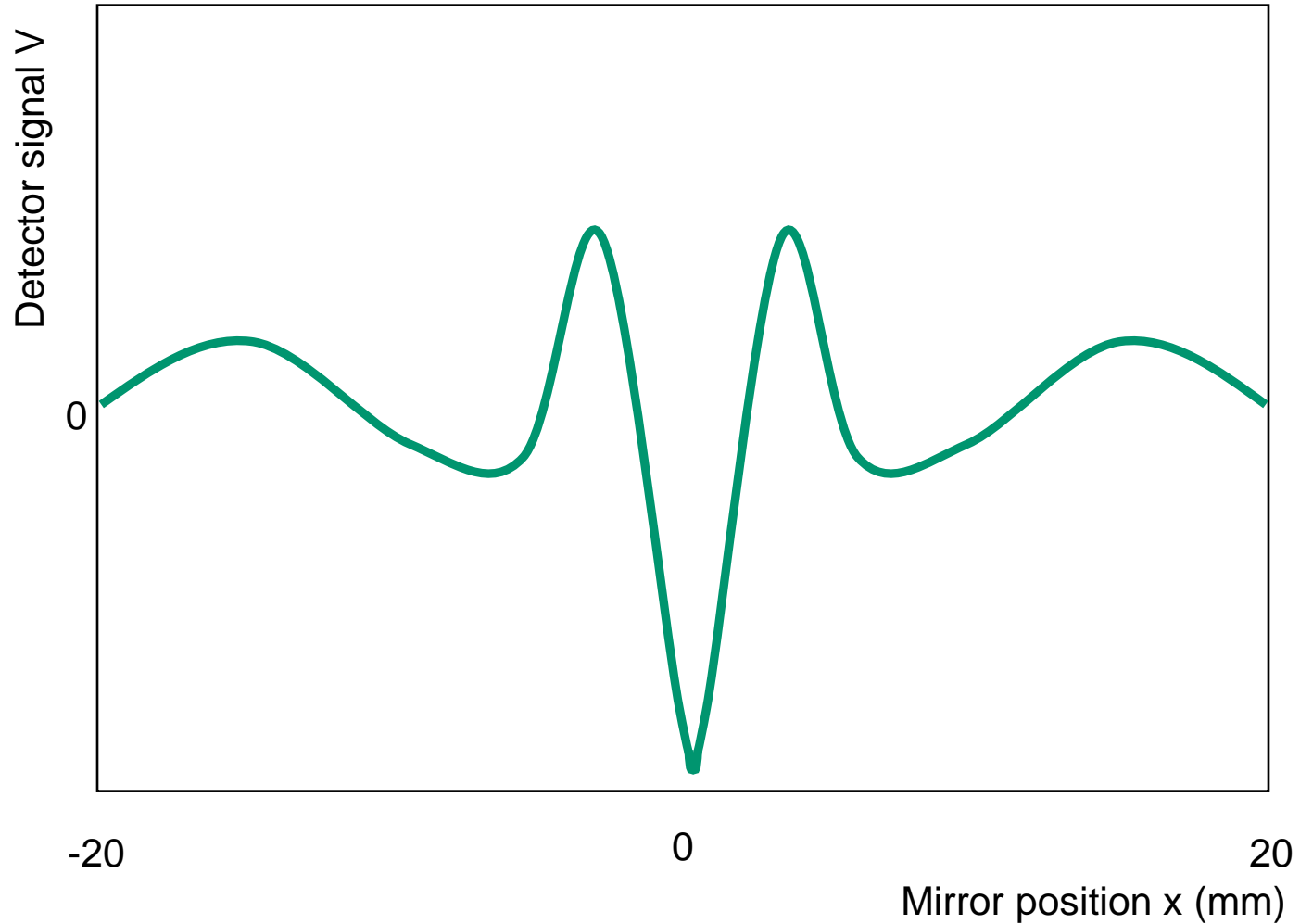
# Spectral Distortions of the CMB

- The final measurement must be carried out from space. PIXIE, CORE, PRISTINE, FOSSIL proposals not selected yet. Meanwhile, ground and near-space efforts are useful to test and refine methods, and possibly to detect the largest distortions (COSMO, BISOU).
- The target now shifts from producing an upper limit to obtaining a detection, and the requirements for the instrument are much more stringent. In fact, what was actually measured by FIRAS was ZERO (within the noise)



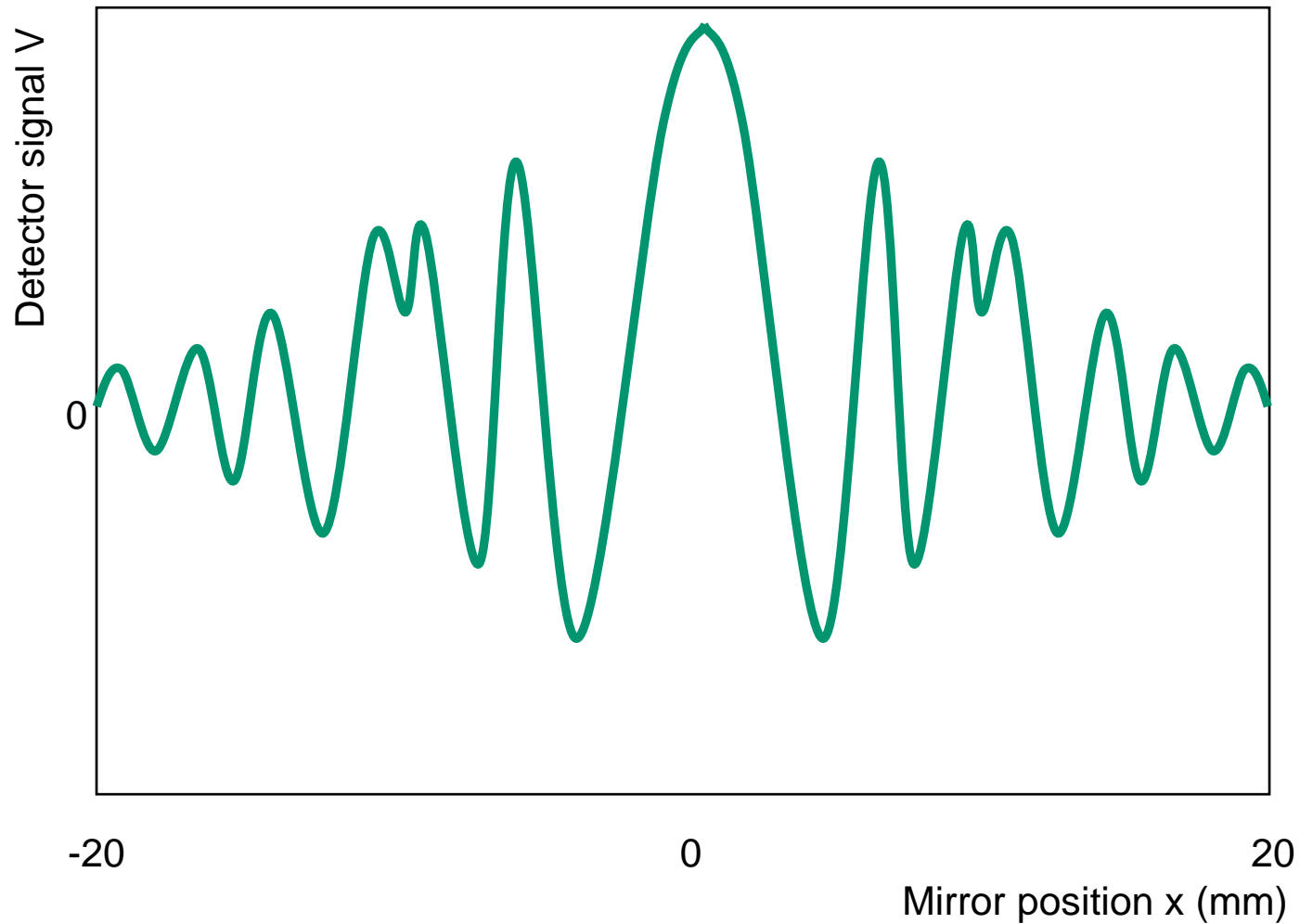
What was NOT measured :

i.e. what you expect if, whatever they are, the internal reference and the sky brightness are not the same.



What was NOT measured :

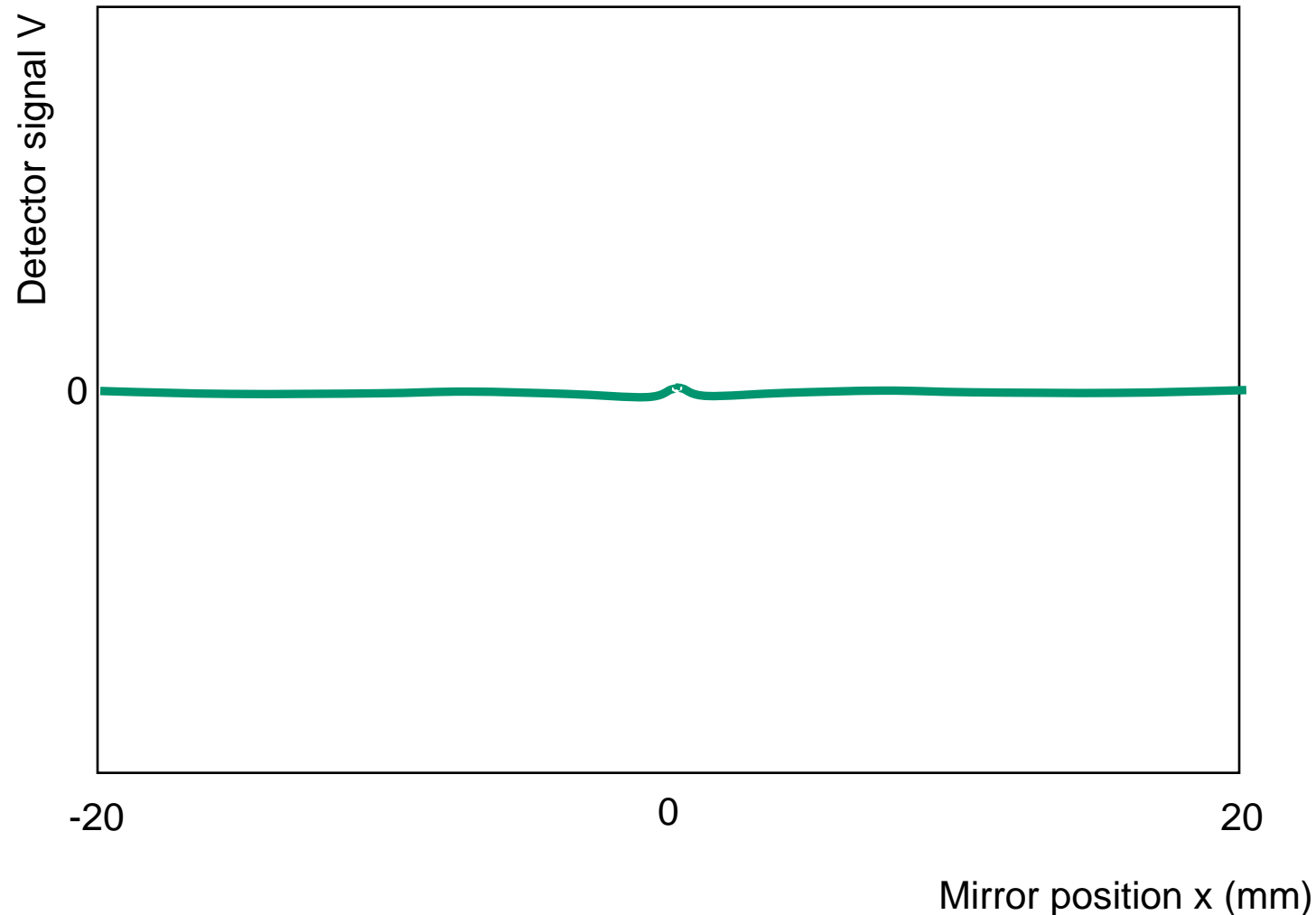
i.e. what you expect if, whatever they are, the internal reference and the sky brightness are not the same.



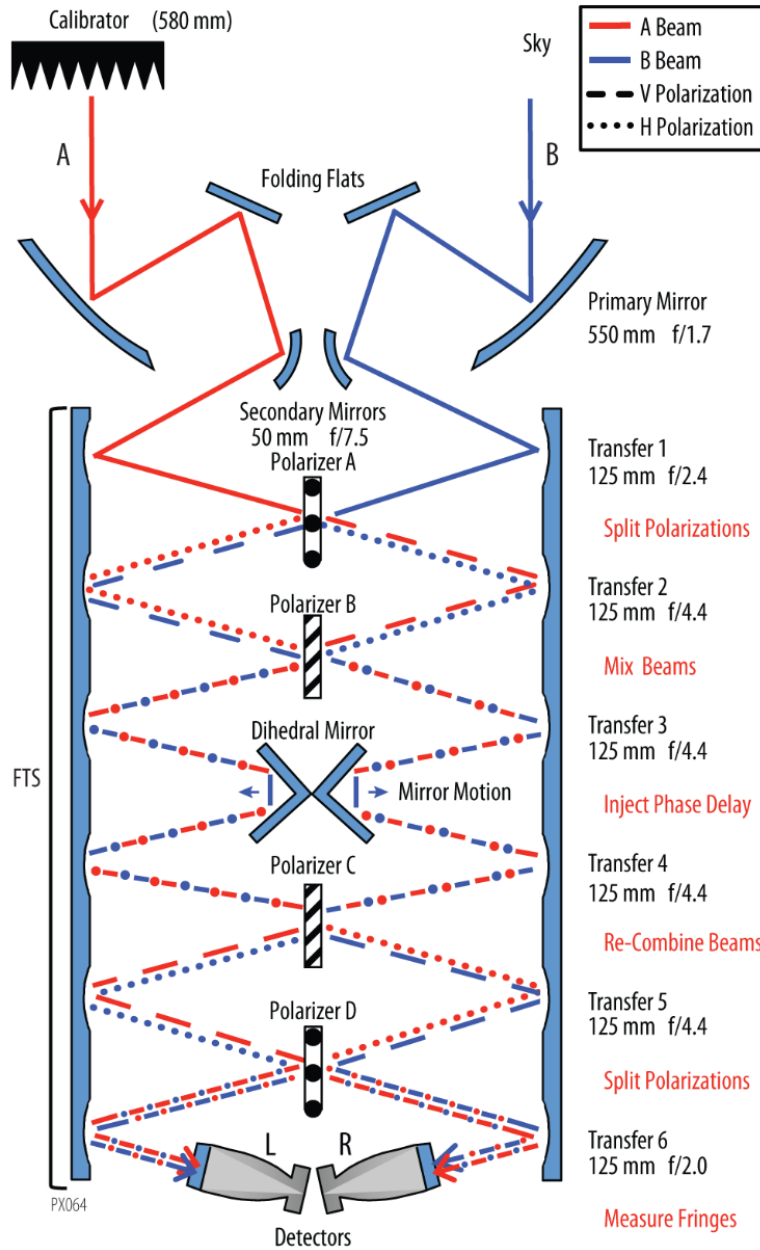
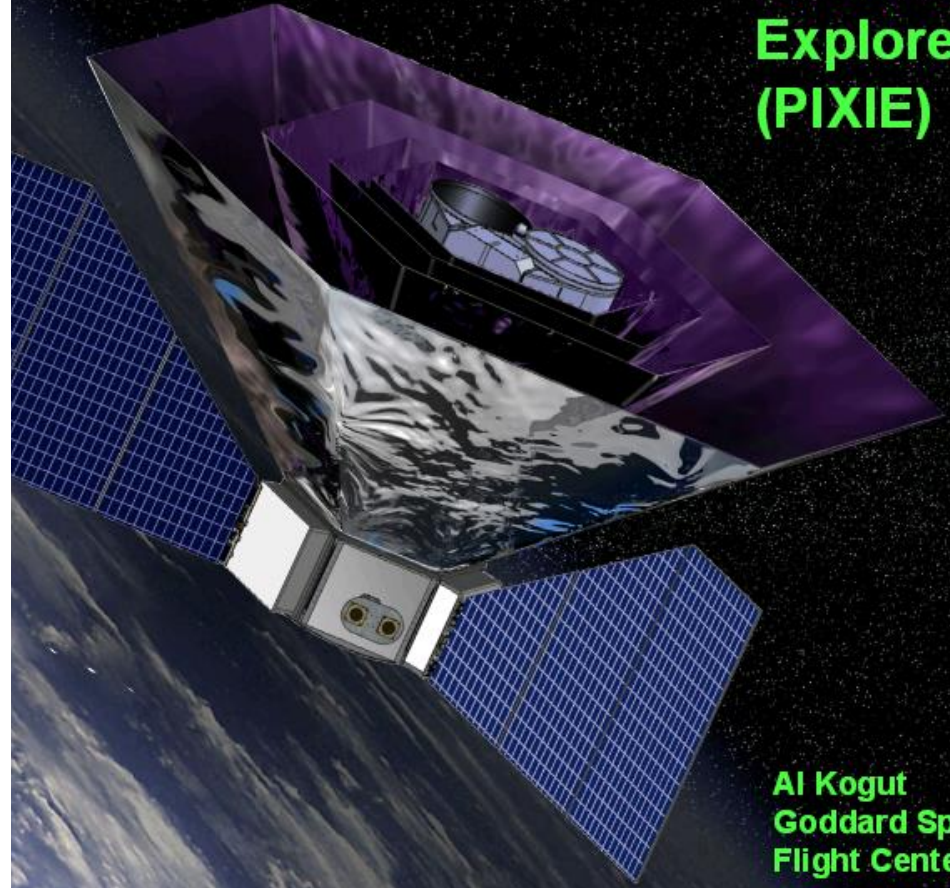
Note that as soon as you start to detect any small deviation from zero ..

- 1) You need accurate calibration of  $C$  and  $rt(\sigma)$  to convert it into a  $S_{\text{sky}} - S_{\text{ref}}$  signal
- 2) You start asking yourself if this deviation is in the sky or is in your reference blackbody

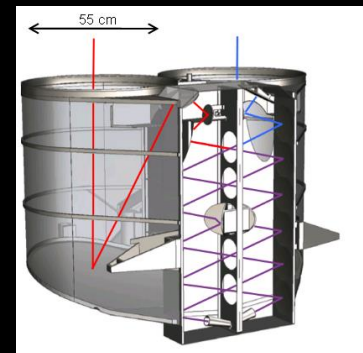
Being a differential instrument, your FTS cannot tell you the answer. You have to be sure that your reference blackbody is really black, i.e. reflectivity  $< -80\text{dB}$  (!!)



# Primordial Inflation Explorer (PIXIE)

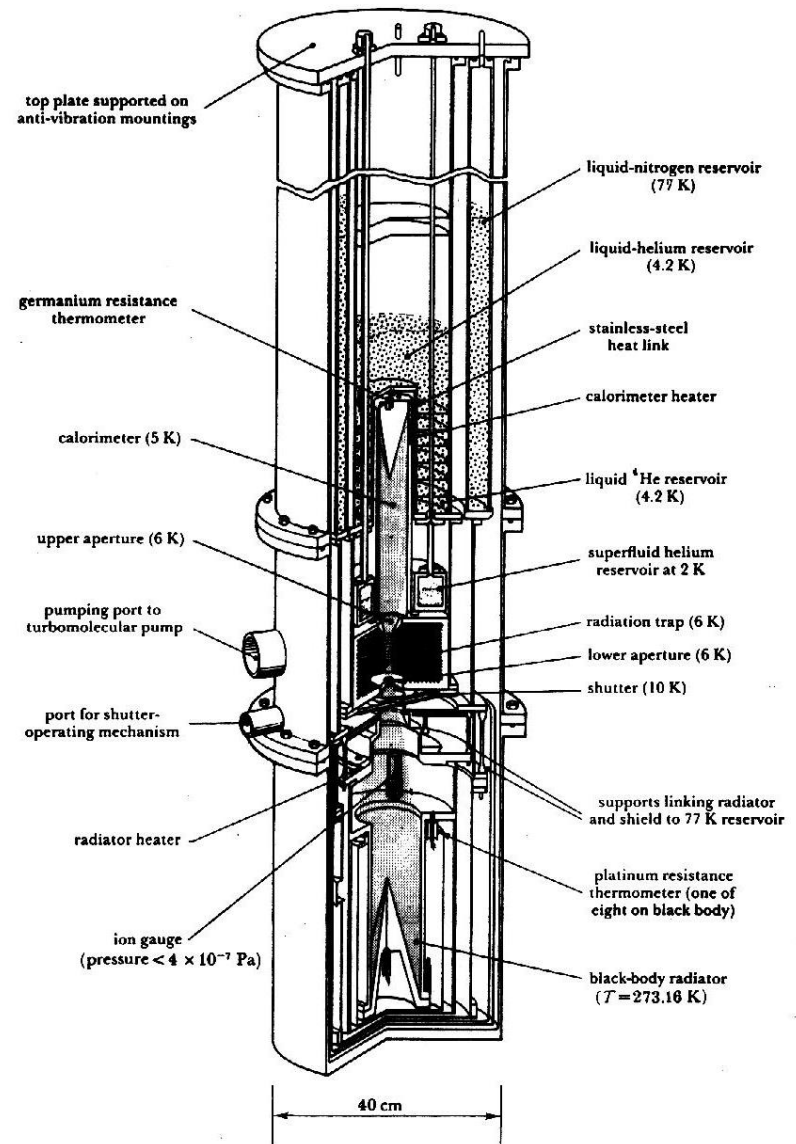


Looking at CMB deviations from Planck's law of the order of  $<10^{-7}$  !



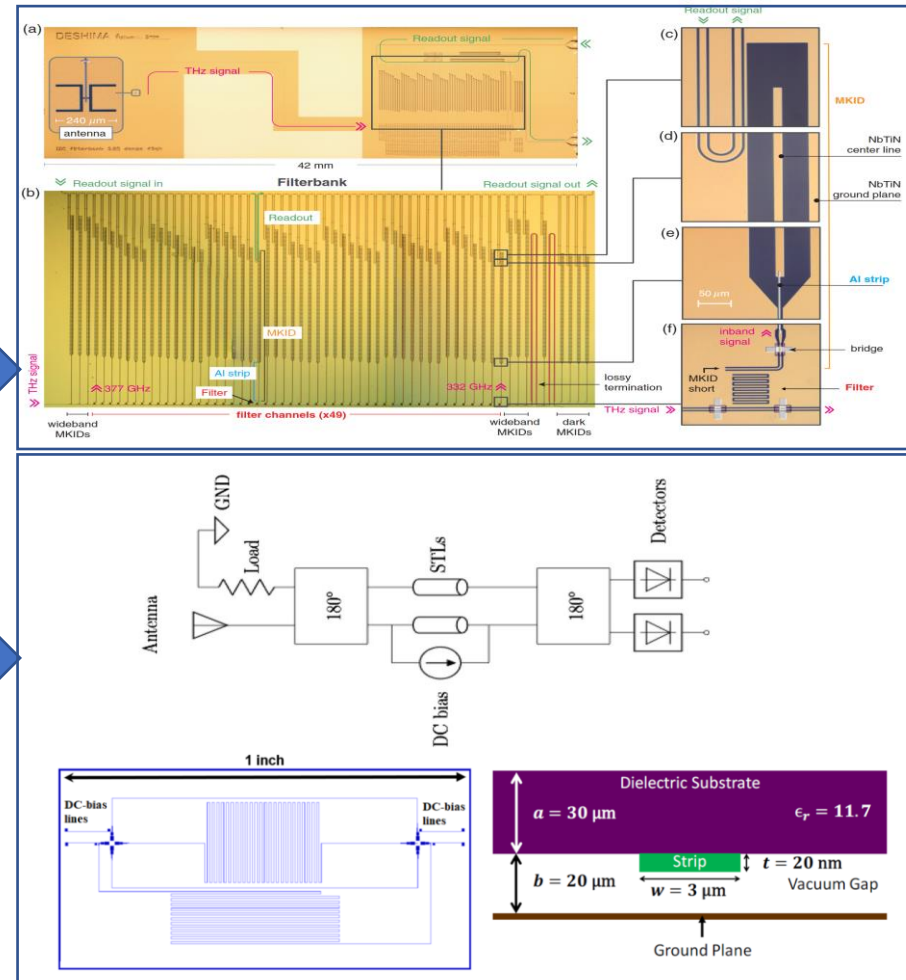
# Accurate reference blackbodies

- To measure a few K blackbody, you need a cryogenic reference blackbody, with variable temperature. Otherwise you do not null the signal.
- Practical design of a Blackbody cavity: see e.g. Quinn T.J., Martin J.E., (1985), *Phil. Trans. R. Soc. Lond.*, A316, 85: who made a radiometric measurement of the Boltzmann constant (precise to 5 significant digits !)
- Test, test, test: use a VNA to measure S11 of the BB in the entire frequency range: if it is less than -80dB, you are fine !



# On-chip spectroscopic capabilities

- mm-wave spectrometers (usually FTSs) are very effective instruments, but have a bulky structure, and are not easy to implement in a cryogenic environment, as needed to fully exploit the advantage of the low background conditions in space-based experiments.
- A filterbank, feeding a KID for each band can be efficiently built on-chip using planar transmission lines and filters. See e.g. Endo &, JATIS, 5, 035004 (2019).
- Delay lines for an **on-chip Fourier Transform Spectrometer**, encoding all the frequencies of interest on a single detector, can be obtained on the same wafer as the detectors using superconducting transmission lines (STL) as delay lines. A DC current can be used to modulate the *kinetic inductance of the STL* and thus the delay. See e.g. Faramarzi & JLTP 199, 867 (2020) and Basu et al., arXiv:2111.06558, expecting up to 2000 rad of phase shift ( $R=1000$  @100 GHz) from 700 mm long NbN STL.
- Very important developments, in view of a space-based mission. Drawbacks: calibration, CMRR, **frequency coverage**.



# COSMO

## (COSmic Monopole Observer)



\*E. Battistelli, P. de Bernardis, S. Cibella, F. Columbro, A. Coppolecchia, M. Bersanelli, G. D'Alessandro, M. De Petris, C. Franceschet, M. Gervasi, A. Limonta, L. Lamagna, E. Manzan, E. Marchitelli, S. Masi, L. Mele, A. Mennella, A. Paiella, G. Pettinari, F. Piacentini, L. Piccirillo, G. Pisano, S. Realini, C. Tucker, M. Zannoni

<https://cosmo.roma1.infn.it>

